Aus dem Experimental and Clinical Research Center
der Medizinischen Fakultät Charité – Universitätsmedizin Berlin

DISSERTATION

„Repositioned drugs against the MACC1-β-catenin-S100A4 axis of metastasis suppress colon cancer metastasis in a synergistic manner“

„Repositionierte Arzneistoffe gegen die MACC1-β-Catenin-S100A4-Achse der Metastasierung unterdrücken Darmkrebs-metastasen in synergistischer Weise“

zur Erlangung des akademischen Grades

Doctor of Philosophy (PhD)

vorgelegt der Medizinischen Fakultät
Charité – Universitätsmedizin Berlin

von

Benedikt Kortüm
aus Schwalmstadt

Datum der Promotion: 30. Juni 2024

Contents

List of tables

List of figures

List of abbreviations

APC	Adenomatous-polyposis-coli
CAF	Cancer-associated fibroblast
CDS	Coding Sequence
CMV	Cytomegaly Virus
Co-IP	Co-Immunoprecipitation
CRC	Colorectal Cancer
CRISPR	Clustered Regularly Interspaced Short Palindromic Repeats
CTC	Circulating Tumor Cell
DAPI	4',6-Diamidin-2-phenylindol dihydrochloride
DMEM	Dulbecco's Modified Eagle Medium
DNA	Desoxyribonucleic Acid
FACS	Fluorescence Activated Cell Sorting
FBS	Fetal Bovine Serum
GFP	Green-Fluorescent Protein
G6PDH	Glucose-6-phosphat-Dehydrogenase
LDS	Lithium dodecyl sulfate
MACC1	Metastasis-Associated in Colon Cancer-1
MFS	Metastasis-Free Survival
MMR	Mismatch Repair
MS	Mass-Spectrometry
MSI	Microsatellite Instability
OS	Overall Survival
PBS	Phosphate-Buffered Saline
PPI	Protein-Protein Interaction
RIPA	Radio-Immunoprecipitation Buffer
RNA	Ribonucleic Acid; messenger RNA (mRNA)
RPMI	Roswell Park Memorial Institute
RT-qPCR	Reverse Transcription and quantitative Polymerase Chain Reaction
SILAC	Stable Isotope Labeling by/with Amino acids in Cell Culture
S100A4	S100 protein A4
TCF	T-Cell Factor
Wnt	Wingless/Integrin

Zusammenfassung

Einleitung: Metastasen sind Haupttodesursache des kolorektalen Karzinoms (KRK). Trotz kurativer Therapie entwickeln 50% der nicht-metastasierten KRK-Fälle metachrone Metastasen. Das Sekretom des Primärtumors könnte eine frühe Metastasierung fördern. Metastasis-associated in colon cancer-1 (MACC1) ist ein Treiber der Tumorprogression, aber seine Rolle im Tumorsekretom ist unbekannt. Hier wurde versucht durch Hemmung der MACC1-abhängigen Tumorzellmotilität die metachrone Metastasierung zu verhindern.

Methoden: MACC1-konditioniertes Medium wurde funktionell und in seiner Peptid-Zusammensetzung analysiert. Kaplan-Meier Schätzer bewertete das KRK-Risiko anhand der RNA-Expression von MACC1 und S100A4 in Tumor- und Blutproben. Korrelation von MACC1 und S1000A4 wurde in drei Kohorten von KRK-Tumorproben analysiert. S100A4-Regulation wurde auf Promoter-, RNA- und Proteinebene gemessen. In funktionellen Versuchen wurde S100A4 mittels CRISPR-Cas9 oder mit pharmakologischen Inhibitoren unterdrückt. Proteininteraktionen wurden mit Massen-Spektrometrie und Ko-Immunopräzipitation untersucht. Wundheilungsversuche ermittelten die KRK-Zellmigration unter Gabe von Statinen (Atorvastatin, Fluvastatin, Lovastatin) und Niclosamid. Metastasen wurden modelliert durch Injektion von KRK-Zellen in die Milz von SCID bg/bg Mäusen und unter oraler Gabe von Statinen und Niclosamid monitiert. Mikrometastasen wurden anhand der Last an humaner Satelliten-DNA in tumorfrei erscheinendem Lebergewebe gemessen.

Ergebnisse: MACC1 induzierte KRK-Zellmotilität und S100A4-Sekretion in das Kulturmedium. Hohe MACC1- und S100A4-Expression im Tumorgewebe und in Patientenblut sagte ein schlechtes metastasenfreies und gesamtes Überleben voraus. MACC1 stimulierte die Promoteraktivität, die RNA- und Proteinexpression von S100A4 in Zellkultur und in Tumoren von ApcMin-Mäusen mit ektopischem MACC1. MACC1 steigerte die Motilität nur in KRK-Zellen mit intakter S100A4-Expression, aber nicht unter S100A4-Depletion. Wnt/β-Catenin-Inhibitoren unterdrückten MACC1-abhängige Hochregulation von S100A4. MACC1 interagierte mit β-Catenin und verstärkte dessen Phosphorylierung und Interaktion mit TCF4. Kombinierte Gabe von Statinen und Niclosamid unterdrückte die Motilität von KRK-Zellen. Orale Gabe von Statin und Niclosamid verhinderte nicht das

Auswachsen von Metastasen, aber unterdrückte die Absiedelung von Mikrometastasen in Mauslebern.

Schlussfolgerungen: MACC1 treibt die Krebsprogression durch sekretorisches S100A4, und Überexpression beider Biomarker zeichnet Hochrisiko-KRK aus. MACC1 induziert S100A4 via Wnt/β-Catenin durch Interaktion mit β-Catenin und Stimulation seiner transkriptionellen Aktivität. Die Kombination transkriptioneller Inhibitoren von MACC1 und S100A4 unterdrücken synergistisch das metastatische Potential von KRK-Zellen *in vitro* und *in vivo*. MACC1 und S100A4 kooperieren in der KRK-Progression als Induktor und Effektor innerhalb einer MACC1-β-Catenin-S100A4-Achse der Metastasierung.

Abstract

Introduction: Metastasis is the main cause of colorectal cancer CRC death. Despite curative therapy, 50% of non-metastasized CRC cases will develop metachronous metastasis. Factors secreted by the primary tumor might facilitate early metastasis into distant organs. Metastasis-associated in colon cancer-1 (MACC1) drives cancer progression, yet it's involvement in the tumor secretome is unknown. This project aimed to target MACC1-driven motility of cancer cells to prevent metachronous metastasis.

Methodology: MACC1-conditioned medium was analyzed functionally and for peptide composition. CRC risk assessment employed Kaplan-Meier estimation on MACC1 and S100A4 RNA expression in patient-derived tumor and blood samples. Correlation of MACC1 and S1000A4 expression was analyzed in three cohorts of CRC tumor specimens. Regulation of S100A4 was measured with promoter reporters, and on RNA and protein level. CRISPR-Cas9 knock-out and pharmacological inhibitors were employed to inhibit S100A4 in functional assays. Protein-protein interactions were examined via Mass-spectrometry and Co-Immunoprecipitation. Wound healing experiments assessed CRC cell migration under statins (atorvastatin, fluvastatin or lovastatin) and niclosamide. Metastasis was modelled by injection of CRC cell into the spleen of SCID bg/bg mice and monitored non-invasively under oral administration of statins and niclosamide. Micrometastases were quantified by measuring loads of human satellite DNA in tumor-free appearing liver tissue.

Results: MACC1 induced CRC cell motility and S100A4 secretion into culture medium. High MACC1 and S100A4 expression in tumor tissue and in patient blood predicted dismal metastasis-free and overall survival. MACC1 stimulated promoter activity, RNA, and protein expression of S100A4 in cell culture and in tumors of ApcMin mice with ectopic MACC1. MACC1 enhanced motility only in CRC cells with intact S100A4 expression, but not in S100A4-depleted cells. Wnt/β-catenin signaling inhibitors suppressed S100A4 upregulation by MACC1. MACC1 interacted with β-catenin and enforced its phosphorylation and interaction with TCF4. Combined administration of statins and niclosamide synergistically suppressed the motility of CRC cells. Oral combinations of statin and niclosamide did not prevent metastatic outgrowth but suppressed the abundance of micrometastases in mouse liver.

Conclusion: MACC1 drives cancer progression via secretory S100A4, and combined overexpression of these biomarkers hallmarks high-risk CRC tumors. MACC1 induces S100A4 via Wnt/β-catenin by interacting with β-catenin and stimulating its transcriptional activity. Combination of respective transcriptional inhibitors synergistically suppress the metastatic potential of CRC cells *in vitro* and *in vivo*. MACC1 and S100A4 cooperate in CRC progression as inducer and effector within a druggable MACC1-β-catenin-S100A4 axis of metastasis.

1 Introduction

1.1 Colorectal cancer

1.1.1 Clinical relevance of CRC

Colorectal cancer (CRC) is not only the third-most common cancer but also the second-most common cause of cancer-related deaths worldwide [Fig. 1] [1]. Rather than local progression of the primary tumor, which is usually removed surgically upon diagnosis, it is the development and outgrowth of distant metastases that remains the main culprit of CRC-related deaths. In fact, 20 to 40% of patients are diagnosed with CRC at a stage where distant metastases have developed (stage IV) [2,3]. Recent advantages in surgical and medical oncology allow management of metastatic CRC at relatively good health, yet this disease stage is still regarded incurable and terminal. However, also the CRC patients without detectable metastases at time of diagnosis face risk of up to 30% of distant recurrence within 5 years after initial treatment [4].

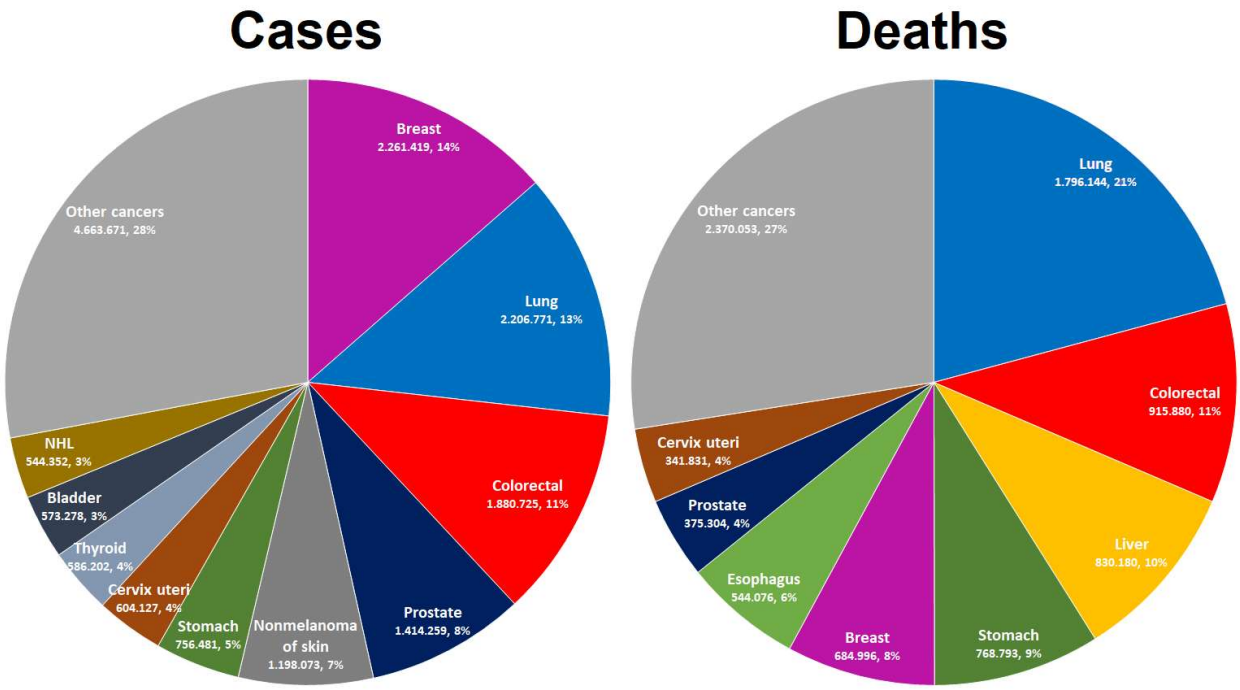

Figure 1: Cancer statistics 2020. Colorectal is the third-most frequent type of cancer, and the second-most frequent cause of cancer deaths (figures taken from Sung et al., 2020).

1.1.2 Current state of the art disease management

In present day CRC diagnosis and therapy, the Union intérnationale contre le cancer (UICC) staging system is the main therapy decision aid in clinical use, which is based solely on histopathological criteria such as tumor size and depth of invasion, presence of regional lymph node metastases, and presence of distant metastases. Recently however, it has been hypothesized that primary tumors of would-be metastatic CRC shed metastatic cells very early during tumor progression [5]. Therefore, conventional staging is insufficient to assign patients to the least toxic and most efficient therapy possible [6,7].

Post-operative treatment of non-metastasized CRC patients is limited to chemotherapy in current guidelines, while antibodies and kinase inhibitors are given exclusively to patients with inoperable metastatic CRC. Conventional chemotherapy is limited by its poor selectivity and extensive toxicity, but in the present scarcity of clinically safe and effective small molecular inhibitors it remains the mainstay of the postoperative management of CRC patients [8,9]. Recently, microsatellite instability (MSI) found in about 15% of CRC cases was shown to qualify patients for adjuvant immunotherapy in post-surgical cancer management [10]. The field of translational oncology is growingly interested in tailoring cancer therapies to the molecular Achilles' heel of a given tumor to prevent recurrence or to halt tumor progression, while complementing or even replacing conventional chemotherapy.

There have been numerous approaches to employ gene expression analysis from the tissue of the primary tumor and blood for risk stratification in order to predict survival and to assign patients to more or less aggressive therapies [11–13]. Moreover, a vast majority of genetic markers merely predict poor survival. Purely prognostic markers are of limited clinical value due to their sole potential to identify whom to treat. In order to inform clinicians of how to treat, true predictive biomarkers are strongly desired so as to tailor adjuvant therapy to the individual molecular vulnerabilities of the tumor and the success of targeted therapies [14–16].

1.1.3 Mechanisms of CRC genesis and progression

It is hypothesized that CRC arises from single transformed cells within the crypts of the colorectal mucosa, to form abnormal crypt foci. These will eventually grow to adenomas, detectable macroscopically in colonoscopy procedures. If left in situ, the benign neoplasia

will progress to a carcinoma-in-situ and adopt features of epithelial-to-mesenchymal transition and invasion into the basal lamina. Further mutations enable recruitment of neoangiogenesis, i.e., the establishment of new blood vessels. In parallel, the ensuing inflammation attracts lymphocytes, that infiltrate the nascent neoplasia. At the constant threat of elimination by the immune cells, progressing tumors maintain an intricate interaction between the tumor-infiltrating lymphocytes (TIL) and the surrounding cancer-associated fibroblasts (CAF). Eventually, the tumor invades blood and lymphatic vessels and sheds circulating tumor cells (CTCs) that colonize regional lymph nodes and distant organs such as the liver [17,18]. It is hypothesized, that metastasis is heavily controlled by the primary tumor. Not only do exosomes shed by tumor cells of certain phenotypes create pre-metastatic niches in the liver, but also prevent implantation by recruiting monocytes to these niches in the case of non-metastatic cancer cells[19,20]. Remarkably, primary tumors can suppress the outgrowth of undetectable metastases by the release of angiopoietin-like 4 (ANGPTL4), and the removal of the tumor triggers the metastatic outgrowth [21].

The vast majority of colon adenomas arise from a hyperactivation of the Wnt/β-catenin signaling cascade due to loss of APC or activating mutations within exon 3 of the CTNNB1 locus, allowing β-catenin to evade physiological inactivation by a destruction complex formed by APC, Axin, casein kinase-1 and GSK-3β [22,23]. Additional mutations in tumor suppressor genes such as p53 and in oncogenes such as K-Ras lead to persistent activation of MAPK/ERK, TGF-β and PI3K-Akt signaling, amongst others, resulting in malignant transformation of CRC, hallmarked by epithelial-mesenchymal transition, increased cell motility and invasion, recruitment of de-novo blood vessel formation (neoangiogenesis), and eventually metastasis. Wnt/β-catenin signaling regulates a multitude of target genes and continues to contribute to all stages of CRC progression, fueling hyperproliferation and adenoma formation as well as less proliferative states such as stemness and senescence [23–25]. During cancer progression, β-catenin experiences stabilization even in absence of physiological Wnt-dependent activation [26–28]. In fact, β-catenin harbors multiple phosphorylation sites, of which the N-terminal serine-33, -37, -45 and threonine-41 mediate swift proteasomal degradation via CK1 and GSK-3β, while residues towards the C-terminus are substrates to various kinases that support β-catenin stability: serine-552 (Akt, PKA) [29], serine-552 and -675 (PKA) [30,31], tyrosine-654 and -670 (MET), serine-663 and -675 (PAK1) [32–35]. Lacking DNA-binding domains, β-catenin relies on recruitment of TCF transcription factors to induce a plethora of target genes, such as Cyclin-D1, MMP7, MET, Oct4 and Nanog [23,36].

1.2 Drug repositioning against cancers

There is an ever-growing body of knowledge about non-oncologic drugs that either reduce cancer incidence (primary prevention) or mitigate cancer morbidity and mortality by either controlling the aggressiveness of localized tumors (secondary prevention) or the development of systemic, metastatic disease (tertiary prevention).
Daily intake of acetylsalicylic acid reduces risk of CRC by 25%, while statins achieve a risk reduction of up to 47% [37–39]. Even more surprisingly, endometrial cancer incidence is reduced by oral contraceptives [40]. While preventing tumorigenesis is of universal interest, combatting the progress of cancer and development of metachronous metastasis is a pressing demand after diagnosis and initial therapy of cancer. Through competitive antagonism of estrogen, the abortifacients mifepristone and metapristone inhibit adhesion and invasion of breast cancer and trophoblastic cells, suggesting that similar molecular pathways underly zygotic implantation in the uterine mucosa and dissemination of CTCs to form metastasis [41,42].
Small molecules are being developed to intervene in signaling cascades deregulated in cancer. In fact, inhibitors of receptor tyrosine kinases (RTKs) have been a paradigm-shifting supplement to hitherto chemotherapy-based tumor therapy. However, blocking growth receptor signaling is toxic also to normal organ tissue and further burdened by the capability of tumors to develop resistance to RTK-inhibitors. An ideal drug would target a molecular mechanism that is exclusive to the malignant tissue while being orally bioavailable. Therefore, drug discovery involves screens of large compound libraries for transcriptional inhibitors of cancer-specific genes, followed by elimination of cytotoxic candidates and establishing dosages effective *in vivo*. Screening clinically approved drugs for novel transcriptional inhibitor circumvents the necessity of preclinical safety testing and *de novo* drug approval, as antitumoral efficacy can be tested in clinical trials immediately [43].

1.3 Mechanistic and predictive biomarkers

Our group has identified two gene products, MACC1 and S100A4, that independently (1) predict poor metastasis-free survival, (2) evidentially promote distant metastasis by induction of cell motility *in vitro* and metastasis *in vivo*, and (3) have been successfully targeted pharmacologically by repositioned FDA-approved drugs [44–49]. Given their

high specificity to predict distant metastasis and the availability of effective small molecular inhibitors, we set out to (1) study the effectiveness of a hypothesis-driven, gene-based risk stratification of CRC patients, (2) to demonstrate how a MACC1-Wnt/β-catenin-S100A4 axis drives cell motility and metastasis in CRC and (3) to gauge synergistic effects of combinatorial inhibition in preventing CRC cell motility and metastasis.

MACC1 has been discovered in CRC of stage I-III as being highly expressed in tumors which yielded metachronous metastases, while being lowly expressed in non-metastasizing CRC. In fact, upregulation of MACC1 was found already in late adenomas, indicating that a MACC1-driven metastatic career is laid out even before the tumor presents hallmarks of malignant progression [46,50]. The prognostic biomarker capabilities of MACC1 has since been confirmed in over 22 (solid) cancer entities in individual reports and 5 meta-analyses (extensively reviewed in [49]). Of note, the absence of MACC1 in mismatch-repair (MMR) proficient CRC identified patients with a low risk of metachronous metastases, comparable to the favorable outcome of MSI CRC [51]. This finding promises value as a predictive biomarker in that absent MACC1 expression in MSS-CRC could warrant omitting adjuvant chemotherapy. While it has been established that MACC1 is a versatile inducer of cancer progression and metastasis, there is not much known about molecular details of its mechanism. MACC1 is a 852 amino acid containing protein, and *in silico* predictions have suggested the existence of several conserved structural domains frequently implemented in protein-protein interactions, such as a proline-rich motif (PRM), ZU5, UPA, Src homologue 3 (SH3) and Death domains (DD) [52]. In previous works we found that MACC1 itself occupies promoter regions of MET, SPON2 and Nanog [46,53,54]. In the absence of DNA-binding motifs within the MACC1 gene product, it must be assumed that MACC1 mediates transcription by recruiting proper transcription factors to these promoter regions.

S100A4, a target gene of Wnt/β-catenin signaling, is a versatile mediator of cancer cell migration, invasion and metastasis [44,55]. Intracellular as well as extracellular mechanisms of cancer metastasis by S100A4 have been described. S100A4 modulates the turnover of non-muscle-myosin-II, the contractible component of stress fibers that hallmark migrating cells [56,57]. Extracellularly, soluble S100A4 triggers CRC motility through binding to the receptor of advanced-glycosylation-end-products (RAGE), which in turn feeds into MEK/ERK signaling [58]. S100A4 itself potently induces Wnt/β-catenin

signaling by suppressing the transcription of DKK1, a physiological inhibitor of Wnt activation [59]. Interactions between the tumor and the underlying stroma are crucial in the progression of cancer. Secretion of prometastatic factors such as S100A4 leads to T-cell recruitment and reprogramming of fibroblasts, which aid in tumor invasion and metastasis [60,61]. Furthermore, solid tumors have been shown to secrete proteins and shed exosomes, i.e., microvesicles containing RNA, DNA and proteins, into the blood stream, which effectively contribute to the formation of pre-metastatic niches in distant organs such as the liver. Kupffer cells within the liver sinusoids internalize cancer-derived exosomes and initiate secretion of TGF-β and fibronectin, leading to microenvironment fibrosis and recruitment of macrophages from the bone marrow. These niches facilitate the engraftment of circulating tumor cells (CTCs) [62–64].

Both S100A4 and MACC1 are stage-independent prognostic biomarkers of metachronous metastases in CRC and other malignancies [44,46,49]. We previously demonstrated that combined elevation of MACC1 and S100A4 transcripts reads in liquid biopsies in CRC, gastric and ovary cancer best identifies patients at high risk for dismal cancer-specific and overall survival [65–67].

1.4 Aims and hypotheses

Here we set out to identify secreted factors that exert MACC1-dependent cancer cell migration by functional experiments and proteomic analyses.

Thereafter, assays in preclinical and clinical samples and expression data were performed to scrutinize the relevance of such associations in the real world.

Subsequently, we probed the mechanism by which MACC1 induces the transcription of factors exerting cancer cell migration.

Finally, we attempted to explore whether combining already established transcriptional inhibitors to achieve antimetastatic efficacy is superior to use of single repositioned drugs.

2 Methodology

2.1 Cell culture and manipulation of gene expression

CRC cell lines employed in this study are listed in Table 1. A clone with ectopic overexpression of MACC1 (SW480/MACC1) was obtained by lipofection of a recombinant DNA vector encoding the human CDS of MACC1 driven by a CMV promoter (pcDNA3.1-MACC1-V5), followed by selection of stable clones with geneticin. Cells transfected with an identical vector without insertion of the MACC1 CDS served as a negative control (SW480/vector). SW620, a cell line with high levels of MACC1 was depleted of MACC1 via lentiviral RNA-interference (SW620/shMACC1), or a non-functional construct as a negative control (SW620/shCtrl). All cell lines are listed in **Table *1***.

Table 1: Cell lines used in the study

Cell line	Entity	Origin	ATCC	MMR	APC	CTNNB1
SW480	**CRC**	**Primary tumor**	**CCL-228**	**Stable**	**wt/mut**	**wt/wt**
SW480/vector			Transfected with CMV-V5			
SW480/MACC1			Transfected with CMV-MACC1-V5			
SW620	**CRC**	**Metastasis**	**CCL-227**	**Stable**	**wt/mut**	**wt/wt**
SW620/Cas9-ev			Transfected with Cas9 and no sgRNA			
SW620/MACC1-KO			Transfected with Cas9 and MACC1 sgRNA			
SW620/shCtrl			Transduced with pU6-shScrambled-RFP			
SW620/shMACC1			Transduced with pU6-shMACC1-RFP			
HCT116	**CRC**	**Primary tumor**	**CCL-247**	**Instable**	**wt/wt**	**wt/delS45**
HCT116/vector			Transduced with CMV-GFP			
HCT116/MACC1			Transduced with CMV-MACC1-GFP			
HCT116/Cas9-ev			Transfected with Cas9 and no sgRNA			
HCT116/S100A4-KO			Transfected with Cas9 and S100A4 sgRNA			
HCT116/CMV-Luc			Transduced with CMV-driven Luciferase			
HT-29	**CRC**	**Primary tumor**	**HTB-38**	**Stable**	**wt/mut**	**wt/wt**
LS174T	**CRC**	**Primary tumor**	**CL-188**	**Instable**	**wt/wt**	**wt/S45F**

(author's own representation)

In HCT116, MACC1-GFP was overexpressed by lentiviral transduction, while GFP served as empty vector control. GFP-positive (i.e. fluorescent in the GFP channel) cells were collected for further cultivation using a LSR Fortessa™ FACS device (BD Bioscience).

Table 2: sgRNA and knockout-sequencing primer

Oligonucleotide		Sequence
sgMACC1	forward	5' - CAC ATC AAG TTC ATC ACC GGA GG - 3'
sgS100A4	forward	5' - TTT GCC CGA GTA CTT GTG GAT GG - 3'
MACC1 sequencing	forward	5' - GTA ACT CAC AGT GCC ACC TT - 3'
	reverse	5' - AGC CAC TCT AAG TCG TGT AGT - 3'
S100A4 sequencing	forward	5' - GAA TCT CCA GAG CTT GCG C - 3'
	reverse	5' - AGC CAC CCC ACT GAT AGA TG - 3'

(author's own representation)

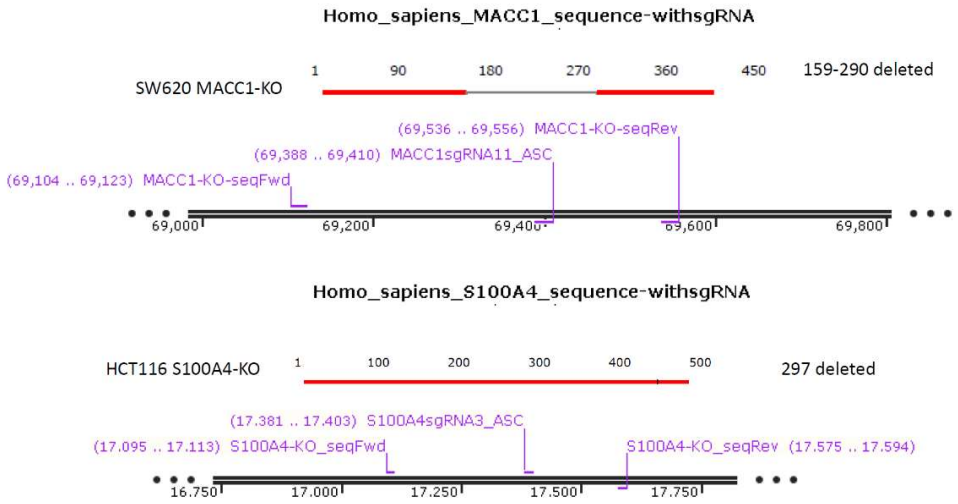

Figure 2: CRISPR-Cas9 mediated knockout of MACC1 and S100A4. The SW620 MACC1-KO clone used for all studies showed a major deletion of 141 bp, and the HCT116 S100A4-KO clone used for cell motility assays showed a single nucleotide deletion.

MACC1 and S100A4 were depleted from SW620 and HCT116 cells using the CRISPR-Cas9 system. A Cas9-puromycin- and a Cas9-GFP-sgRNA-plasmid specific for either MACC1 or S100A4 (Applied StemCell Inc., Milpitas CA, USA) were co-lipofected into SW620 and HCT116 cells to inflict double strand breaks, provoking error-prone non-homologous end joining within the respective gene locus. Upon puromycin selection for 48 h, single cell clones were raised and tested for knockout of either MACC1 (SW620/MACC1-KO) or S100A4 (HCT116/S100A4-KO) by Western blot. A mixed population of SW620 or HCT116 lipofected with Cas9-puromycin alone served as empty vector

(Cas9-ev) control. Knock-out was confirmed by Western blot and by Sanger sequencing of the genomic locus with primers reported in **Table *2***.

2.2 Compositional and functional analysis of the MACC1-specific secretome

MACC1-conditioned medium was obtained from SW620 wildtype, SW480/MACC1 and SW480/vector cells. Cells were seeded at 50% confluence and incubated at 37°C, 5% atmospheric CO_2 and 100% relative humidity. After 48 h medium was collected, cleared of floating cells and subcellular particles by centrifugation at 500 g for 10 min.
The composition of cell media from SW480/MACC1 and SW480/vector cells were comparatively analyzed employing SILAC. Cells were grown in DMEM SILAC media containing heavy lysine and arginine ($^{15}N_2$ $^{13}C_6$ Lys, $^{15}N_4$ $^{13}C_6$ Arg). Secreted proteins collected after 24 h were concentrated using a 30 kDa molecular filter cartridge (Millipore) to be analyzed in Mass-Spectrometry (section 2.6).
To assess functional signaling properties of MACC1-conditioned medium, the CRC cell lines SW480, HCT116, HT-29, LS14T, SW620-shMACC1 and SW620-shCtrl were seeded and grown to 50% confluency. At 70% confluency, half of the medium was exchanged with MACC1-conditioned medium from SW480/MACC1 or SW480/vector cells, and additionally from SW620 wildtype cells.

2.3 RNA expression analysis

RNA transcripts were quantified in RT-qPCR assays. Briefly, RNA of 2×10^5 cells treated as indicated for 24 h was isolated with the Universal RNA purification kit (Roboklon). After quantification of RNA yield (Nanodrop), 50 ng of RNA was reverse transcribed with random hexamers in a reaction mix (10 mM $MgCl_2$, 1 × RT Buffer, 250 µM pooled dNTPs, 1 U RNAse inhibitor, 2.5 U Moloney murine leukemia virus reverse transcriptase) at 30°C for 10 min, 50°C for 40 min and 99°C for 5 min, followed by cooling at 4°C. PCR was carried out on a LightCycler 480 II system at 95°C for 2 min followed by 40 cycles of 95°C for 5 s and 60°C for 20 s using exon-spanning primers. Primer sequences are listed in **Table *3***.

2.4 Protein expression analysis

PBS-washed cells were lysed with RIPA buffer supplemented with cOmplete protease inhibitor cocktail and phosStop phosphatase inhibitor (Roche), when indicated. For fractionation of cytoplasmic and nuclear protein, cell monolayers were scraped off with NE-PER buffer and processed further according to manufacturer's protocol. After 30 min of lysis on ice and centrifugation at 12,000 g for 10 min at 4°C, protein concentration was quantified with the Pierce BCA system (Thermo Fisher) and spectrometry using Magellan v7 software (Tecan). 2 µg (for total protein analysis) or 30 µg (for phospho-protein analysis) of protein were boiled with 0.1 M DTT (Sigma-Aldrich) and 1 × LDS loading buffer (NuPage). Cellular proteins were resolved in SDS page and transferred onto PVDF membranes (BioRad), followed by blocking with 5% w/v skim milk powder in TBS-T for 1 h. Proteins of interest were detected by probing membranes with specific primary antibodies at 4°C overnight and secondary HRP-conjugated antibodies for 1 h at room temperature, and subsequent visualization with WesternBright and exposure of Fuji medical X-ray film SuperRX. X-ray films exposed to chemoluminesence from Western blot experiments were digitally scanned. Densitometric measurements in Western blots were performed by band analysis routines in AlphaView 3.4.0 software (ProteinSimple, Minneapolis MN, USA). For supernatant WB, 1 × 10^6 cells were seeded into a 6-well plate, and complete medium was replaced with 1.5 ml serum-free culture medium. After 24 h, the cell culture supernatant was carefully collected, and floating cells were eliminated by centrifugation at 500 g for 5 min. a portion of clarified cell culture medium was boiled with 0.1 M DTT and 1 × LDS loading buffer. Meanwhile, cells from the same well were counted to load proportional medium samples into SDS page. To study the post-translational phosphorylation of β-catenin, cells were seeded at 50% confluence. On the following day cells were synchronized by starvation for 18 h. The cell monolayers were washed with PBS on ice and immediately lysed on the culture dish with RIPA buffer. The fraction of β-catenin phosphorylated at Ser-552 relative to total β-catenin was assessed by Western blot. Antibodies employed in Western blot experiments are listed in **Table *4***, buffers are described in **Table *5***.

2.5 Protein-protein interaction analysis

Co-Immunoprecipitation (Co-IP) experiments were carried out from cell lysates and in cell-free mixtures of human recombinant proteins. Cells were grown to ~80% confluence

in 10 cm dishes, washed twice with ice-cold PBS and scraped off with 1 ml Co-IP buffer to obtain cell lysates. Aliquots of 500 µg cellular protein were topped up to 1 ml with Co-IP buffer. 200 µg human recombinant MACC1 (TP324774) and β-catenin (TP308947) were dissolved in 1 ml of Co-IP buffer. Each 1 ml aliquot was incubated with 1 µg specific antibody (MACC1: HPA020081, β-catenin: 610154) or non-specific immunoglobulin G under constant agitation overnight at 4°C on a test tube rotator to form immune complexes of antibodies and the respective protein-of-interest. Protein-G coated agarose beads (AlphaBiosciences) were added to absorb immune complexes during 4h on the test tube rotator, followed by centrifugation for 45 mins at 2,500 g to precipitate immune complexes. The agarose bead pellets were washed at least 4 times with lysis buffer (resuspension, centrifugation for 5 mins at 2,500 g) and protein precipitations were eluted with LDS buffer at 95°C for 10 min for SDS page. In Western blot experiments β-catenin was detected in MACC1-specific and non-specific immunoprecipitations, and MACC1 was detected in β-catenin-specific and non-specific precipitations. To identify the MACC1-interactome, MACC1-specific immunoprecipitations were processed as described in 2.6.

2.6 Mass-Spectrometry

Proteins were digested according to Kanashova[68], purified and measured in a Q-Exactive plus mass spectrometer (Thermo-Fisher) coupled to a Proxeon nano-LC system (Thermo-Fisher). MaxQuant software suite (version 1.5.2.8)[69] was used to interprete the data, employing the human UniProt database (downloaded 06.08.2014)[70] with carbamylation of cysteins set as a fixed modification and oxidation of methionines and N-terminal protein acetylation set as variable modifications[70,71]. MS data were statistically analyzed with R-software[72].

2.7 Immunohistochemistry

Protein expression in organ tissue was assessed using immunohistochemistry (IHC). Frozen human tumor tissues were cryosectioned at a thickness of 5 mm, draped on glass slips, thawed, and fixed with ethanol. Formalin-fixed and paraffin-embedded mouse tumors were cut at ambient temperature and draped on glass slips, followed by deparaffinization and rehydration with xylol and ethanol. Primary antibodies against MACC1 (HPA020081, 1:100 in 2% BSA/PBS), S100A4 (A5114, 1:400 in 2% BSA/PBS) and human cytokeratin 19 (TA336845, 1:200 in 2% BSA/PBS) were incubated overnight at 4°C.

After washing with PBS-T, a Rabbit-IgG-specific antibody (Horseradish-conjugated, 1:1000 in 2% BSA/PBS) was incubated on the tissue slides for 1 h at ambient temperature. After washing with PBS-T and PBS, secondary antibodies were detected with a biotin-based ABC kit. Cell nuclei were counterstained with hematoxylin. Slides incubated without any primary antibody served as a control for unspecific staining. Microscopic images were taken at 20x and 63x magnification using the Axiovision 4.2 software (Zeiss).

2.8 CRC cohorts and biomarker tests

In a cohort of primary CRC tumors (UICC Stages I-III, n = 60) and in another cohort of plasma samples of newly diagnosed CRC (n = 49) RNA was purified from cryopreserved tumor tissue or patient blood drawn before surgery, respectively, and the amount of MACC1 and S100A4 messenger RNA (mRNA) was quantified by RT-qPCR. To predict patient survival from continuous mRNA expression values, binary classifiers for MACC1 and S100A4 were established by receiver operating characteristic (ROC) curve against the endpoints “death” and “distant metastasis” to be used in the prognosis of Overall Survival (OS) and Metastasis-Free Survival (MFS). All cases were sorted into the four subgroups “MACC1 and S100A4 low”, MACC1 low and S100A4 high”, “MACC1 high and S100A4 low”, “MACC1 and S100A4 high”. Subsequently, patient survival was compared using log rank rest. All patients gave their written informed consent to take part in our tumor biobank. We obtained expression data of CRC tumor microarrays from the public functional genomics data repository Gene Expression Omnibus (www.ncbi.nlm.nih.gov/geo). Two RNA expression datasets comprising 98 CRC cases (GDS4393 and GDS4718)[73,74] and an additional dataset of 117 CRC tissue sample from the OncoTrack consortium[75] dataset were obtained. RNA expression values of MACC1 and S100A4 were normalized to G6PDH and analyzed for their correlation using Spearman statistics. Spearman coefficients were calculated and plotted along with scatter plots of MACC1 and S100A4 expression values.

2.9 Reporter assays of promoter activity and pathway signaling activity

Wnt/β-catenin and S100A4-promoter activity was examined in firefly luciferase-based assays. Plasmids encoding a CDS of firefly luciferase under the transcriptional control of a series of TCF4 binding sites or the genomic sequence of the S100A4 promoter were lipofected into CRC cells (500 ng per 250,000 cells)[44]. A plasmid encoding a CDS of

renilla luciferase under the transcriptional control of a constitutively active CMV promoter served as a transfection control (25 ng per 250,000 cells). After incubation for 48 h, the cells were lysed and the chemiluminescence (indicative of abundance of firefly and renilla luciferase) was measured with proprietary substrates (Promega) in a microplate reader (Tecan), according to the manufacturer's protocol.

2.10 Application of small molecular inhibitors *in vitro* and *in vivo*

The small molecule inhibitors FH535, LF3 (Selleckchem LLC, Houston TX, USA) and niclosamide (Sigma-Aldrich St. Louis MO, USA) were used to probe Wnt/β-catenin signaling in the context of S100A4 regulation [45,76,77]. Prochlorpromazine (Selleckchem LLC, Houston TX, USA) is an allosteric inhibitor of S100A4[78]. Atorvastatin, fluvastatin and lovastatin (Selleckchem) were employed as transcriptional inhibitors of MACC1[47]. For application in cell culture compounds were dissolved in DMSO to obtain a 1000x stock solution. Stock solutions were then diluted in cell culture medium at a ratio of 1:1000. Pure DMSO in culture medium was used as negative control. For application in animal experiments compounds were dissolved in 10% Kolliphor EL in 0.9% NaCl, while identical, compound-free formulations served as control treatment.

2.11 CRC cell motility *in vitro* and metastasis *in vivo.*

CRC cell motility was assessed *in vitro* using Boyden chamber and wound healing assays. The Boyden chamber setup tests chemotaxis and transwell migration of cells towards a positive gradient of FBS through a membrane with pores of 8 µm in diameter, while the wound healing assay assesses the cells' capacity to repopulate a cell-free area of the dish after mechanic abrasion of a portion of the cell monolayer by lateral movement. For transwell migration assays, cells were seeded at 50% confluence to settle overnight. The next day, the medium was changed to implement conditioning by specific media or drug treatment for another 24 to 48 h. After this period, the complete medium on the subconfluent cell monolayers was replaced with pure, FBS-free culture medium, to starve and synchronize the cells for 8 h. 24-well and 96-well setups were employed throughout the study. In either case, standard 24-well or 96-well cell culture plates were prefilled with complete medium (DMEM or RPMI, supplemented with 10% v/v FBS). Size-appropriate transwell inserts (Corning) were placed into the wells and left for about 10 min for com-

plete removal of air entrapments. Meanwhile, the cells were recovered by enzymatic detachment with trypsin for 2-3 min and were carefully resuspended under gentle pipetting to break up cell clusters. In 24-well setups, 2.5×10^5 cells were pipetted onto the transwell insert membrane, while in 96-well setups, 5×10^4 cells were inserted, with a final concentration of about 700 cells per µl. After 20 h, the number of cells that have migrated to the bottom face of the transwell insert membrane (towards the FBS-containing medium in the bottom well) was assessed by fixation, nuclear staining with DAPI (which intercalates in DNA to fluoresce under excitation with UV light at 405 nm wavelength) and counting under a microscope. Alternatively, and in 96-well plate format, medium in the bottom well was removed and replaced with trypsin to detach cells present at the lower face of the membrane. After 5 min, the cell-trypsin suspensions were transferred into 200 µl reaction tubes, and the cells were collected by centrifugation at 500 g for 5 min. Following removal of the supernatant, the cell pellets were lysed with CellTiter Glo®, and transferred by pipetting to an opaque, white-bottom plate. The lysing reagent produces a fluorescent light signal with an intensity proportional to the amount of ATP present in the entirety of cells in the pellet, thus providing a readout of viable cells collected.

Synergisms of statins and niclosamide in suppressing cell motility *in vitro* were examined in wound healing assays. 1×10^5 HCT116 cells per well were seeded into 96-well plates, to reach confluence after 8 h. Subsequently, cell monolayers were wounded by shaving off cells using a proprietary WoundMaker device (EssenBioScience), followed by thorough removal of floating cells by washing with PBS, and replenishing of culture medium with the respective treatment. Niclosamide was applied in concentrations of 0.25, 0.5 and 1 µM and the statins atorvastatin, fluvastatin and lovastatin were applied in concentrations of 1.25, 2.5 and 5 µM. Wound closure was monitored for 7 days in an IncuCyte system. Using IncuCyte Zoom software, the repopulation of wounds relative to their size at zero minutes was computationally measured.

Splenohepatic metastasis of HCT116 cells served as an *in vivo* model of CRC metastasis. 1×10^6 HCT116/CMV-Luc cells, constitutively expressing luciferase, were xenografted by laparotomic injection into the spleen of immunodeficient SCID bg/bg mice (Charles River; Wilmington MA, USA). Niclosamide and either atorvastatin, fluvastatin or lovastatin, or combinations thereof, were administered by daily oral gavage. The dosage of niclosamide was 250 mg/day, to match human equivalent doses of 1.5 g per patient per day, while all statins were given at 3.25 mg/kg, equivalent to 20 mg per patient per day[79]. Following CRC cell xenografting, SCID mice were caged (n = 60, 10 animals per

group). Luciferin (VivoGlo®) was administered by tail-vein injection to evoke bioluminescence in the xenografted HCT116/CMV-Luc cells, which allowed non-invasive measurement of the size of any tumors present in the mice in an imaging chamber (Berthold Technologies; done at EPO GmbH, Berlin-Buch). Tumor and metastasis bioluminescence data from *in vivo* studies were processed using ImageJ (NIH, Bethesda MD, USA).
Mice were euthanized after 24 days or as soon as ethical endpoints (signs of significant suffering, immobility, reduced feeding and/or drinking, tumor burden, enlarged abdomen) were observed. Mice were immediately dissected to retrieve the spleen (site of xenotransplant injection) and liver (site of distant metastasis), which were shock frozen in liquid nitrogen. Cryosections were obtained for isolation of genomic DNA and mRNA, and for immunohistochemistry.
To assess abundance of micrometastases, tumor-free appearing mouse liver tissue was collected at a distance of at least 2 mm of any visible tumor metastasis and lysed to obtain genomic DNA. Human satellite DNA was quantified in qPCR experiments using specific primers (Table 3) on identical amounts of mouse liver DNA.

2.12 Computational evaluation of data and statistical analysis.

Numeric results shown means ± SEM of 3 independent experiments, test for significance with ANOVA and Tukey correction for multiple testing. All graphs show means ± SEM of 3 independent experiments, test for significance with Student's t-test. When applicable, ANOVA and Dunnett's correction for multiple testing were applied to establish levels of significance. Statistical software products used were SPSS 28.0 (IBM, Armonk NY, USA) and GraphPad Prism v8.0 and v9.0 (GraphPad, San Diego CA, USA). Drug synergisms were quantified using the Combenefit software v2.02, which employs a Loewe interaction analysis [80].

Devices used throughout at the study are listed in **Table *6*: Devices used in the experimentsTable *6***, while reagents are listed in **Table *7***.

Table 3: Primers

Oligonucleotide		Sequence
hMACC1	forward	5' - TTC TTT TGA TTC CTC CGG TG - 3'
	reverse	5' - TTC TTT TGA TTC CTC CGG TG - 3'
hS100A4	forward	5' - CTC AGC GCT TCT TCT TTC - 3'
	reverse	5' - GGG TCA GCA GCT CCT TTA - 3'
mS100a4	forward	5' - TGA GCA ACT TGG ACA GCA ACA - 3'
	reverse	5' - CTT CTT CCG GGG CTC CTT ATC - 3'
mGapdh	forward	5' - AAC CTG CCA AGT ATG ATG AC - 3'
	reverse	5' - CTG TTG CTG TAG CCG TAT T - 3'
hRP-II	forward	5' - GAA GAT GGT GAT GGG ATT TC - 3'
	reverse	5' - GAA GGT GAA GGT CGG AGT - 3'
hCyclin-D1	forward	5' - CTG TTT GGC GTT TCC CAG AGT CAT C - 3'
	reverse	5' - AGC CTC CTC CTC ACA CCT CCT C - 3'
hMMP7	forward	5' - TCG GAG GAG ATG CTC ACT TCG A - 3'
	reverse	5' - GGA TCA GAG GAA TGT CCC ATA CC - 3'
hCTNNB1	forward	5' - GTG CTA TCT GTC TGC TCT AGT A - 3'
	reverse	5' - CTT CCT GTT TAG TTG CAG CAT C - 3'
human satellite DNA	forward	5' - GGG ATA ATT TCA GCT GAC TAA ACA G - 3'
	reverse	5' - AAA CGT CCA CTT GCA GAT TCT AG - 3'

(author's own representation)

Table 4: Antibodies, recombinant proteins

Specificity	Host; Dilution in Western blot	Manufacturer
Primary antibodies		
Anti-MACC1 (HPA020081)	Rabbit, polyclonal IgG; 1:10,000	Sigma-Aldrich (St. Louis MO, USA)
Anti-S100A4 (A5114)	Rabbit, polyclonal IgG; 1:1,000	DAKO (Carpinteria CA, USA)
Anti-β-catenin (610154)	Mouse, monoclonal IgG; 1:20,000	Thermo Fisher Scientific (Waltham MA, USA)
Anti-pSer552-β-catenin (#9566)	Rabbit, polyclonal IgG; 1:2,000	Cell Signaling Technology (Cambridge, UK)
Anti-TCF7L (ab76151)	Rabbit, polyclonal IgG; 1:1,000	Abcam (Cambridge, UK)
Anti-β-actin (clone AC-15)	Mouse, monoclonal IgG; 1:20,000	Thermo Fisher Scientific (Waltham MA, USA)
Anti-human CK19 (TA336845)	Rabbit, polyclonal IgG; 1:400 (IHC only)	OriGene (Rockville MD, USA)
Secondary antibodies		
Anti-Rabbit-HRP (W401B)	HRP-conjugated antibody; 1:10,000	Promega Corporations (Madison WI, USA)
Anti-Mouse-IgG-HRP (HP-03)	HRP-conjugated antibody; 1:30,000	Thermo Fisher Scientific (Waltham MA, USA)
Human recombinant proteins		
MACC1 (TP324774)	cell-free interaction studies	Origene (Herford, Germany)
β-catenin (TP308947)	cell-free interaction studies	Origene (Herford, Germany)

(author's own representation)

Table 5: Buffers used in wet-lab experiments

Buffer Name	Ingredients
1 × PBS(-T)	155 mM NaCl, 0.2 g, 1 mM KH_2PO_4, 3 mM Na_2HPO_4 (, Tween® 20)
1 × RIPA Buffer	50 mM Tris-HCl pH 7.5, 150 mM NaCl, 1% Nonidet P-40, 0.5 % sodium deoxycholate, Protease inhibitor
IP-lysis Buffer	20 mM Tris-HCl pH 7.5, 150 mM NaCl, 0.1% NP40, 1 mM EDTA, 1% Triton X, 1 tbl./10 ml protease and phosphatase inhibitors
1 × Transfer Buffer	25 mM Tris-HCl pH 7.5, 200 mM Glycine, 0.1 % SDS, 20 % Methanol
1 × TBS-T	50 mM Tris-HCl pH 7.5, 150 mM NaCl, 0.1%, Tween®20
Skim milk Blocking Buffer	1 × TBS-T in 5 % skim milk
BSA Blocking Buffer	1 × TBS-T in 5 % BSA
Mild Stripping Buffer	15 g/L Glycine, 1 g/L SDS, 10 ml Tween® 20, pH2.2

(author's own representation)

Table 6: Devices used in the experiments

Device	Purpose	Manufacturer
Cell culture incubator	Cell incubation at 37°C, 5% CO2, 5% humidity	Heraeus Instruments (Hanau, Germany)
CountessTM cell counter	Cell counting in cell-medium suspension	Invitrogen (Karlsruhe, Germany)
Transwell inserts, 8 mm pores	Assessment of cell migration through 8 mm pores	Corning Inc. (Corning NY, USA)
LSR Fortessa™ FACS device	Sorting of fluorescent cells	BD Bioscience (San Jose CA, USA)
Cooling Centrifuge 5804 R	Centrifugation at ambient and 4°C temperature	Eppendorf (Hamburg, Germany)
NanoDrop 1000	Quantification of DNA and RNA concentration	Peqlab (Erlangen, Germany)
Light Cycler® 480 II	Reverse transcription and quantitative PCR	Roche Diagnostic (Mannheim, Germany)
Infinite F200 PRO	Spectrometry and chemoluminescence assays	Tecan (Männedorf, Switzerland)
Belly Dancer	Mild agitation of Western blot membranes	Stovall Life Science (Greensboro, USA)
Transblot® TurboTM	Transfer from SDS page gel to PVDF membranes	BioRad Laboratories Inc. (Singapore)
SuperRX Medical X-Ray Film	Recording chemiluminescence in Western blot	Fujifilm (Tokyo, Japan)
Vortex Genie 2TM	Harsh agitation of reaction tubes	Scientific Industries, Inc. (New York, USA)
IncuCyte® ZOOM	Automated wound healing monitoring	EssenBioScience (Ann Arbor MI, USA)
NightOWL LB 981 system	*In vivo* bioluminescence measurements	Berthold Technologies (Bad Wildbad, Germany).
Cryomicrotome	Tumor sections of 3-5 mm	Thermo Scientific (Waltham MA, USA).
Zeiss Axioplan 2	Microscope	Zeiss (Oberkochen, Germany)
Axiocam HRc camera	Digital microscopic camera	Zeiss (Oberkochen, Germany)
Amicon Ultra-2 Centrifugal Filter	Concentration of proteins of up to 30 kDa size	Sigma-Aldrich (St. Louis MO, USA)
Q-Exactive plus	Mass spectrometer	Thermo Scientific (Waltham MA, USA).
Proxeon nano-LC system	Sample feed into Mass spectrometer	Thermo Scientific (Waltham MA, USA).

(author's own representation)

Table 7: Reagents used in cell culture, animal experiments and wet-lab analyses

Reagent	Manufacturer
DMEM medium; RPMI-1640 medium	Gibco - Thermo Fisher Scientific (Waltham MA, USA)
Fetal calf serum (FBS)	PAA Laboratories (Cölbe, Germany)
Trypsin-EDTA	Thermo Fisher Scientific (Waltham MA, USA)
Trypan-Blue	Invitrogen (Karlsruhe, Germany)
Opti-MEM medium	PAA Laboratories (Cölbe, Germany)
TransIT 2020	Invitrogen (Karlsruhe, Germany)
Geneticin (G418)	Sigma-Aldrich (St. Louis MO, USA)
Puromycin	Thermo Fisher Scientific (Waltham MA, USA)
Dimethylsulfoxid (DMSO)	Carl Roth (Karlsruhe, Germany)
MycoAlert™ Mycoplasma Detection Kit	Lonza (Basel, Switzerland)
Dual-Luciferase® Reporter Assay, CellTiter Glo®	Promega (Madison WI, USA)
NE-PER™ Nuclear and Cytoplasmic Extraction Reagents	Thermo Fisher Scientific (Waltham MA, USA)
DNA Extraction and Purification Kit	Qiagen (Hilden, Germany)
Universal RNA Purification Kit	Roboklon (Berlin, Germany)
$MgCl_2$ (25 mM)	Applied Biosystems (Foster City, USA)
10 × PCR-buffer II	Invitrogen (Karlsruhe, Germany)
Desoxyribonucleotide (dNTPs) mix	Biozym (Hessisch Oldendorf, Germany)
RNase Inhibitor	Biozym (Hessisch Oldendorf, Germany)
Random Hexamers	Biozym (Hessisch Oldendorf, Germany)
MuLV Reverse Transcriptase	Biozym (Hessisch Oldendorf, Germany)
Ethanol, Isopropanol, Methanol	Carl Roth (Karlsruhe, Germany)
GoTaq® qPCR Master Mix	Promega (Madison, USA)
PierceTM BCA Protein Assay Kit	Thermo Fisher Scientific (Waltham MA, USA)
Bovine Serum Albumin (BSA)	Standard Pierce (Rockford, USA)
NuPAGE® LDS Sample Buffer	Invitrogen (Karlsruhe, Germany)
Dithiothreitol (DTT)	Sigma-Aldrich (St. Louis MO, USA)
NuPAGE® 10% Bis-Tris Gel	Invitrogen (Karlsruhe, Germany)
SpectraTM Multicolor Broad Range Protein Ladder	Fermentas (Sankt Leon-Rot, Germany)
Ponceau S solution	Sigma-Aldrich (St. Louis MO, USA)
LDS Buffer	Thermo Fisher Scientific (Waltham MA, USA)
WesternBright™ ECL	Advansta (San Jose CA, USA)
Protein G-agarose beads	Alpha Diagnostic International Inc. (San Antonio, Texas)
Skim milk and Bovine Serum Albumin (BSA) powder	Sigma-Aldrich (St. Louis MO, USA)
cOmplete protease inhibitor cocktail	Roche Diagnostics (Risch, Switzerland)
PhosStop® phosphatase inhibitors	Roche Diagnostics (Risch, Switzerland)
Polysorbate 20 (Tween® 20)	Carl Roth (Karlsruhe, Germany)
VivoGlo®	Promega (Madison WI, USA)
Kolliphor® EL	Sigma-Aldrich (St. Louis MO, USA)
ABC Peroxidase Standard Staining Kit	Thermo Fisher Scientific (Waltham MA, USA)
Hematoxylin	Carl Roth (Karlsruhe, Germany)

(author's own representation)

3 Results

3.1 MACC overexpression confers a promigratory secretome via S100A4.

To test whether the secretome of CRC cells expressing MACC1 induces cell motility in a paracrine fashion, culture medium of two SW480/MACC1 clones and SW620 cells was obtained, cleared of floating cells and debris by centrifugation. Cell lines with low endogenous expression levels of MACC1 (SW480, HCT116, HT-29 and LS14T) were cultured to be conditioned by these culture media for 24 or 48 h, followed by assessment of transwell migration in Boyden chamber experiments [Fig. 3A]. SW480 cells demonstrated increased motility after 24 and 48 h of medium treatment [Fig. 3B].

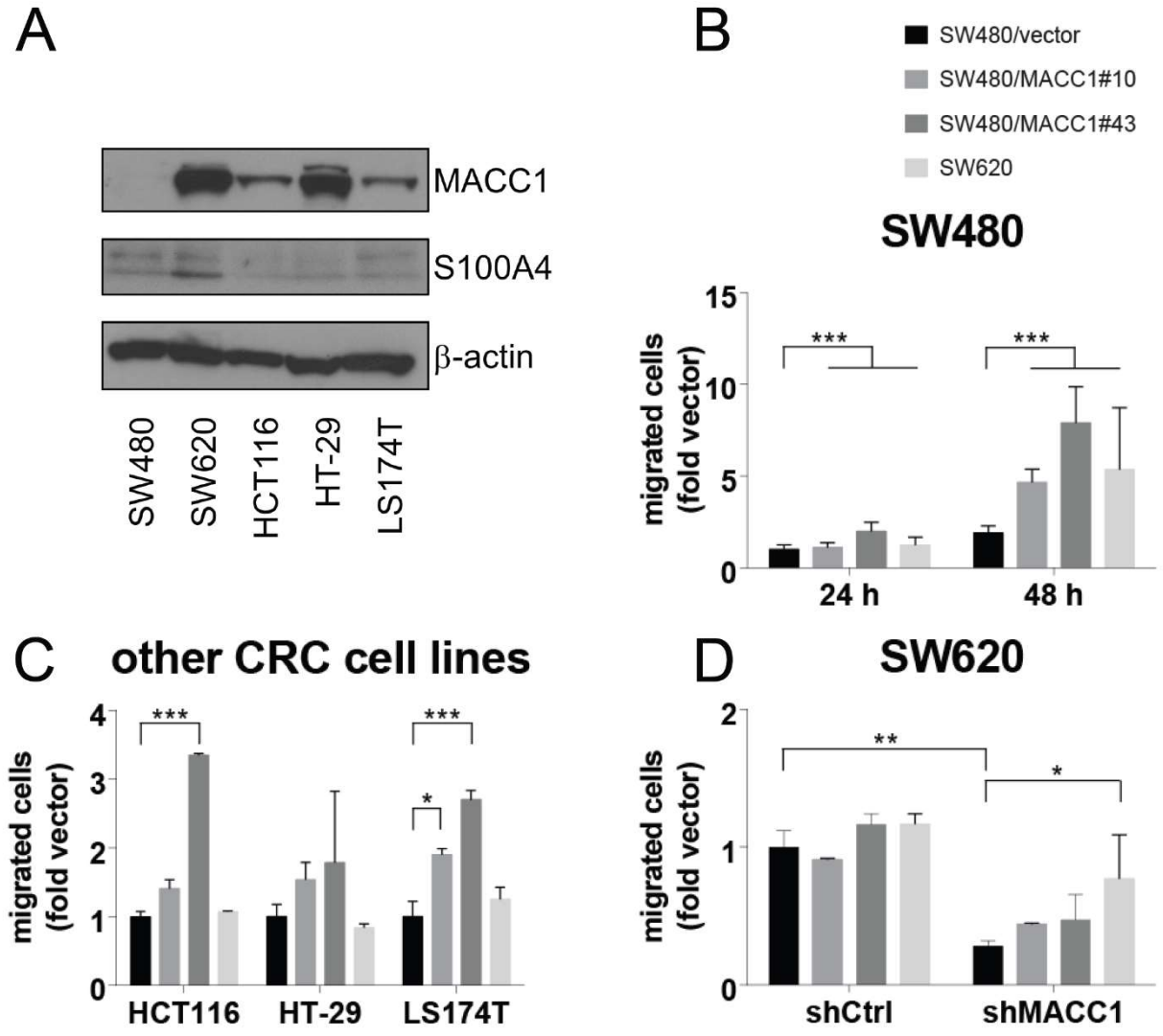

Figure 3: The MACC1 secretome induces CRC cell migration via S100A4. Baseline protein expression of MACC1 and S100A4 in the human colon carcinoma cell lines SW480, SW620, HCT116, HT-29 and LS174T (A). Culture medium of MACC1-overexpressing cells stimulated migration of SW480 cells (B), and in HCT116, HT-29 and LS174T (C). The same culture supernatants rescued migration of SW620/shMACC1 that was diminished after depletion of MACC1 (D) (modified after Kortüm et al., 2022).

Since results were more pronounced after 48 h, further experiments were carried out with the longer incubation period. HCT116, HT-29 and LS174T all experienced significant induction of migration after treatment with media of SW480/MACC1 cells, while medium of wildtype SW620 did not share this effect [Fig. 3C]. Medium of SW480/vector cells served as a negative control and did not elicit promigratory effects. SW620 is a cell line raised from a CRC lymph node metastasis and features extremely high levels of MACC1. In fact, the SW480 cell line originates from the primary tumor of the same patient. Following depletion of MACC1 through RNA-interference, SW620/shMACC1 cells demonstrate reduced migration as compared to SW620-shCtrl controls with high endogenous expression of MACC1 left intact. We probed whether MACC1-conditioned media can restore migration in MACC1-depleted cells. Indeed, only medium of wildtype SW620 cells, but none of the SW480 clones, was able to partially restore migration.

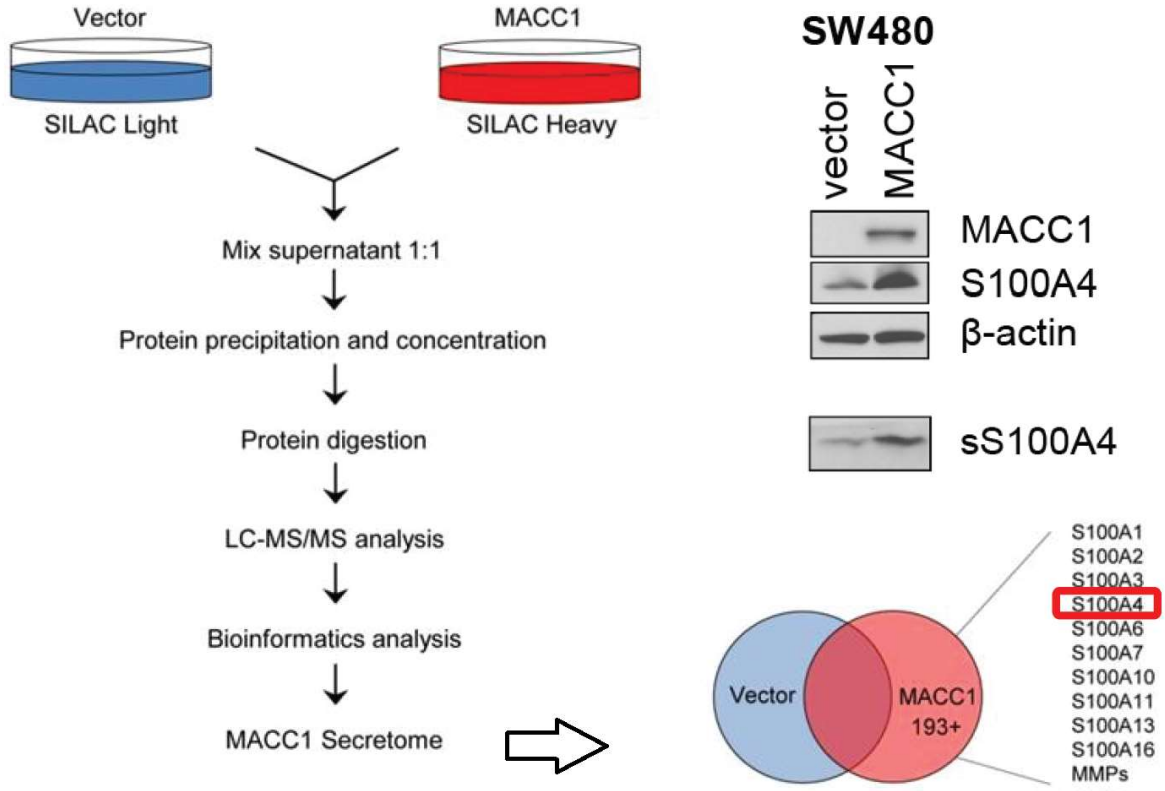

Figure 4: The MACC1 secretome features S100A4. Cell culture medium of SW480/vector and SW480/MACC1 cells differed in SILAC analysis, in that S100 proteins were overrepresented in medium of MACC1-overexpressing cells. Western blot from cell culture supernatant (sample volume proportional to respective cell count at time of medium harvest) confirmed increased presence of soluble S100A4 (sS100A4) in the secretome of SW480/MACC1 cells. (modified after Kortüm et al., 2022).

We hypothesized that MACC1 itself is not part of the secretome, but rather its overexpression within the cells shapes the proteome of the culture medium. To ascertain the MACC1-specific secretome we employed SILAC to compare the cell-free media of SW480/vector and SW480/MACC1 cells. Several S100 proteins, including S100A4, were dramatically enriched in SW480/MACC1 medium compared to SW480/vector medium. Increased soluble S100A4 in the cell free supernatant of MACC1-overexpressing cells was confirmed by direct Western blotting [Fig. 4].

3.2 CRC metastasis involves MACC1 and S100A4 co-expression.

We took advantage of a tumor tissue bank from 60 CRC patients and obtained 5 µm thick sections. Immediately adjacent sections were fixed, permeated, and stained immunohistochemically with antibodies against MACC1 or S100A4. Tumors with pronounced staining of MACC1 were predominantly enriched in S100A4 expression. Conversely, sections with faint immunoreactivity against MACC1 demonstrated weak expression of S100A4 [Fig. 5].

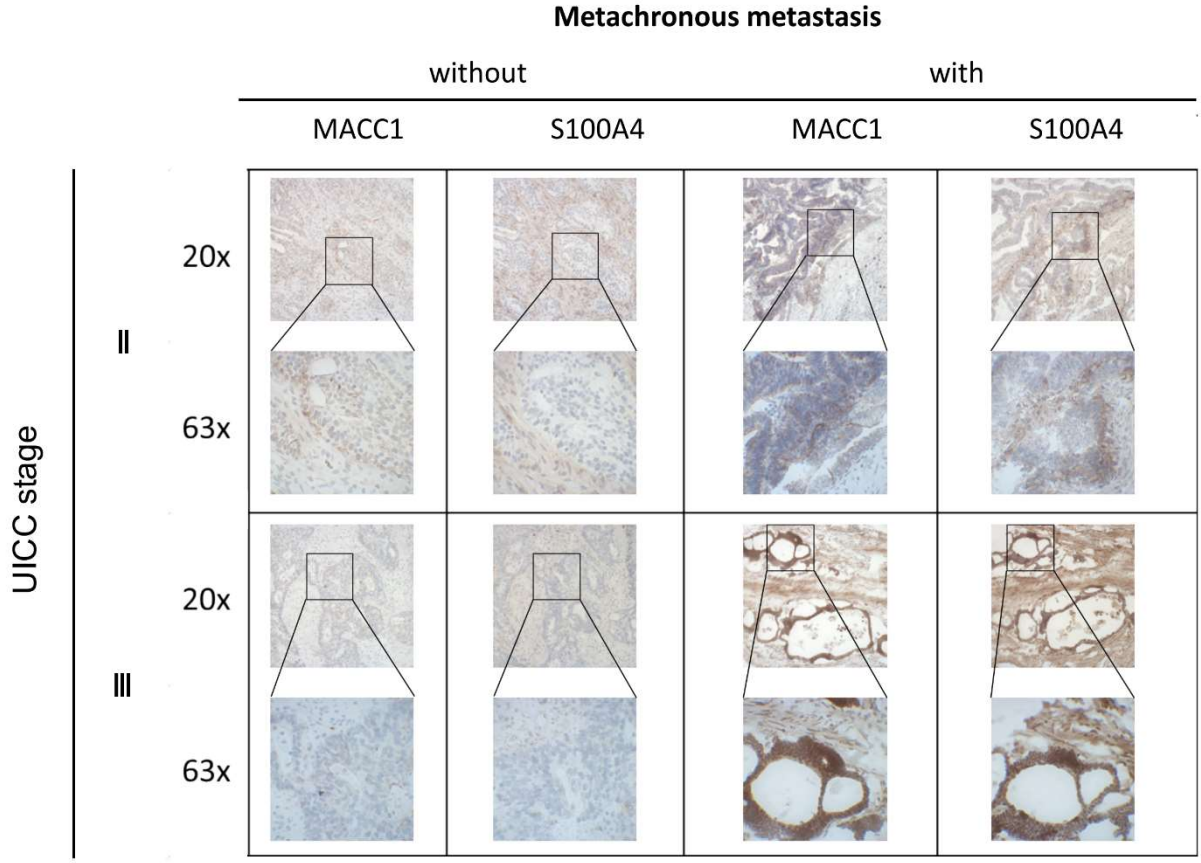

Figure 5: Co-expression of MACC1 in human CRC sections. Tumors that did not yield metachronous metastases expressed faint amounts of MACC1 and S100A4, while recurrent CRC (tumors with metachronous metastases) showed pronounced expression of MACC1 and S100A4. Also note the marked positivity for S100A4 in the stroma (modified after Kortüm et al., 2022).

Of note, in S100A4-rich sections, a substantial staining was observable also outside of the tumor cells, throughout the surrounding stroma tissue. In three external CRC cohorts MACC1 and S100A4 correlated significantly with Spearman ρ values of 0.392, 0.431 and 0.317, respectively [Fig. 6].

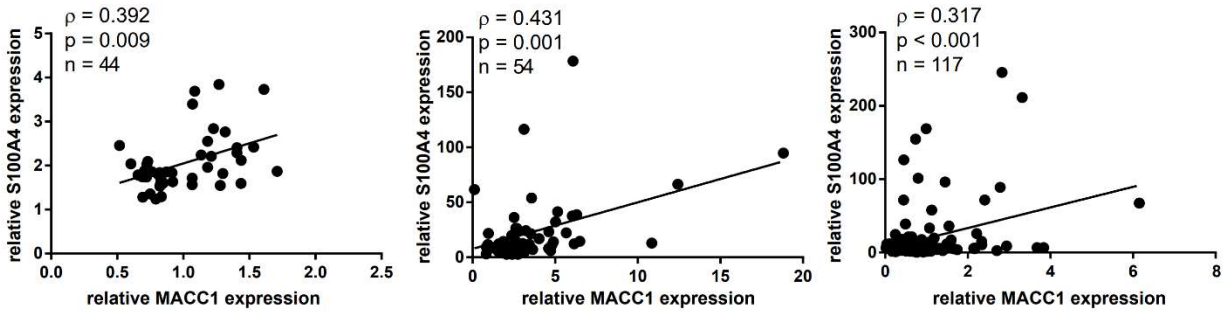

Figure 6: Co-expression of MACC1 and S100A4 in patient cohorts. In publicly available of three independent clinical cohorts, the expression of MACC1 and S100A4 mRNA correlated positively (modified after Kortüm et al., 2022).

These findings suggest a potential co-regulation of both biomarkers. Therefore, and since MACC1 and S100A4 have independently been shown to predict dismal cancer survival, we examined whether combined upregulation would define high risk CRC patients. In a cohort of 60 CRC patients, we established Youden's J cut-off values of MACC1 and S100A4 mRNA expression for the endpoints Overall Survival and Metastasis-Free Survival to stratify all cases for survival analysis. The combination of "high MACC1 and S100A4" expression was associated with the shortest OS, while the longest OS was found in "MACC1 and S100A4 low" [Fig. 7].

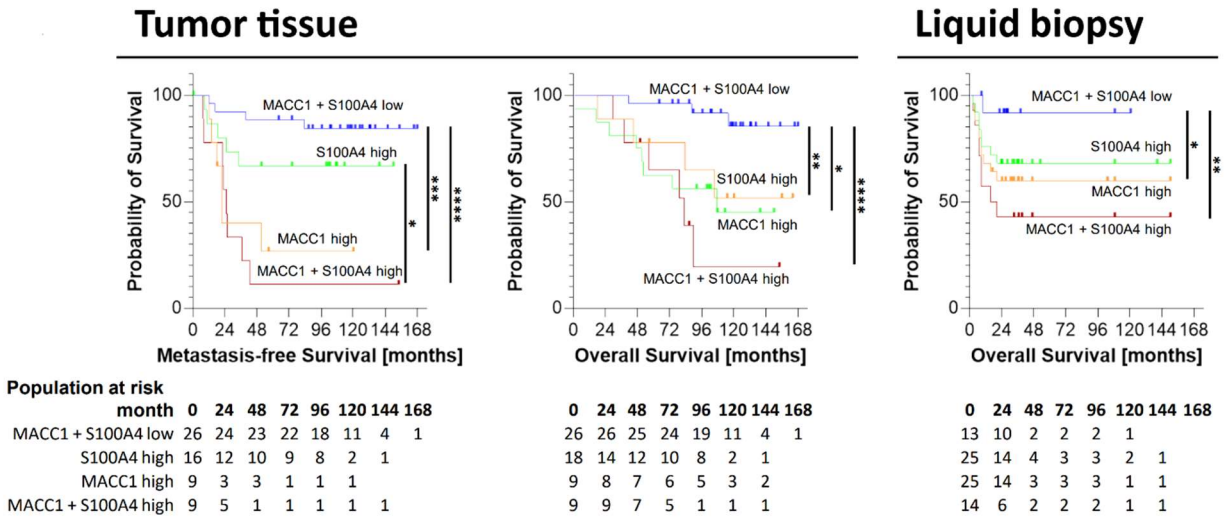

Figure 7: Prognostic biomarker combination of MACC1 and S100A4. High tumor RNA expression of both markers predicts poor metastasis-free and overall survival. Patients with elevated transcript levels of MACC1 and S100A4 in blood samples face poor overall survival (modified after Kortüm et al., 2022).

Similarly, combined overexpression of MACC1 and S100A4 identified patients with the shorted MFS. In an unrelated collection of 49 preoperative serum samples, “high MACC1 and S100A4” expression was associated with the shortest OS, while “MACC1 and S100A4 low” was associated with the longest MFS, conversely. This underlines that combining both biomarkers result in robust prediction of high risk in CRC patients and demonstrates that MACC1 and S100A4-level assessments in the primary tumor and in patient blood are similarly informative.

3.3 MACC1 induces S100A4 via Wnt/β-catenin to exert cancer cell migration.

We hypothesized a transcriptional connection between MACC1 and S100A4. To test this hypothesis *in vitro*, we overexpressed MACC1 in HCT116 (low intrinsic expression) cells by lentiviral transduction, while we depleted MACC1 in SW620 (high intrinsic expression) cells using CRISPR-Cas9 technology. Indeed, overexpression of MACC1 in HCT116 cells led to increased luciferase activity in the S100A4-promoter driven luciferase activity. Finally, HCT116/MACC1 cells expressed significantly more S100A4 mRNA and protein than HCT116/vector cells, while SW620/MACC1-KO showed reduction of S100A4 mRNA and protein compared to SW620/Cas9-ev cells [Fig. 8].

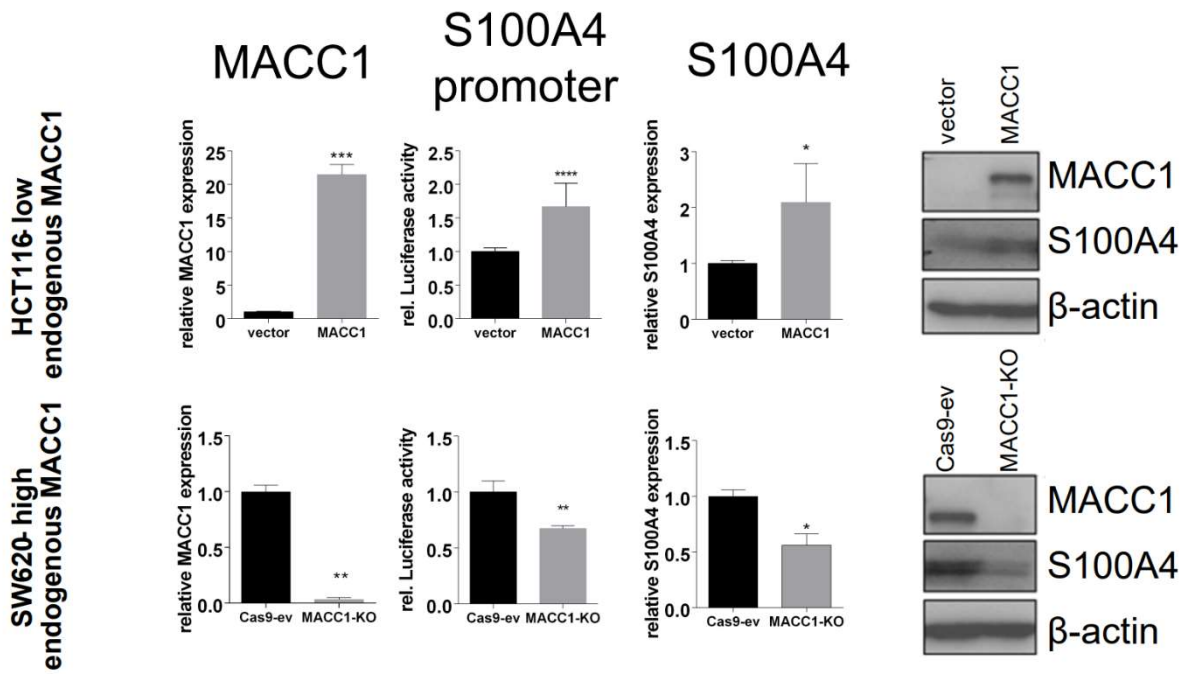

Figure 8: MACC1-regulated S100A4 expression. Overexpressing MACC1 in HCT116 increases S100A4 promoter activity, RNA, and protein expression. Elimination of MACC1 in SW620 had the opposite effect (modified after Kortüm et al., 2022).

Ectopic MACC1 (vil-MACC1-ApcMin) leads to malignant transformation of non-invasive ApcMin tumors model, accompanied by upregulated Wnt/β-catenin signaling [54]. To answer whether S100A4 was involved in this process, we sectioned vil-MACC1-ApcMin and ApcMin tumors for immunohistochemical detection of MACC1 and S100A4 protein. S100A4 immunoreactivity was stronger in vil-MACC1-ApcMin tissue than in ApcMin tissues [Fig. 9A]. Tumor tissue was scraped off with a sterile scalpel for extraction of mRNA. We found that villin-promoter driven overexpression of MACC1 was detectable in vil-MACC1-ApcMin tissue, but not in tissues of ApcMin littermates. This finding was reflected in higher concentrations of human MACC1 (hMACC1) in RT-qPCR [Fig. 9B]. Importantly, we assessed murine mRNA of S100a4 (mS100a4) by mouse-specific primers and found increased expression levels of mS100a4 in tumors of vil-MACC1-ApcMin mice [Fig. 9C].

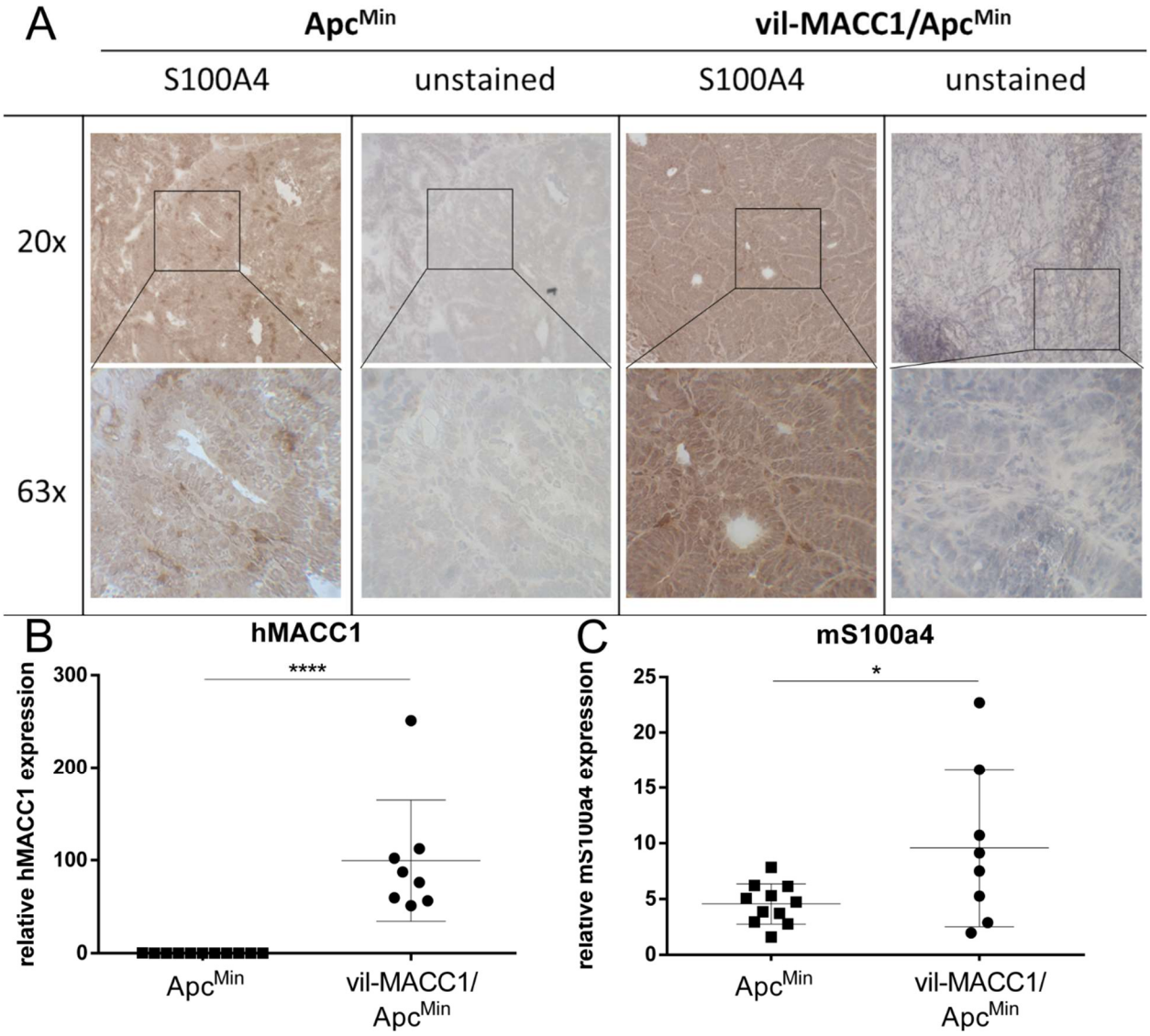

Figure 9: Co-expression of MACC1 and S100A4 in a transgenic mouse model. Immunoreactivity against S100A4 was stronger in vil-MACC1/ApcMin mice in comparison to ApcMin littermates. The ectopic human MACC1 transgene (hMACC1) leads to upregulation of mouse intrinsic S100a4 (mS100a4) (modified after Kortüm et al., 2022).

We examined whether MACC1 can induce cell migration independently of S100A4. MACC1 was overexpressed in HCT116/Cas9-ev cells and HCT116 S100A4-KO cells. MACC1 increased the transwell migration of S100A4-competent HCT116 Cas9-ev cells but did not increase cell migration of HCT116 S100A4-KO cells [Fig. 10A].

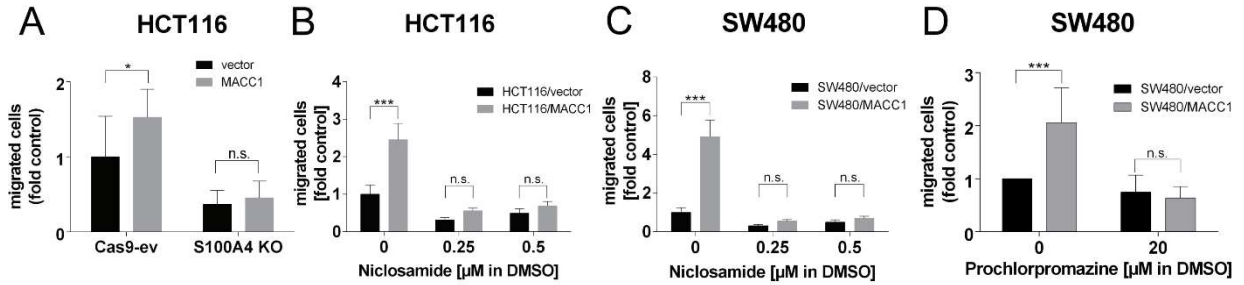

Figure 10: MACC1-specific migration via S100A4. Deletion (A), transcriptional inhibition (B, C) and pharmacological blocking (D) of S100A4 halts MACC1-driven cancer cell migration (modified after Kortüm et al., 2022).

To replicate S100A4 deficiency pharmacologically, we pretreated HCT116/vector and HCT116/MACC1 cells and SW480/vector and SW480/MACC1 cells with niclosamide for 24 h and performed Boyden chamber experiments. Under 0.25 µM and 0.5 µM, niclosamide significantly eliminated the increased migration of MACC1-overexpressing cells in comparison to negative controls [Fig. 10B and C]. We also ventured into testing whether prochlorpromazine, a phenothiazine that was able to complex and polymerize S100A4 in cell-free experiments, can mitigate migration of cells [78]. Indeed, migration of SW480/MACC1 was reduced to SW480/vector levels after treatment with 20 µM prochlorpromazine [Fig. 10D].

To test whether MACC1 upregulates S100A4 transcriptionally, we employed three different Wnt/β-catenin inhibitors, FH535, LF3 and niclosamide. In HCT116/MACC1 cells, all inhibitors were able to revert S100A4 upregulation to expression levels of HCT116/vector cells [Fig. 11].

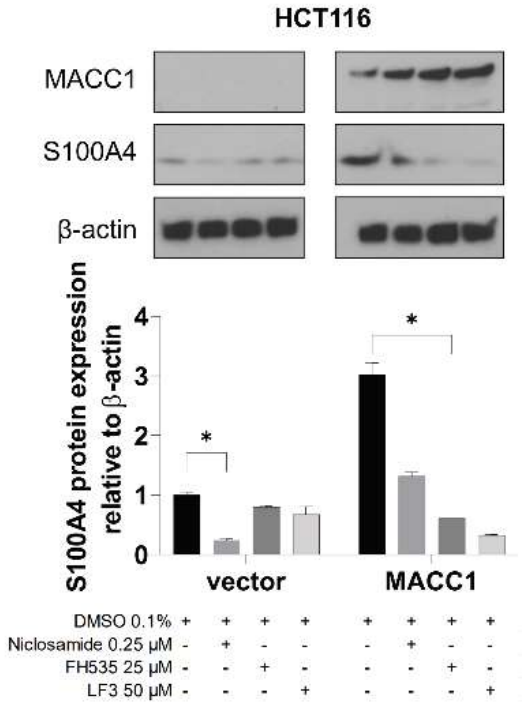

Figure 11: Wnt inhibitors revert MACC1-driven S100A4 overexpression. S100A4 expression is elevated in HCT116/MACC1, and returned to HCT116/vector levels by niclosamide, FH535 and LF3 (modified after Kortüm et al., 2022).

3.4 β-catenin is directly engaged by MACC1.

We have established that MACC1 and β-catenin engage in direct protein-protein interaction (PPI). By deciphering the interactome of MACC1 using mass-spectrometry, seven peptides could be mapped to β-catenin [Fig. 12A].

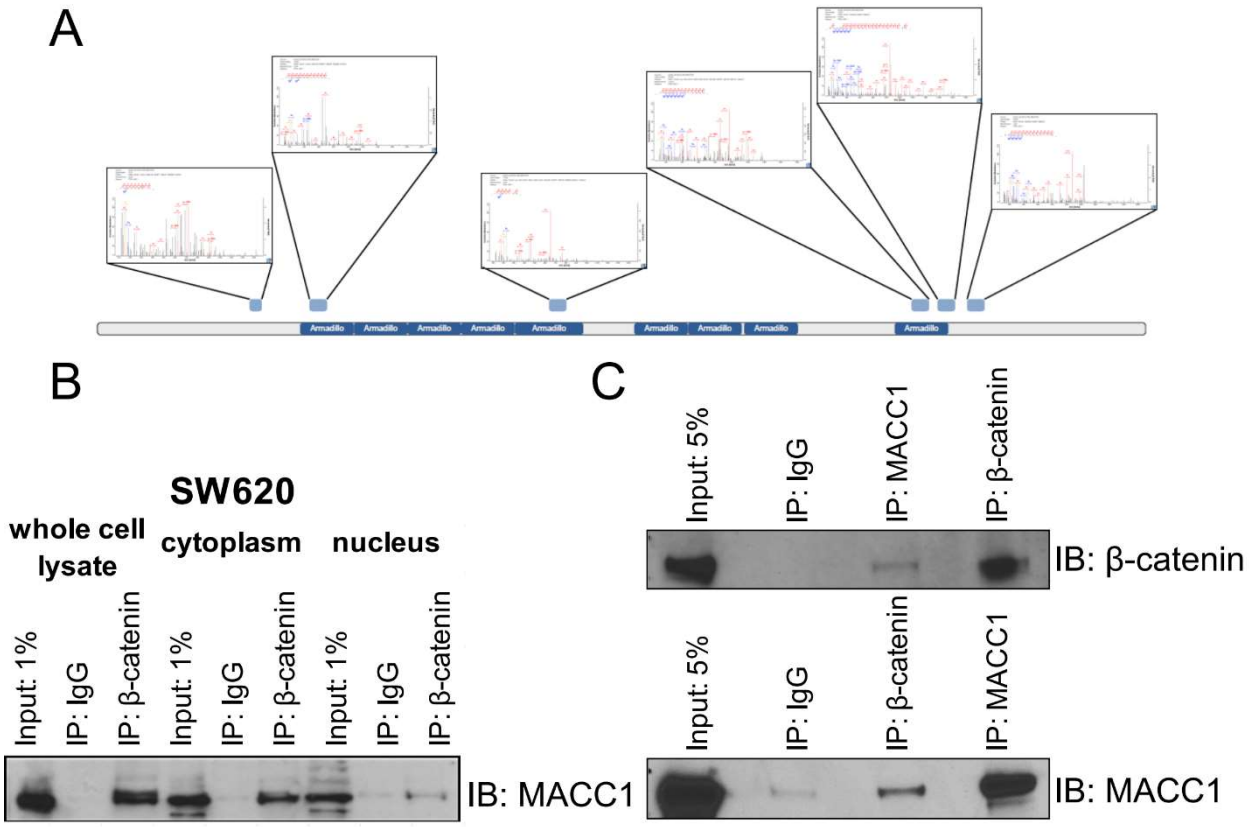

Figure 12: MACC1 binds β-catenin. Mass-Spectrometry of the MACC1 interactome identified 6 peptide fragments of β-catenin (A). This interaction occurred also in co-Immunoprecipitation experiments with whole and fractioned cell lysate (B) and in cell-free assays (C) (modified after Kortüm et al., 2022).

We verified this PPI in co-immunoprecipitation experiments. In whole lysate of SW620 cells, MACC1 was immune-absorbed to a specific antibody, followed by incubation with protein-G coated agarose beads. Centrifugation and stringent and repeated washing of these beads exposed complexes of antibody bound MACC1 and interacting proteins. Western blotting of the eluate with a β-catenin-specific antibody resulted in a band matching β-catenin in the input control, while no band was detectable in the eluate of IgG control pulldown. These findings could be replicated in cytoplasmatic as well as nuclear protein lysates [Fig. 12B]. Furthermore, recombinantly produced MACC1 and β-catenin protein also interacted in entirely cell-free experiments [Fig. 12C].

To elucidate the significance of this hitherto unknown PPI, we examined implications on the transcriptional activity of β-catenin. TOP-flash assay for Wnt/β-catenin signaling, while knock-out of MACC1 in SW620 cells decreased TOP-flash activity. Similar results were found on mRNA-expression levels of the Wnt target genes Cyclin-D1 MMP7 and S100A4, while β-catenin mRNA was not induced [Fig. 13A].

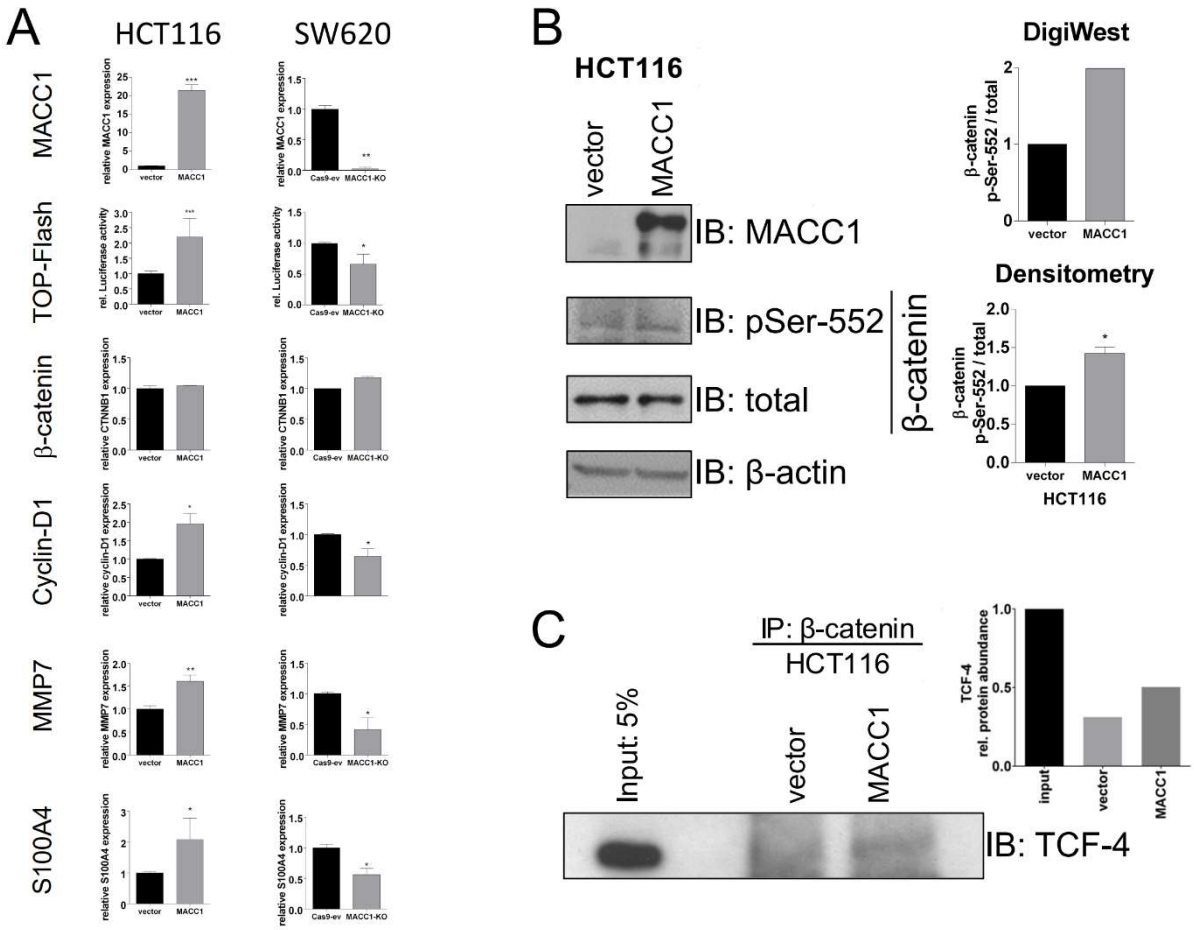

Figure 13: MACC1 enhances β-catenin signaling. Overexpression of MACC1 in HCT116 increased activity of TOP-Flash reporter for Wnt/β-catenin/TCF signaling, and upregulated the Wnt targets cyclin D1, MMP7 and S100A4. Depletion of MACC1 in SW620, conversely, had the opposite effect. Expression of β-catenin RNA (CTNNB1) was unaffected (A). phosphorylation of Ser-552 of β-catenin is increased under MACC1 overexpression (B), concomitant with increased interaction with TCF4 (C) (modified after Kortüm et al., 2022).

The activity and stability of β-catenin is mainly regulated by post-translational modifications. It has been shown that activating phosphorylation of β-catenin is sufficient to promote its translocation into the nucleus [29]. We observed increased phosphorylation of β-catenin at Ser-552 in HCT116/MACC1 compared to HCT116/vector, and decreased phosphorylation of these sites in SW620/MACC1-KO compared to SW620/Cas9-ev [Fig. 13B]. TCF4 is crucial for β-catenin-dependent gene transcription. We assessed the intensity of β-catenin/TCF4 interaction under MACC1 overexpression by simultaneous Co-IP

experiments in HCT116/vector and HCT116/MACC1 cells and found higher abundance of TCF4 protein in precipitates of β-catenin in MACC1 overexpressing cells [Fig. 13C]. The MACC1 protein itself lacks sequences suggesting kinase activity [52]. Given these findings, we hypothesize that MACC1 acts as an adapter protein by interacting with both a kinase and its substrate, thus increasing the efficiency of post-translational stabilization of β-catenin and potentially modifying the target gene spectrum.

3.5 Niclosamide and statins synergistically halt CRC cell motility.

To test the potential clinical feasibility of MACC1-S100A4-targeted therapy in CRC, we combined transcriptional inhibitors against MACC1 and S100A4 in wound healing and metastasis assays. A combination of 2.5 µM atorvastatin and 0.5 µM niclosamide was the most effective combination in restricting wound healing of HCT116 cells [Fig. 14A].

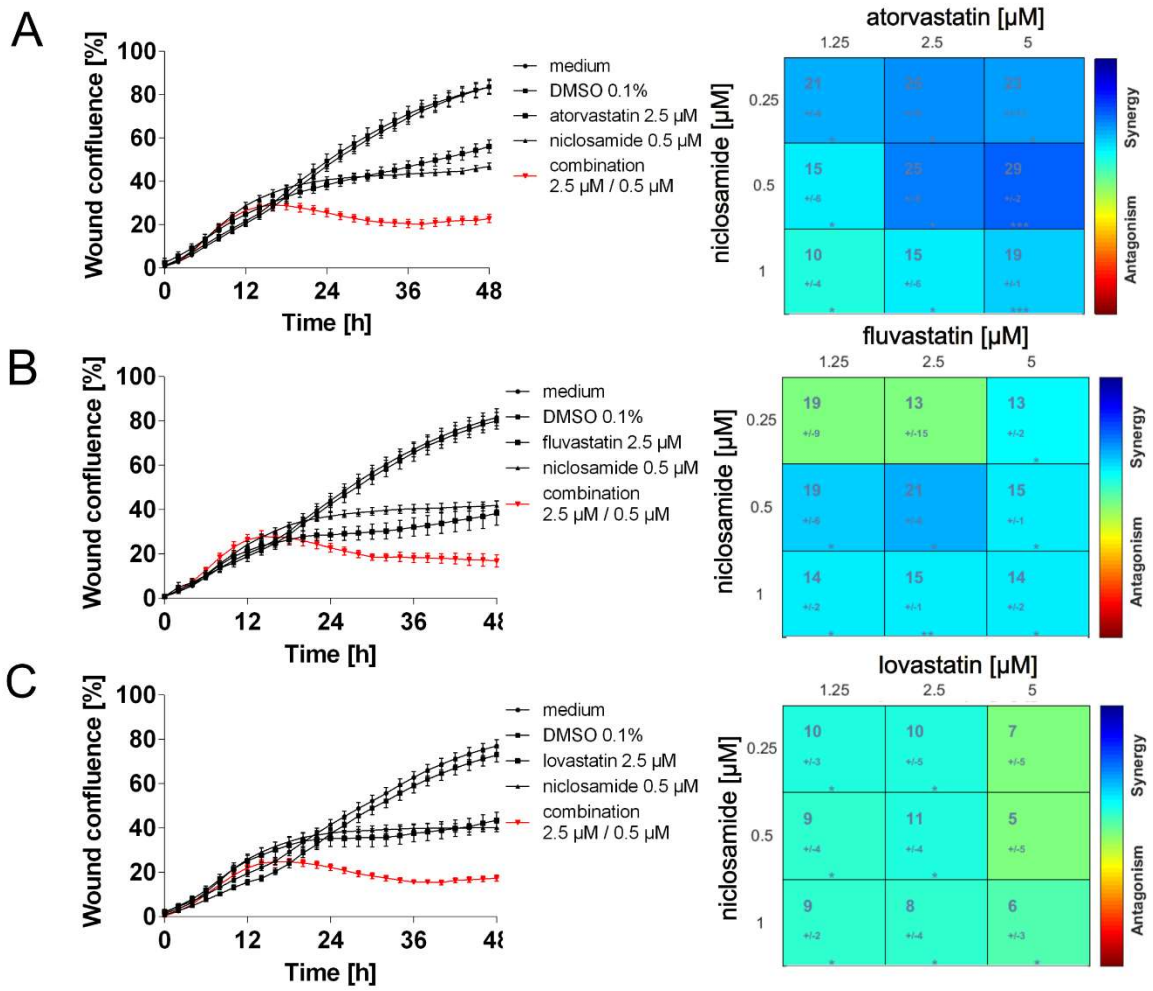

Figure 14: Statins synergize with niclosamide against CRC motility. The statins atorvastatin (A), fluvastatin (B) and lovastatin (C) were combined with niclosamide in wound healing assays for cell motility. In Loewe interaction analyses, atorvastatin showed the strongest synergy with niclosamide, at 5 µM and 0.5 µM, respectively (modified after Kortüm et al., 2022).

In comparison, fluvastatin or lovastatin and niclosamide given alone at higher concentrations (5 µM and 1 µM, respectively) did suppress HCT116 cell migration, but less effectively than in combination [Fig. 14B, C].

3.6 Niclosamide and statins synergistically suppress CRC cell metastasis.

We sought to validate the synergisms of niclosamide and statins in restricting cell motility *in vitro* in an *in vivo* model of metastasis. To this end, SCID bg/bg mice were injected with 1×10^6 HCT116/CMV-Luc, forming a xenograft of human CRC cells. Starting from day 5 after xenotransplantation, the animals were orally administered either statins or niclosamide, or combination thereof, while solvent-treated animals served as a control cohort. For each experiment, 60 animals were randomly assigned to one of 6 treatment groups (n = 10). Luciferin, a substrate of luciferase expressed by HCT116/CMV-Luc cells, was administered into the tail vein of the mice, eliciting bioluminescence in the HCT116/CMV-Luc cells. This allowed non-invasive monitoring of tumors and metastases. An initial experiment using 100% of the human equivalent dose of statins (13 mg/kg) and 164 mg/kg niclosamide was performed to assess toxicity and efficacy of the pharmaceuticals to mitigate macroscopic and microscopic metastasis. Luminescence data from day 20 showed significant suppression of tumor growth in all statin-based treatments, so that any potential synergistic effects were obfuscated [Fig. 15A]. Conversely, administration of 12.5% of the human equivalence dose of statins (1.5 mg/kg) and niclosamide (164 mg/kg) did not, neither in single dose nor in combination, elicit any significant suppression of tumor and metastasis growth [Fig. 15B]. Nevertheless, the highest doses of statins and niclosamide were found to be safe. Mouse body weights were equal in all treatments [Fig. 15C]. Under administration of statins at 25% of the human equivalent dose (3.25 mg/kg) and 250 mg/kg niclosamide, both fluvastatin + niclosamide and atorvastatin + niclosamide groups showed the lowest reads of tumor bioluminescence [Fig. 15D]. We sought to also compare the load of micrometastases between the treatment groups. Immediately after euthanasia, mouse livers were shock frozen in liquid nitrogen to be cryosectioned and immunostained with antibodies specific for human cytokeratin 19 (hCK19) to detect human HCT116 cells that have disseminated into the tumor-free appearing mouse liver [Fig. 15E]. Treatment with solvent and monotherapy with either statin or niclosamide (1-4) was associated with high abundance of hCK19, while both combinatorial treatments (5, 6) showed virtually no hCK19 signal.

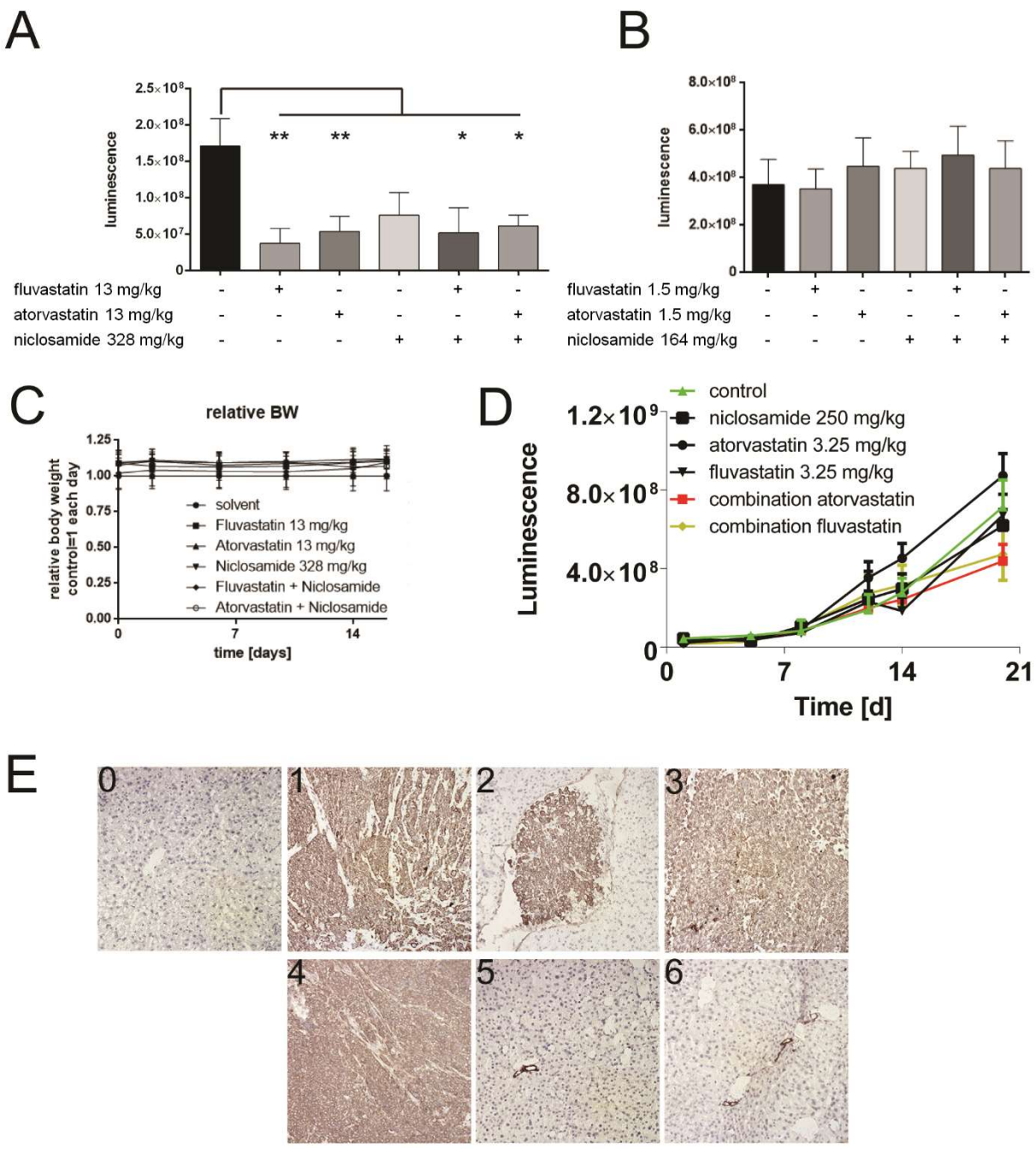

Figure 15: Dose-finding for statin-niclosamide synergy for suppression of CRC metastasis. Luminescence of metastases in murine livers following CRC cell xenografts under treatment with 100 % (A) and 12.5 % (B) human equivalent dosage of respective drug. Under 100 % dosage, all drugs significantly reduced liver metastases, and synergistic effects were obscured, while at 12.5 % no effects were observed, and dosage was not sufficient to elicit synergism of niclosamide and statin. Body weight curves normalised to control treated mice showed no toxicity of either treatment (C). Luminescence over time in the final experiment (D). IHC against hCK19 detected disseminated human CRC cells in murine liver (E) Representative murine liver sections show abundance of hCK19, indicating micrometastases (0 = healthy liver, 1 = solvent, 2 = niclosamide, 3 = fluvastatin, 4 = atorvastatin, 5 = fluvastatin + niclosamide, 6 = atorvastatin + niclosamide) (modified after Kortüm et al., 2022).

Statins (3.25 mg/kg) and niclosamide (250 mg/kg) did not affect macroscopic tumor growth and liver metastases [Fig. 16A, B]. However, loads of human satellite DNA, indicative of micrometastases, were reduced by monotherapies, and more potently by combinations of statin and niclosamide [Fig. 16C].

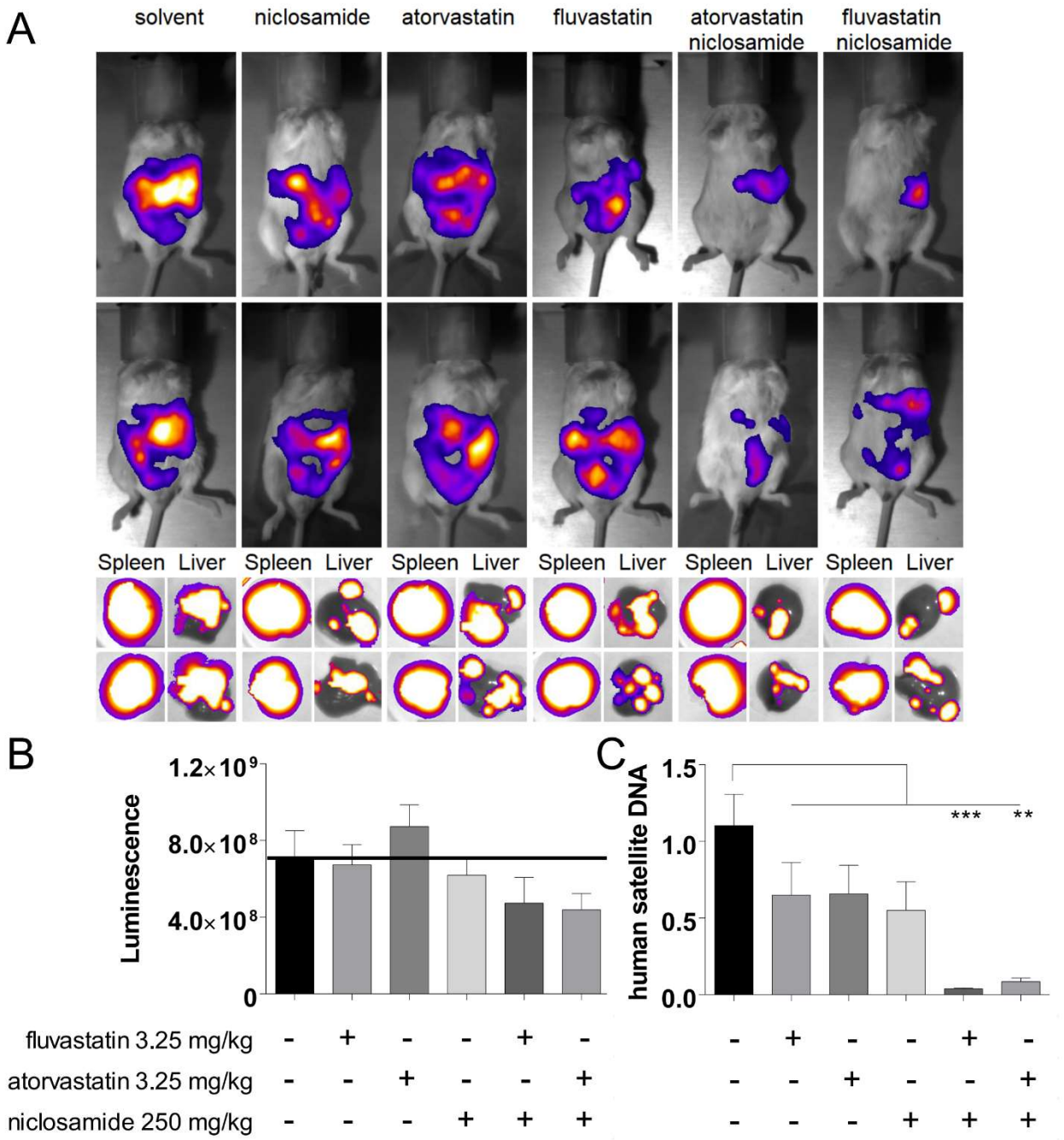

Figure 16: Synergistic suppression of CRC metastasis. Under treatment with either atorvastatin (3.25 mg/kg, 20 mg per patient per day), fluvastatin (3.25 mg/kg, 20 mg per patient per day) or niclosamide (250 mg/day, 1.5 g per patient per day). Growth of macroscopic liver metastases did not differ amongst the treatment groups. However, micrometastases in tumor-free appearing liver tissue were only diminished in combinations of statin and niclosamide (C) (modified after Kortüm et al., 2022).

4 Discussion

4.1 Brief summary of results

CRC cells with intrinsically or extrinsically high levels of MACC1 secrete S100A4. Cell culture medium of MACC1-overexpressing cells stimulates migration of CRC cell lines with low expression levels of MACC1. S100A4 and MACC1 are co-expressed in tumor samples, and combined overexpression of both markers in tumors and clinical blood samples identifies high risk patients with dismal MFS and OS. MACC1 directly promotes S100A4 expression through enforced β-catenin-dependent transcriptional activity. Induction of cancer cell migration relies on S100A4 and is druggable by small molecule transcriptional inhibitors of Wnt/β-catenin signaling and S100A4. Niclosamide (S100A4 inhibitor) and statins (MACC1 inhibitors) are individually able to halt cancer cell motility *in vitro.* In combinatorial use, the effects on cultured cells are potentiated and in a mouse model of CRC, niclosamide and statins synergize in prevention of metastasis.

4.2 Interpretations of results

Upregulation of MACC1 is associated with overexpression and secretion of S100A4. CRC cells with high levels of MACC1 demonstrate high expression of intracellular S100A4 and elevated secretion of soluble S100A4. In tumor samples of patients and mice, S100A4 was not only found upregulated within the tumor cells, but also in the surrounding stromal tissue. Both biomarkers are positively correlated in expression and, potentially due to being, mechanistically linked, in that MACC1 interacts with β-catenin, a translational activator of S100A4, leading to its posttranslational stabilization and an enforced interaction with downstream transcription factors. Combinatorial transcriptional inhibition of MACC1 and S100A4 is superior to separate use in the restriction of migration *in vitro* and metastasis *in vivo*, in line with antineoplastic drug synergism.

We report here the mechanistic link between two seemingly unrelated metastasis inducers. MACC1 enforces Wnt/β-catenin signaling and expression of its target gene S100A4 by direct modification of β-catenin. Furthermore, phosphorylation of β-catenin is increased at serine-552, which has been described in a variety of cancers. In the absence of intrinsic kinase activity, MACC1 might act as an adapter protein and bind to β-catenin to shift the stoichiometry of β-catenin interacting with its kinases Akt, MET or PAK1. An

interaction with a kinase able to phosphorylate β-catenin with MACC1 has yet to be established.
We established, that macroscopic metastasis (i.e., detectable by bioluminescence) was not affected by either treatment, but that the abundance of micrometastases in the liver tissue around the large tumor masses was reduced only in combinatorial treatments. This means, that statins and niclosamide overall decrease the risk of metastasis development, but do not prevent the outgrowth of some metastatic lesions once they have escaped pharmacological inhibition.

4.3 Strengths and limitations

We have been able to test the combination of both biomarkers in tumor samples and liquid biopsies in predicting cancer survival. Of note, these CRC cohorts are independent. It would have been ideal to have matched tumor and blood samples from the same cohort of patients to compare risk stratification from blood plasma and tumor samples side-by-side. Nevertheless, being able to predict OS from tumor samples and then liquid biopsies demonstrates a certain robustness of our biomarker combination, and our approach of isolating RNA transcripts from unprocessed blood plasma, without ultracentrifugation or material-intensive purification of subcellular vesicles, is potentially easy to implement in routine laboratory medicine. Furthermore, artificial release of S100A4 protein from blood cells after sampling as well as elevated S100A4 protein in non-cancerous diseases disqualify its assessment as a biomarker [81,82].
Supernatant of SW480/MACC1 cells drives migration of SW480 and all other cell lines, but not SW620, while supernatant of SW620 only drives (restores) SW620-shMACC1 migration. Clearly, ectopic overexpression of MACC1 in SW480 is by far not sufficient to render them SW620 cells, and the very different origin of both cell lines only emphasize that highly contextual mechanisms are at play. High expression and activity of MACC1 must be studied functionally in cellular models of benign and malign tumor stages as well as healthy and developmental contexts.
It must be noted that we did not distinguish between S100A4 in free solution in the medium and within subcellular vehicles, or exosomes. In fact, both MACC1 and S100A4 proteins were more abundant in exosomes of the metastatic SW620 cell line compared to the primary tumor-derived SW480 counterpart [83]. Tumor-derived exosomes, shed into the blood stream, have been found to be assimilated by Kupffer cells in the liver of

mice and induce formation of premetastatic niches [64]. It remains to be clarified, whether upregulation of S100A4 in the tumor stroma is attributable to secretion of S100A4 by the tumor cells alone or by hitherto unknown mechanisms through which MACC1-expressing cancer cells induce the fibroblasts to increase synthesis of S100A4 themselves.
To strengthen the evidence for the mechanisms by which Wnt/β-catenin is activated by MACC1, it would have been desirable to inactivate the phosphorylation site at serine-552 of β-catenin by site-directed mutagenesis. Furthermore, this study did not specify which kinase phosphorylates β-catenin downstream of MACC1.

4.4 Implications for the standard of care and future research of CRC

We have characterized the interplay of MACC1 and S100A4 in CRC, *in vitro* and *in vivo* models of CRC, and pharmaceuticals primarily targeting β-catenin/TCF4 signaling. CRC is a cancer entity largely driven by aberrantly active Wnt/β-catenin signaling – 85% of cases demonstrate either loss-of-function of APC or gain-of-function of β-catenin. However, clearly this pathway is not equally prevalent in most other cancer entities.
Therefore, we must regard our findings limited to the majority of CRC, and not directly applicable to other entities. Nevertheless, we postulate that similarly to our study, repositioning drugs against pathways that are decisive in progression of other tumor entities would be feasible. Our group has demonstrated that the lipid profile of patient plasma is informative for CRC risk [84]. Extensive work is being done on circulating tumor cells and cell-free DNA, RNA and proteins, either dissolved freely in blood plasma or contained in extracellular vesicles (exosomes) [85]. Focusing on feasibility, we have isolated RNA from blood plasma without prior enrichment of extracellular vesicles. While important biological information is lost, we argue that this approach is more easily adoptable in clinical routine by avoiding the need of ultracentrifugation.
The problematic toxicity profile of currently used chemotherapies calls for a quest for supplementary or even alternative pharmaceuticals for the management of cancers and the prevention of metastasis. Our group has outlined several of the emerging non-cytotoxic strategies such as inhibiting transcription and biosynthesis of tumor-promoting genes or alternatively, targeting the proteins that effect cancerous phenotypes [86]. Most notably in the context of this study, single molecules of phenothiazine-type antipsychotic drugs bind to S100A4 protein, coercing the formation of pentamers that are biologically inert within the cell [78]. An efficacy in cell culture has yet to be tested, yet in initial experiments

we were able to suppress MACC1-driven CRC cell migration with 20 µM prochlorpromazine [Fig. 10]. To our best knowledge, this is the first translation of an interesting biochemical report into cell culture. While novel biologics such as recombinant antibodies are poised to become a new mainstay of cancer therapy, the prospect of combatting cancer metastasis with already available, and orally taken, drugs warrants further development and research [87].

5 Conclusions

We have identified a novel MACC1-Wnt/β-catenin-S100A4 axis, which directly fuels cell motility and metastasis, the most dreaded complication of CRC. Contrary to most risk stratification studies that derive novel biomarkers from unsupervised data analyses, our approach is hypothesis-driven, therefore provides a molecular rationale and, in the case of MACC1 and S100A4, also a set of small molecule inhibitors already confirmed to have anti-metastatic effects in CRC. Additional to MACC1-targeting strategies, neutralization of S100A4 might be beneficial in preventing MACC1-dependent cancer progression.

Literature

1. Sung H, Ferlay J, Siegel RL, Laversanne M, Soerjomataram I, Jemal A, Bray F. Global Cancer Statistics 2020: GLOBOCAN Estimates of Incidence and Mortality Worldwide for 36 Cancers in 185 Countries. CA Cancer J Clin [Internet]. 2021 May;71(3):209–49.
2. Weitz J, Koch M, Debus J, Höhler T, Galle PR, Büchler MW. Colorectal cancer. Lancet [Internet]. 2005 Jan;365(9454):153–65.
3. Elferink MAG, de Jong KP, Klaase JM, Siemerink EJ, de Wilt JHW. Metachronous metastases from colorectal cancer: a population-based study in North-East Netherlands. Int J Colorectal Dis [Internet]. 2015 Feb 12;30(2):205–12.
4. Manfredi S, Lepage C, Hatem C, Coatmeur O, Faivre J, Bouvier AM. Epidemiology and management of liver metastases from colorectal cancer. Ann Surg [Internet]. 2006 Aug;244(2):254–9.
5. Hu Z, Ding J, Ma Z, Sun R, Seoane JA, Scott Shaffer J, Suarez CJ, Berghoff AS, Cremolini C, Falcone A, Loupakis F, Birner P, Preusser M, Lenz H josef, Curtis C. Quantitative evidence for early metastatic seeding in colorectal cancer. Nat Genet [Internet]. 2019;51(7):1113–22.
6. Sveen A, Kopetz S, Lothe RA. Biomarker-guided therapy for colorectal cancer: strength in complexity. Nat Rev Clin Oncol [Internet]. 2020 Jan;17(1):11–32.
7. Koulis C, Yap R, Engel R, Jardé T, Wilkins S, Solon G, Shapiro JD, Abud H, McMurrick P. Personalized Medicine—Current and Emerging Predictive and Prognostic Biomarkers in Colorectal Cancer. Cancers (Basel) [Internet]. 2020 Mar 28;12(4):812.
8. Sepulveda AR, Hamilton SR, Allegra CJ, Grody W, Cushman-Vokoun AM, Funkhouser WK, Kopetz SE, Lieu C, Lindor NM, Minsky BD, Monzon FA, Sargent DJ, Singh VM, Willis J, Clark J, Colasacco C, Rumble RB, Temple-Smolkin R, Ventura CB, Nowak JA. Molecular biomarkers for the evaluation of colorectal cancer: Guideline from The American Society for Clinical Pathology, College of American Pathologists, Association for Molecular Pathology, and the American Society of Clinical Oncology. J Clin Oncol. 2017;35(13):1453–96.
9. Iveson TJ, Kerr RS, Saunders MP, Cassidy J, Hollander NH, Tabernero J, Haydon A, Glimelius B, Harkin A, Allan K, McQueen J, Scudder C, Boyd KA, Briggs A, Waterston A, Medley L, Wilson C, Ellis R, Essapen S, Dhadda AS, Harrison M, Falk

S, Raouf S, Rees C, Olesen RK, Propper D, Bridgewater J, Azzabi A, Farrugia D, Webb A, Cunningham D, Hickish T, Weaver A, Gollins S, Wasan HS, Paul J. 3 versus 6 months of adjuvant oxaliplatin-fluoropyrimidine combination therapy for colorectal cancer (SCOT): an international, randomised, phase 3, non-inferiority trial. Lancet Oncol [Internet]. 2018;19(4):562–78.

10. Chang L, Chang M, Chang HM, Chang F. Microsatellite Instability: A Predictive Biomarker for Cancer Immunotherapy. Appl Immunohistochem Mol Morphol AIMM [Internet]. 2018 Feb;26(2):e15–21.
11. Gray RG, Quirke P, Handley K, Lopatin M, Magill L, Baehner FL, Beaumont C, Clark-langone KM, Yoshizawa CN, Lee M, Watson D, Shak S, Kerr DJ. Validation Study of a Quantitative Multigene Reverse Transcriptase – Polymerase Chain Reaction Assay for Assessment of Recurrence Risk in Patients With Stage II Colon Cancer. 2020;29(35):4611–9.
12. Yamanaka T, Oki E, Yamazaki K, Yamaguchi K, Muro K, Uetake H, Sato T, Nishina T, Ikeda M, Kato T, Kanazawa A, Kusumoto T, Chao C, Lopatin M, Krishnakumar J, Bailey H, Akagi K, Ochiai A, Ohtsu A, Ohashi Y, Yoshino T. 12-Gene Recurrence Score Assay Stratifies the Recurrence Risk in Stage II/III Colon Cancer With Surgery Alone: The SUNRISE Study. J Clin Oncol [Internet]. 2016 Aug 20;34(24):2906–13.
13. Fadaka AO, Pretorius A. Biomarkers for Stratification in Colorectal Cancer : MicroRNAs. 2019;26:1–11.
14. Schmoll HJ, Cutsem E Van, Stein A, Valentini V, Glimelius B, Haustermans K, Nordlinger B, Velde CJ Van De, Balmana J, Regula J, Nagtegaal ID. ESMO Consensus Guidelines for management of patients with colon and rectal cancer . A personalized approach to clinical decision making. Ann Oncol [Internet]. 2012;23(10):2479–516.
15. Lawler M, Alsina D, Adams RA, Anderson AS, Brown G, Fearnhead NS, Fenwick SW, Halloran SP, Hochhauser D, Hull MA, Koelzer VH, Mcnair AGK, Monahan KJ, Näthke I, Norton C, Novelli MR, Steele RJC, Thomas AL, Wilde LM, Wilson RH, Tomlinson I. Critical research gaps and recommendations to inform research prioritisation for more effective prevention and improved outcomes in colorectal cancer. 2018;179–93.
16. Koncina E, Haan S, Rauh S, Letellier E. Prognostic and Predictive Molecular Biomarkers for Colorectal Cancer : Updates and Challenges. 2020;1–25.

17. Obenauf AC, Massagué J. Surviving at a Distance: Organ-Specific Metastasis. Trends in cancer [Internet]. 2015 Sep;1(1):76–91.
18. Massagué J, Obenauf AC. Metastatic colonization by circulating tumour cells. Nature [Internet]. 2016 Jan 20;529(7586):298–306.
19. Sceneay J, Smyth MJ, Möller A. The pre-metastatic niche: finding common ground. Cancer Metastasis Rev [Internet]. 2013 Dec;32(3–4):449–64.
20. Plebanek MP, Angeloni NL, Vinokour E, Li J, Henkin A, Martinez-Marin D, Filleur S, Bhowmick R, Henkin J, Miller SD, Ifergan I, Lee Y, Osman I, Thaxton CS, Volpert O V. Pre-metastatic cancer exosomes induce immune surveillance by patrolling monocytes at the metastatic niche. Nat Commun [Internet]. 2017;8(1):1319.
21. Hübers C, Abdul Pari AA, Grieshober D, Petkov M, Schmidt A, Messmer T, Heyer CM, Schölch S, Kapel SS, Gengenbacher N, Singhal M, Schieb B, Fricke C, Will R, Remans K, Utikal JS, Reissfelder C, Schlesner M, Hodivala-Dilke KM, Kersten S, Goerdt S, Augustin HG, Felcht M. Primary tumor–derived systemic nANGPTL4 inhibits metastasis. J Exp Med [Internet]. 2023 Jan 2;220(1).
22. Fearon ER, Vogelstein B. A genetic model for colorectal tumorigenesis. Cell [Internet]. 1990 Jun 1 [cited 2014 Mar 24];61(5):759–67.
23. Klaus A, Birchmeier W. Wnt signalling and its impact on development and cancer. Nat Rev Cancer. 2008;8(5):387–98.
24. Holland JD, Klaus A, Garratt AN, Birchmeier W. Wnt signaling in stem and cancer stem cells. Curr Opin Cell Biol [Internet]. 2013 Apr;25(2):254–64.
25. Milanovic M, Fan DNY, Belenki D, Däbritz JHM, Zhao Z, Yu Y, Dörr JR, Dimitrova L, Lenze D, Monteiro Barbosa IA, Mendoza-Parra MA, Kanashova T, Metzner M, Pardon K, Reimann M, Trumpp A, Dörken B, Zuber J, Gronemeyer H, Hummel M, Dittmar G, Lee S, Schmitt CA. Senescence-associated reprogramming promotes cancer stemness. Nature [Internet]. 2018;553(7686):96–100.
26. Monga SPS, Mars WM, Pediaditakis P, Bell A, Mulé K, Bowen WC, Wang X, Zarnegar R, Michalopoulos GK. Hepatocyte growth factor induces Wnt-independent nuclear translocation of beta-catenin after Met-beta-catenin dissociation in hepatocytes. Cancer Res. 2002;62(7):2064–71.
27. Zeng G, Apte U, Micsenyi A, Bell A, Monga SPS. Tyrosine residues 654 and 670 in β-catenin are crucial in regulation of Met-β-catenin interactions. Vol. 312, Experimental Cell Research. 2006. p. 3620–30.
28. Gherardi E, Birchmeier W, Birchmeier C, Woude G Vande. Targeting MET in

cancer: Rationale and progress. Nat Rev Cancer. 2012;12(2):89–103.

29. Fang D, Hawke D, Zheng Y, Xia Y, Meisenhelder J, Nika H, Mills GB, Kobayashi R, Hunter T, Lu Z. Phosphorylation of beta-catenin by AKT promotes beta-catenin transcriptional activity. J Biol Chem [Internet]. 2007 Apr 13;282(15):11221–9.
30. Hino S i., Tanji C, Nakayama KI, Kikuchi A. Phosphorylation of -Catenin by Cyclic AMP-Dependent Protein Kinase Stabilizes -Catenin through Inhibition of Its Ubiquitination. Mol Cell Biol. 2005;25(20):9063–72.
31. Taurin S, Sandbo N, Qin Y, Browning D, Dulin NO. Phosphorylation of beta-catenin by cyclic AMP-dependent protein kinase. J Biol Chem [Internet]. 2006 Apr 14;281(15):9971–6.
32. Dammann K, Khare V, Harpain F, Lang M, Kurtovic A, Mesteri I, Evstatiev R, Gasche C. PAK1 promotes intestinal tumor initiation. Cancer Prev Res. 2015;8(11):1093–101.
33. Park MH, Kim DJ, You ST, Lee CS, Kim HK, Park SM, Shin EY, Kim EG. Phosphorylation of β-catenin at serine 663 regulates its transcriptional activity. Biochem Biophys Res Commun [Internet]. 2012;419(3):543–9.
34. He H, Shulkes A, Baldwin GS. PAK1 interacts with β-catenin and is required for the regulation of the β-catenin signalling pathway by gastrins. Biochim Biophys Acta - Mol Cell Res. 2008;1783(10):1943–54.
35. Zhu G, Wang Y, Huang B, Liang J, Ding Y, Xu a, Wu W. A Rac1/PAK1 cascade controls β-catenin activation in colon cancer cells. Oncogene [Internet]. 2012 Feb 23 [cited 2013 Jan 7];31(8):1001–12.
36. Nusse R, Clevers H. Wnt/β-Catenin Signaling, Disease, and Emerging Therapeutic Modalities. Cell [Internet]. 2017 Jun;169(6):985–99.
37. Bosetti C, Santucci C, Gallus S, Martinetti M, La Vecchia C. Aspirin and the risk of colorectal and other digestive tract cancers: an updated meta-analysis through 2019. Ann Oncol [Internet]. 2020 May;31(5):558–68.
38. Poynter JN, Gruber SB, Higgins PDR, Almog R, Bonner JD, Rennert HS, Low M, Greenson JK, Rennert G. Statins and the risk of colorectal cancer. N Engl J Med [Internet]. 2005 May 26;352(21):2184–92.
39. Gohlke BO, Zincke F, Eckert A, Kobelt D, Preissner S, Liebeskind JM, Gunkel N, Putzker K, Lewis J, Preissner S, Kortüm B, Walther W, Mura C, Bourne PE, Stein U, Preissner R. Real-world evidence for preventive effects of statins on cancer incidence: A trans-Atlantic analysis. Clin Transl Med [Internet]. 2022;12(2):e726.

40. Endometrial cancer and oral contraceptives: an individual participant meta-analysis of 27 276 women with endometrial cancer from 36 epidemiological studies. Lancet Oncol [Internet]. 2015 Sep;16(9):1061–70.
41. Wang J, Yu X, Peng H, Lu Y, Li S, Shi Q, Liu J, Dong H, Katanaev V, Jia L. Embedding similarities between embryos and circulating tumor cells: fundamentals of abortifacients used for cancer metastasis chemoprevention. J Exp Clin Cancer Res [Internet]. 2021 Sep 23;40(1):300.
42. Xu H, Wan L, Xu J, Liu J, Zheng N, Jia L. HAMPT, A Novel Quadruple Drug Combination Designed for Cancer Metastatic Chemoprevention: From Hypothesis to Proof-of-concept. Curr Cancer Drug Targets [Internet]. 2019;19(4):296–303.
43. Pantziarka P, Vandeborne L, Bouche G. A Database of Drug Repurposing Clinical Trials in Oncology. Front Pharmacol [Internet]. 2021 Nov 10;12.
44. Stein U, Arlt F, Walther W, Smith J, Waldman T, Harris ED, Mertins SD, Heizmann CW, Allard D, Birchmeier W, Schlag PM, Shoemaker RH. The Metastasis-Associated Gene S100A4 Is a Novel Target of ß-catenin/T-cell Factor Signaling in Colon Cancer. Gastroenterology. 2006;131(5):1486–500.
45. Sack U, Walther W, Scudiero D, Selby M, Kobelt D, Lemm M, Fichtner I, Schlag PM, Shoemaker RH, Stein U. Novel effect of antihelminthic niclosamide on s100a4-mediated metastatic progression in colon cancer. J Natl Cancer Inst. 2011;103(13):1018–36.
46. Stein U, Walther W, Arlt F, Schwabe H, Smith J, Fichtner I, Birchmeier W, Schlag PM. MACC1, a newly identified key regulator of HGF-MET signaling, predicts colon cancer metastasis. Nat Med [Internet]. 2009 Jan;15(1):59–67.
47. Juneja M, Kobelt D, Walther W, Voss C, Smith J, Specker E, Neuenschwander M, Gohlke BO, Dahlmann M, Radetzki S, Preissner R, von Kries JP, Schlag PM, Stein U. Statin and rottlerin small-molecule inhibitors restrict colon cancer progression and metastasis via MACC1. PLoS Biol [Internet]. 2017 Jun;15(6):e2000784.
48. Dahlmann M, Kobelt D, Walther W, Mudduluru G, Stein U. S100A4 in Cancer Metastasis: Wnt Signaling-Driven Interventions for Metastasis Restriction. Cancers (Basel) [Internet]. 2016 Jun 20;8(6):59.
49. Radhakrishnan H, Walther W, Zincke F, Kobelt D, Imbastari F, Erdem M, Kortüm B, Dahlmann M, Stein U. MACC1-the first decade of a key metastasis molecule from gene discovery to clinical translation. Cancer Metastasis Rev [Internet]. 2019 Jan 3;37(4):805–20.

50. Ashktorab H, Hermann P, Nouraie M, Shokrani B, Lee E, Haidary T, Brim H, Stein U. Increased MACC1 levels in tissues and blood identify colon adenoma patients at high risk. J Transl Med [Internet]. 2016 Dec 20;14(1):215.
51. Rohr UP, Herrmann P, Ilm K, Zhang H, Lohmann S, Reiser A, Muranyi A, Smith J, Burock S, Osterland M, Leith K, Singh S, Brunhoeber P, Bowermaster R, Tie J, Christie M, Wong HL, Waring P, Shanmugam K, Gibbs P, Stein U. Prognostic value of MACC1 and proficient mismatch repair status for recurrence risk prediction in stage II colon cancer patients: the BIOGRID studies. Ann Oncol Off J Eur Soc Med Oncol [Internet]. 2017 Aug 1;28(8):1869–75.
52. Stein U, Dahlmann M, Walther W. MACC1 - more than metastasis? Facts and predictions about a novel gene. J Mol Med [Internet]. 2010 Jan;88(1):11–8.
53. Schmid F, Wang Q, Huska MR, Andrade-Navarro MA, Lemm M, Fichtner I, Dahlmann M, Kobelt D, Walther W, Smith J, Schlag PM, Stein U. SPON2, a newly identified target gene of MACC1, drives colorectal cancer metastasis in mice and is prognostic for colorectal cancer patient survival. Oncogene [Internet]. 2015 Dec 21;(October):1–11.
54. Lemos C, Hardt MS, Juneja M, Voss C, Forster S, Jerchow B, Haider W, Blaker H, Stein U, Förster S, Jerchow B, Haider W, Bläker H, Stein U. MACC1 Induces Tumor Progression in Transgenic Mice and Colorectal Cancer Patients via Increased Pluripotency Markers Nanog and Oct4. Clin Cancer Res [Internet]. 2016 Jan 12;
55. Garrett SC, Varney KM, Weber DJ, Bresnick AR. S100A4, a Mediator of Metastasis. J Biol Chem [Internet]. 2006 Jan 13;281(2):677–80.
56. Garrett SC, Hodgson L, Rybin A, Toutchkine A, Hahn KM, Lawrence DS, Bresnick AR. A biosensor of S100A4 metastasis factor activation: inhibitor screening and cellular activation dynamics. Biochemistry [Internet]. 2008 Jan 22;47(3):986–96.
57. Ramagopal UA, Dulyaninova NG, Varney KM, Wilder PT, Nallamsetty S, Brenowitz M, Weber DJ, Almo SC, Bresnick AR. Structure of the S100A4/myosin-IIA complex. BMC Struct Biol [Internet]. 2013 Nov 20;13(8):31.
58. Dahlmann M, Okhrimenko A, Marcinkowski P, Osterland M, Herrmann P, Smith J, Heizmann CW, Schlag PM, Stein U. RAGE mediates S100A4-induced cell motility via MAPK/ERK and hypoxia signaling and is a prognostic biomarker for human colorectal cancer metastasis. Oncotarget [Internet]. 2014;5(10):3220–33.
59. Dahlmann M, Monks A, Harris ED, Kobelt D, Osterland M, Khaireddine F, Herrmann P, Kemmner W, Burock S, Walther W, Shoemaker RH, Stein U.

Combination of Wnt/β-Catenin Targets S100A4 and DKK1 Improves Prognosis of Human Colorectal Cancer. Cancers (Basel) [Internet]. 2021 Dec 22;14(1).

60. Schmidt-Hansen B, Klingelhöfer J, Grum-Schwensen B, Christensen A, Andresen S, Kruse C, Hansen T, Ambartsumian N, Lukanidin E, Grigorian M. Functional significance of metastasis-inducing S100A4(Mts1) in tumor-stroma interplay. J Biol Chem. 2004;279(23):24498–504.
61. Li ZH, Dulyaninova NG, House RP, Almo SC, Bresnick AR. S100A4 regulates macrophage chemotaxis. Mol Biol Cell [Internet]. 2010 Aug 1;21(15):2598–610.
62. Hoshino A, Costa-Silva B, Shen TL, Rodrigues G, Hashimoto A, Tesic Mark M, Molina H, Kohsaka S, Lyden D, et al. Tumour exosome integrins determine organotropic metastasis. Nature [Internet]. 2015 Nov 19;527(7578):329–35.
63. Peinado H, Alečković M, Lavotshkin S, Matei I, Costa-Silva B, Moreno-Bueno G, Hergueta-Redondo M, Williams C, García-Santos G, Ghajar C, Nitadori-Hoshino A, Hoffman C, Badal K, Garcia B a, Callahan MK, Yuan J, Martins VR, Skog J, Kaplan RN, Brady MS, Wolchok JD, Chapman PB, Kang Y, Bromberg J, Lyden D. Melanoma exosomes educate bone marrow progenitor cells toward a pro-metastatic phenotype through MET. Nat Med [Internet]. 2012 Jun [cited 2014 Jul 12];18(6):883–91.
64. Costa-Silva B, Aiello NM, Ocean AJ, Singh S, Zhang H, Thakur BK, Becker A, Hoshino A, Mark MT, Molina H, Xiang J, Zhang T, Theilen TM, García-Santos G, Williams C, Ararso Y, Huang Y, Rodrigues G, Shen TL, Labori KJ, Lothe IMB, Kure EH, Hernandez J, Doussot A, Ebbesen SH, Grandgenett PM, Hollingsworth MA, Jain M, Mallya K, Batra SK, Jarnagin WR, Schwartz RE, Matei I, Peinado H, Stanger BZ, Bromberg J, Lyden D. Pancreatic cancer exosomes initiate pre-metastatic niche formation in the liver. Nat Cell Biol [Internet]. 2015 Jun 18;17(6):816–26.
65. Stein U, Burock S, Herrmann P, Wendler I, Niederstrasser M, Wernecke KDD, Schlag PM. Circulating MACC1 transcripts in colorectal cancer patient plasma predict metastasis and prognosis. PLoS One [Internet]. 2012;7(11):e49249.
66. Burock S, Herrmann P, Wendler I, Niederstrasser M, Wernecke KD, Stein U. Circulating Metastasis Associated in Colon Cancer 1 transcripts in gastric cancer patient plasma as diagnostic and prognostic biomarker. World J Gastroenterol [Internet]. 2015 Jan 7;21(1):333–41.
67. Link T, Kuhlmann JD, Kobelt D, Herrmann P, Vassileva YD, Kramer M, Frank K,

Göckenjan M, Wimberger P, Stein U. Clinical relevance of circulating MACC1 and S100A4 transcripts for ovarian cancer. Mol Oncol. 2019 May;13(5):1268–79.

68. Kanashova T, Popp O, Orasche J, Karg E, Harndorf H, Stengel B, Sklorz M, Streibel T, Zimmermann R, Dittmar G. Differential proteomic analysis of mouse macrophages exposed to adsorbate-loaded heavy fuel oil derived combustion particles using an automated sample-preparation workflow. Anal Bioanal Chem [Internet]. 2015 Aug;407(20):5965–76.
69. Cox J, Mann M. MaxQuant enables high peptide identification rates, individualized p.p.b.-range mass accuracies and proteome-wide protein quantification. Nat Biotechnol [Internet]. 2008 Dec;26(12):1367–72.
70. UniProt: a worldwide hub of protein knowledge. Nucleic Acids Res. 2019 Jan;47(D1):D506–15.
71. Cox J, Neuhauser N, Michalski A, Scheltema RA, Olsen J V, Mann M. Andromeda: a peptide search engine integrated into the MaxQuant environment. J Proteome Res [Internet]. 2011 Apr 1;10(4):1794–805.
72. 3.5.1. RDCT. A Language and Environment for Statistical Computing. R Found Stat Comput. 2018;2:https://www.R-project.org.
73. Tsuji S, Midorikawa Y, Takahashi T, Yagi K, Takayama T, Yoshida K, Sugiyama Y, Aburatani H. Potential responders to FOLFOX therapy for colorectal cancer by Random Forests analysis. Br J Cancer [Internet]. 2012 Jan 3;106(1):126–32.
74. Tsukamoto S, Ishikawa T, Iida S, Ishiguro M, Mogushi K, Mizushima H, Uetake H, Tanaka H, Sugihara K. Clinical significance of osteoprotegerin expression in human colorectal cancer. Clin Cancer Res [Internet]. 2011 Apr 15;17(8):2444–50.
75. Schütte M, Risch T, Abdavi-Azar N, Boehnke K, Schumacher D, Keil M, Yildiriman R, Jandrasits C, Borodina T, Amstislavskiy V, Worth CL, Schweiger C, Liebs S, Lange M, Warnatz HJ, Butcher LM, Barrett JE, Sultan M, Wierling C, Golob-Schwarzl N, Lax S, Uranitsch S, Becker M, Welte Y, Regan JL, Silvestrov M, Kehler I, Fusi A, Kessler T, Herwig R, Landegren U, Wienke D, Nilsson M, Velasco JA, Garin-Chesa P, Reinhard C, Beck S, Schäfer R, Regenbrecht CRA, Henderson D, Lange B, Haybaeck J, Keilholz U, Hoffmann J, Lehrach H, Yaspo ML. Molecular dissection of colorectal cancer in pre-clinical models identifies biomarkers predicting sensitivity to EGFR inhibitors. Nat Commun. 2017;8:14262.
76. Handeli S, Simon JA. A small-molecule inhibitor of Tcf/beta-catenin signaling down-regulates PPARgamma and PPARdelta activities. Mol Cancer Ther [Internet]. 2008

Mar 1;7(3):521–9.

77. Fang L, Zhu Q, Neuenschwander M, Specker E, Wulf-Goldenberg A, Weis WI, Von Kries JP, Birchmeier W. A small-molecule antagonist of the β-catenin/TCF4 interaction blocks the self-renewal of cancer stem cells and suppresses tumorigenesis. Cancer Res. 2016;76(4):891–901.
78. Malashkevich VN, Dulyaninova NG, Ramagopal UA, Liriano MA, Varney KM, Knight D, Brenowitz M, Weber DJ, Almo SC, Bresnick AR. Phenothiazines inhibit S100A4 function by inducing protein oligomerization. Proc Natl Acad Sci [Internet]. 2010 May 11;107(19):8605–10.
79. Nair AB, Jacob S. A simple practice guide for dose conversion between animals and human. J basic Clin Pharm [Internet]. 2016 Mar;7(2):27–31.
80. Di Veroli GY, Fornari C, Wang D, Mollard S, Bramhall JL, Richards FM, Jodrell DI. Combenefit: an interactive platform for the analysis and visualization of drug combinations. Bioinformatics [Internet]. 2016;32(18):2866–8.
81. Flatmark K, Maelandsmo GM, Mikalsen SO, Nustad K, Varaas T, Rasmussen H, Meling GI, Fodstad Ø, Paus E. Immunofluorometric assay for the metastasis-related protein S100A4: release of S100A4 from normal blood cells prohibits the use of S100A4 as a tumor marker in plasma and serum. Tumour Biol [Internet]. 25(1–2):31–40.
82. Peng T, Zamanian R, Krowka MJ, Benza RL, Roberts KE, Taichman DB, Rybak D, Trotter JF, Brown RS, Fallon MB, Kawut SM, Pulmonary Vascular Complications of Liver Disease Study Group. Plasma levels of S100A4 in portopulmonary hypertension. Biomarkers [Internet]. 2009 May;14(3):156–60.
83. Choi DS, Choi DY, Hong BS, Jang SC, Kim DK, Lee J, Kim YK, Kim KP, Gho YS. Quantitative proteomics of extracellular vesicles derived from human primary and metastatic colorectal cancer cells. J Extracell vesicles [Internet]. 2012;1.
84. Zaimenko I, Jaeger C, Brenner H, Chang-Claude J, Hoffmeister M, Grötzinger C, Detjen K, Burock S, Schmitt CA, Stein U, Lisec J. Non-invasive metastasis prognosis from plasma metabolites in stage II colorectal cancer patients: The DACHS study. Int J cancer [Internet]. 2019;145(1):221–31.
85. Hou J, Li X, Xie KP. Coupled liquid biopsy and bioinformatics for pancreatic cancer early detection and precision prognostication. Mol Cancer [Internet]. 2021;20(1):34.
86. Kobelt D, Dahlmann M, Dumbani M, Güllü N, Kortüm B, Vílchez MEA, Stein U, Walther W. Small Ones to Fight a Big Problem-Intervention of Cancer Metastasis

by Small Molecules. Cancers (Basel) [Internet]. 2020 Jun 3;12(6).

87. Kortüm B, Radhakrishnan H, Zincke F, Sachse C, Burock S, Keilholz U, Dahlmann M, Walther W, Dittmar G, Kobelt D, Stein U. Combinatorial treatment with statins and niclosamide prevents CRC dissemination by unhinging the MACC1-β-catenin-S100A4 axis of metastasis. Oncogene [Internet]. 2022 Aug 25;

Statutory Declaration

“I, Benedikt Kortüm, by personally signing this document in lieu of an oath, hereby affirm that I prepared the submitted dissertation on the topic : „Repositioned drugs against the MACC1-β-catenin-S100A4 axis of metastasis suppress colon cancer metastasis in a synergistic manner“ / „Repositionierte Arzneistoffe gegen die MACC1-β-Catenin-S100A4-Achse der Metastasierung unterdrücken Darmkrebsmetastasen in synergistischer Weise“, independently and without the support of third parties, and that I used no other sources and aids than those stated.

All parts which are based on the publications or presentations of other authors, either in letter or in spirit, are specified as such in accordance with the citing guidelines. The sections on methodology (in particular regarding practical work, laboratory regulations, statistical processing) and results (in particular regarding figures, charts and tables) are exclusively my responsibility.

Furthermore, I declare that I have correctly marked all of the data, the analyses, and the conclusions generated from data obtained in collaboration with other persons, and that I have correctly marked my own contribution and the contributions of other persons (cf. declaration of contribution). I have correctly marked all texts or parts of texts that were generated in collaboration with other persons.

My contributions to any publications to this dissertation correspond to those stated in the below joint declaration made together with the supervisor. All publications created within the scope of the dissertation comply with the guidelines of the ICMJE (International Committee of Medical Journal Editors; www.icmje.org) on authorship. In addition, I declare that I shall comply with the regulations of Charité – Universitätsmedizin Berlin on ensuring good scientific practice.

I declare that I have not yet submitted this dissertation in identical or similar form to another Faculty.

The significance of this statutory declaration and the consequences of a false statutory declaration under criminal law (Sections 156, 161 of the German Criminal Code) are known to me.”

Date	Signature

Contribution in detail

Benedikt Kortüm, contributed to the following publication:

Benedikt Kortüm, Harikrishnan Radhakrishnan, Fabian Zincke, Christoph Sachse, Susen Burock, Ulrich Keilholz, Mathias Dahlmann, Wolfgang Walther, Gunnar Dittmar, Dennis Kobelt, Ulrike Stein. Combinatorial treatment with statins and niclosamide prevents CRC dissemination by unhinging the MACC1-β-catenin-S100A4 axis of metastasis. Oncogene. 2022 Aug 25;
http://dx.doi.org/10.1038/s41388-022-02407-6

Contribution in detail:
I, Benedikt Kortüm, evaluated the data on the induction of CRC cell migration by the MACC1-specific secretome and compiled Fig. 1A-D. I further generated Fig. 1F, which supports Figure 1E (provided by G. Dittmar and U. Stein). I proved coinciding MACC1 and S100A4 immunoreactivity in human CRC tumor sections (Fig. 2A,), and I demonstrated correlating RNA expression of MACC1 and S100A4 in two publicly available cohorts (Tsuji et al. and Tsukamoto et al.) and an additional unpublished dataset (EFRE and Keilholz et al.) of CRC tumor specimens (Fig. 2B-D). I performed the Kaplan-Meier estimates on the prognostic value of MACC1 and S100A4 expression in tumor and blood samples (Fig. 2E and 2F). Taking advantage of a MACC1-overexpressing cell model available in the laboratory, and a MACC1-knock-out cell line established by me, I show MACC1-dependent regulation of S100A4 (Fig. 3A). I found MACC1-dependent regulation of S100a4 in vil-MACC1-ApcMin mice (immunohistochemistry and RT-qPCR, Fig. 3B-D). I found that MACC1 depends on S100A4 to promote cell migration, and that knock-out or pharmacological inhibition of S100A4 suppresses this effect (Fig. 4A-C). Using three different small-molecule inhibitors, I found that MACC1 employs Wnt/β-catenin signaling to upregulate S100A4 (Fig. 4D). I proved direct protein-protein interaction of MACC1 and β-catenin (Fig. 5B and 5C), and that MACC1 induces Wnt/β-catenin signaling in promoter reporter assays and in RNA expression of the target genes Cyclin-D1, MMP7 and S100A4 (Fig. 5D). In Fig. 5E and 5F I elucidate the enforcement of β-catenin-dependent transcription through phosphorylation and interaction with TCF4.
I prepared the entire manuscript, which was read and critically reviewed by Prof. Stein and Dr. Kobelt. I also handled the revision process following peer-review including the commission of additional experimental proofs, and manuscript revision.

The final version of the manuscript was read and approved by all co-authors prior to publication.

_____

Signature of the doctorate student

Excerpt of the Journal Summary List 2020

Journal: Oncogene Impact Factor: 8.756 Eigenfaktor Score: 0.05014

Category: Oncology Rank: 30/242 (JCR Year 2020)

Journal Data Filtered By: **Selected JCR Year: 2020** Selected Editions: SCIE,SSCI
Selected Categories: **"ONCOLOGY"** Selected Category Scheme: WoS
Gesamtanzahl: 242 Journale

Rank	Full Journal Title	Total Cites	Journal Impact Factor	Eigenfactor Score
1	CA-A CANCER JOURNAL FOR CLINICIANS	55,868	508.702	0.105140
2	Nature Reviews Clinical Oncology	17,973	66.675	0.038760
3	NATURE REVIEWS CANCER	62,391	60.716	0.059170
4	JOURNAL OF CLINICAL ONCOLOGY	189,443	44.544	0.249030
5	LANCET ONCOLOGY	72,804	41.316	0.138530
6	Cancer Discovery	27,030	39.397	0.072460
7	ANNALS OF ONCOLOGY	61,542	32.976	0.117180
8	JAMA Oncology	22,382	31.777	0.080430
9	CANCER CELL	50,839	31.743	0.081040
10	Molecular Cancer	24,931	27.401	0.030030
11	Journal of Hematology & Oncology	10,615	17.388	0.018360
12	SEMINARS IN CANCER BIOLOGY	11,552	15.707	0.012110
13	Journal of Thoracic Oncology	24,405	15.609	0.042780
14	Trends in Cancer	4,237	14.226	0.012440
15	Journal for ImmunoTherapy of Cancer	11,042	13.751	0.028830
16	JNCI-Journal of the National Cancer Institute	42,005	13.506	0.038260
17	CANCER RESEARCH	159,236	12.701	0.105150
18	CLINICAL CANCER RESEARCH	105,958	12.531	0.131040
19	NEURO-ONCOLOGY	17,812	12.300	0.029210
20	CANCER TREATMENT REVIEWS	11,834	12.111	0.016910

Rank	Full Journal Title	Total Cites	Journal Impact Factor	Eigenfactor Score
21	Journal of the National Comprehensive Cancer Network	10,050	11.908	0.021920
22	Liver Cancer	1,579	11.740	0.002800
23	LEUKEMIA	34,181	11.528	0.045940
24	Clinical and Translational Medicine	2,201	11.492	0.003110
25	JOURNAL OF EXPERIMENTAL & CLINICAL CANCER RESEARCH	16,717	11.161	0.023310
26	Cancer Immunology Research	11,185	11.151	0.027290
27	Blood Cancer Journal	4,691	11.037	0.011440
28	BIOCHIMICA ET BIOPHYSICA ACTA-REVIEWS ON CANCER	7,025	10.680	0.007000
29	Cancer Communications	1,307	10.392	0.002530
30	ONCOGENE	77,576	9.867	0.059180
31	Annual Review of Cancer Biology-Series	703	9.391	0.002910
32	CANCER AND METASTASIS REVIEWS	7,809	9.264	0.006010
33	EUROPEAN JOURNAL OF CANCER	40,294	9.162	0.046490
34	CANCER LETTERS	42,174	8.679	0.040130
35	npj Precision Oncology	931	8.254	0.002500
36	Therapeutic Advances in Medical Oncology	3,021	8.168	0.005350
37	OncoImmunology	14,987	8.110	0.030230
38	JOURNAL OF PATHOLOGY	22,441	7.996	0.017610
39	BRITISH JOURNAL OF CANCER	54,924	7.640	0.042070
40	Oncogenesis	4,065	7.485	0.008320
41	European Urology Oncology	1,413	7.479	0.004350

Selected JCR Year: 2020; Selected Categories: "ONCOLOGY"

Selected publication

Combinatorial treatment with statins and niclosamide prevents CRC dissemination by unhinging the MACC1-β-catenin-S100A4 axis of metastasis

Benedikt Kortüm, Harikrishnan Radhakrishnan, Fabian Zincke, Christoph Sachse, Susen Burock, Ulrich Keilholz, Mathias Dahlmann, Wolfgang Walther, Gunnar Dittmar, Dennis Kobelt, Ulrike Stein

Oncogene (2022) 41:4446–4458; https://doi.org/10.1038/s41388-022-02407-6

www.nature.com/onc Oncogene

ARTICLE OPEN

Check for updates

Combinatorial treatment with statins and niclosamide prevents CRC dissemination by unhinging the MACC1-β-catenin-S100A4 axis of metastasis

Benedikt Kortüm[1], Harikrishnan Radhakrishnan[1], Fabian Zincke[1,2], Christoph Sachse[3], Susen Burock[4], Ulrich Keilholz[4], Mathias Dahlmann[1,2], Wolfgang Walther[1], Gunnar Dittmar[5], Dennis Kobelt[1,2,5,6] and Ulrike Stein[1,2,6]✉

Colorectal cancer (CRC) is the second-most common malignant disease worldwide, and metastasis is the main culprit of CRC-related death. Metachronous metastases remain to be an unpredictable, unpreventable, and fatal complication, and tracing the molecular chain of events that lead to metastasis would provide mechanistically linked biomarkers for the maintenance of remission in CRC patients after curative treatment. We hypothesized, that Metastasis-associated in colorectal cancer-1 (MACC1) induces a secretory phenotype to enforce metastasis in a paracrine manner, and found, that the cell-free culture medium of MACC1-expressing CRC cells induces migration. Stable isotope labeling by amino acids in cell culture mass spectrometry (SILAC-MS) of the medium revealed, that S100A4 is significantly enriched in the MACC1-specific secretome. Remarkably, both biomarkers correlate in expression data of independent cohorts as well as within CRC tumor sections. Furthermore, combined elevated transcript levels of the metastasis genes MACC1 and S100A4 in primary tumors and in blood plasma robustly identifies CRC patients at high risk for poor metastasis-free (MFS) and overall survival (OS). Mechanistically, MACC1 strengthens the interaction of β-catenin with TCF4, thus inducing S100A4 synthesis transcriptionally, resulting in elevated secretion to enforce cell motility and metastasis. In cell motility assays, S100A4 was indispensable for MACC1-induced migration, as shown via knock-out and pharmacological inhibition of S100A4. The direct transcriptional and functional relationship of MACC1 and S100A4 was probed by combined targeting with repositioned drugs. In fact, the MACC1-β-catenin-S100A4 axis by statins (MACC1) and niclosamide (S100A4) synergized in inhibiting cancer cell motility in vitro and metastasis in vivo. The MACC1-β-catenin-S100A4 signaling axis is causal for CRC metastasis. Selectively repositioned drugs synergize in restricting MACC1/S100A4-driven metastasis with cross-entity potential.

Oncogene (2022) 41:4446–4458; https://doi.org/10.1038/s41388-022-02407-6

INTRODUCTION

CRC is second in tumor incidence and cancer lethality worldwide. Metastatic spread accounts for over 90% of deaths in CRC patients, despite improvements of surgical and adjuvant treatments [1–3]. About 30% of CRC patients without metastases at diagnosis (UICC stage I-III) are expected to develop metachronous metastases in distant organs. Identifying these high risk CRC patients for targeted therapy to prevent relapse remains an unmet clinical need [4].

Upregulation of MACC1 in primary tumors is linked to metachronous metastasis and, independently of the stage of disease, predicts poor metastasis-free survival in CRC and more than 20 other solid tumor entities [5, 6].

MACC1 itself has been identified as an inducer of CRC metastasis through several distinct mechanism [5]. The proto-oncogene MET is induced transcriptionally by MACC1, leading to stabilized HGF/MET signaling [5, 7]. Structurally, the MACC1 molecule serves as a scaffold for MEK1, leading to prolonged and potentiated ERK1 activation [8]. Furthermore, MACC1 promotes the dynamin-dependent restoration of the growth factor receptor EGFR in the cell membrane [9, 10]. These capabilities fuel various cancer hallmarks, such as enhanced survival, proliferation, motility, and metastasis of cancer [6, 11–15].

We have reported previously that the widely used statin drugs effectively downregulate MACC1 expression in CRC cells, accompanied with potent anti-migratory and metastasis-preventive effects in vivo [16–18].

CRC is frequently initiated by hyperactivated Wnt/β-catenin signaling due to loss of APC function or gain of β-catenin function. This allows β-catenin to accumulate in the cytoplasm and to translocate into the nucleus, where it activates Wnt target genes that sustain cell proliferation, motility, and stemness [19, 20]. Additionally, a variety of kinases stabilize β-catenin, resulting in enforcement of its transcriptional effects on cancer promoting target genes [21–23]. The metastasis driver S100A4, one of the calcium binding S100 proteins, is regulated transcriptionally by Wnt/β-catenin signaling [24]. Restriction of β-catenin-dependent

[1]Experimental and Clinical Research Center, Charité—Universitätsmedizin Berlin and Max-Delbrück-Center for Molecular Medicine in the Helmholtz Association, Berlin, Germany. [2]German Cancer Consortium (DKTK), Heidelberg, Germany. [3]NMI-TT Pharmaservices, Berlin, Germany. [4]Charité University Hospital Berlin Centre 10 Charite Comprehensive Cancer Center, Berlin, Germany. [5]Max-Delbrück-Center for Molecular Medicine in the Helmholtz Association, Berlin, Germany. [6]These authors contributed equally: Dennis Kobelt, Ulrike Stein. ✉email: ustein@mdc-berlin.de

Received: 19 December 2021 Revised: 30 June 2022 Accepted: 1 July 2022
Published online: 25 August 2022

expression of S100A4 results in reduced cell motility and prevents metastasis formation in vivo [25, 26]. Intracellularly, S100A4 increases cell motility by interacting with the cytoskeletal proteins F-actin and non-muscle myosin-IIa [27, 28]. In the extracellular space, secreted S100A4 enhances MEK-ERK signaling via its binding to RAGE [29]. It was also reported to shape the premetastatic niche in vivo, and to crucially determine organotropism of solid cancer metastasis [30–32]. As a versatile enforcer of cancer progression and metastasis, S100A4 is a stage-independent predictor for metachronous metastasis in CRC and other solid tumor entities [24, 33].

We were able to demonstrate that circulating transcripts of MACC1 and S100A4 are detectable in blood of cancer patients and serve as reliable biomarkers for OS and MFS. Combined elevation of MACC1 and S100A4 identified patients with the highest risk for unfavorable prognosis in CRC, gastric, and ovarian cancer [34–36]. These findings led us to investigate a potential novel functional link between the strong prognostic markers MACC1 and S100A4. We discovered that through β-catenin signaling, MACC1 directly induces S100A4 expression and secretion, and further mediates MACC1 pro-migratory effect on cancer cells through S100A4 as the enforcing molecule. Here we report on a novel MACC1-β-catenin-S100A4 axis and demonstrate that, based on this rationale, combined transcriptional inhibition of MACC1 and S100A4 restricts cancer cell motility and metastasis in CRC with seminal cross entity potential for cancer therapy.

RESULTS

MACC1 expression stimulates cell motility via secreted proteins

We hypothesized that MACC1-overexpressing tumor cells stimulate cell migration by secretion of pro-metastatic factors. Cell-free culture supernatants from SW480/vector cells, two independent SW480/MACC1 clones (#10, #43) expressing MACC1 ectopically, or SW620 cells, which express high intrinsic MACC1 levels, were added to the CRC cell line SW480, which intrinsically expresses minimal amounts of MACC1. After 48 hours of exposure to MACC1-conditioned medium, the motility of SW480 cells was assessed in Boyden chamber assays. The supernatant of MACC1-overexpressing cells increased the transwell migration capacity of SW480 cells, while the control culture exposed to SW480/vector medium demonstrated poor motility (Fig. 1A). This was verified in three additional CRC cells lines (Fig. 1B). The medium of SW620 cells showed only minor efficacy to induce cell migration in SW480, HCT116, HT-29 and LS174T. Knockdown of MACC1 in SW620 cells (SW620/shMACC1) led to a reduction of migration compared to SW620/shCtrl. None of the conditioned media yielded significant effects on the motility of SW620/shCtrl cells. Intriguingly, SW480/MACC1-conditioned medium failed to rescue migration in SW620/shMACC1 cells, while medium from wildtype SW620 significantly increased migration in SW620/shMACC1 cells (Fig. 1C). MACC1 baseline expression is lowest in SW480 and highest in SW620 cells. HCT116, HT-29 and LS174T feature moderate expression of MACC1. S100A4 is stably expressed in all cell lines, with the highest expression in SW620 cells (Fig. 1D). We carried out a mass-spectrometric SILAC analysis to identify the active principles of the MACC1-specific secretome of SW480/MACC1 cells (vs. SW480/vector cells) (Fig. 1E). Soluble S100A4 was amongst the de novo secreted proteins in MACC1-conditioned cell medium. The increase of S100A4 secretion by SW480/MACC1 cells was confirmed by direct western blotting from cell culture medium (Fig. 1F).

Combination of MACC1 and S100A4 robustly identifies high risk CRC patients

To test whether MACC1-dependent expression of S100A4 is a clinically prevalent phenomenon in CRC, we detected both markers by IHC in representative tumor sections from a previously published cohort. Non-metastasized primary CRC tumors presented a low immunoreactivity for MACC1 and S100A4. Primary tumors associated with metachronous metastases strongly expressed both MACC1 and S100A4 (Fig. 2A). To further validate the co-expression of MACC1 and S100A4 in CRC samples, we correlated both genes in three independent CRC patient cohorts [37–39]. In all cohorts MACC1 and S100A4 showed a significant positive correlation (Spearman-$\rho = 0.392$, $p = 0.009$; Spearman-$\rho = 0.431$, $p = 0.001$; Spearman-$\rho = 0.317$, $p < 0.001$, respectively) (Fig. 2B–D). Since both markers have been reported individually as stage-independent prognostic biomarkers across multiple cancer entities, we assessed the combined prognostic value of MACC1 and S100A4 for MFS and OS. We quantified mRNA levels of MACC1 and S100A4 in primary tumors from a cohort of 60 CRC patients (UICC stage I-III), and of a plasma sample set from a previously published cohort of CRC patients, with RT-qPCR. Based on these data we established respective cut-off values for the primary endpoints "metachronous metastasis" and "death" [5, 34]. Within the primary tumor cohort, the subgroup "MACC1 and S100A4 high" experienced the shortest MFS, while the subgroup "MACC1 and S100A4 low" showed the longest MFS (median follow up: 167.2 months; median MFS of 69 and 131 months, respectively; $p < 0.0001$; Fig. 2E). Similarly, the subgroup "MACC1 and S100A4 high" experienced the shortest OS, while the subgroup "MACC1 and S100A4 low" showed the longest OS ($p = 0.0025$; Fig. 2E). We extended the follow-up on patient survival in the liquid biopsy cohort, and found that also here, combined increased expression of MACC1 and S100A4 was associated with poor OS, while low expression of both markers was found in the subgroup with favorable OS (median follow up: 27.5 months; mean OS of 70 and 111 months, respectively; $p = 0.007$; Fig. 2F).

These findings strongly suggest the existence of a hitherto unknown mechanistic link between MACC1 and S100A4 in metastasis.

MACC1 induces S100A4

The observation of correlated MACC1 and S100A4 expression and activity prompted the examination of a causal link between these initially unrelated mediators of metastasis. Regulation of S100A4 expression by MACC1 was examined with a luciferase-based reporter for S100A4 promoter activity, and at S100A4 mRNA and protein level. In HCT116 cells with endogenously low MACC1 expression, ectopic MACC1 overexpression induced luciferase activity in TOP-flash assays and S100A4-promoter reporter plasmids. This is complemented by increased S100A4 mRNA and protein levels (Fig. 3A, top row). Conversely, CRISPR-Cas9-mediated knockout of MACC1 in SW620 cells with endogenous high MACC1 expression led to decreased TOP-flash and S100A4-promoter activity and concomitant downregulation of S100A4 mRNA and protein (Fig. 3A, bottom row). Additionally, we examined the Apc^{Min} mouse model of APC/β-catenin-dependent intestinal tumors for susceptibility of such effects of MACC1 in vivo by means of IHC and RT-qPCR. In randomly selected tumors of our previously published vil-MACC1/Apc^{Min} mouse model [12], mouse-intrinsic S100a4 (mS100a4) was significantly increased at protein (Fig. 3B) and mRNA level (Fig. 3C) compared to Apc^{Min} littermates, that lack villin-dependent MACC1 overexpression (Fig. 3D).

MACC1 employs S100A4 through β-catenin signaling to drive cancer cell motility

To investigate whether MACC1-induced cell motility is directly mediated by S100A4, we studied the effect of MACC1 overexpression in S100A4-depleted cells. S100A4 was knocked out in HCT116 cells using CRISPR-Cas9 technology, while cells transfected with Cas9 and without sgRNA served as empty vector control (Cas9-ev). MACC1 was overexpressed in both S100A4 competent (Cas9-ev) and in S100A4 deficient (S100A4-KO) HCT116 cells. MACC1 increased transwell migration capability in Cas9-ev

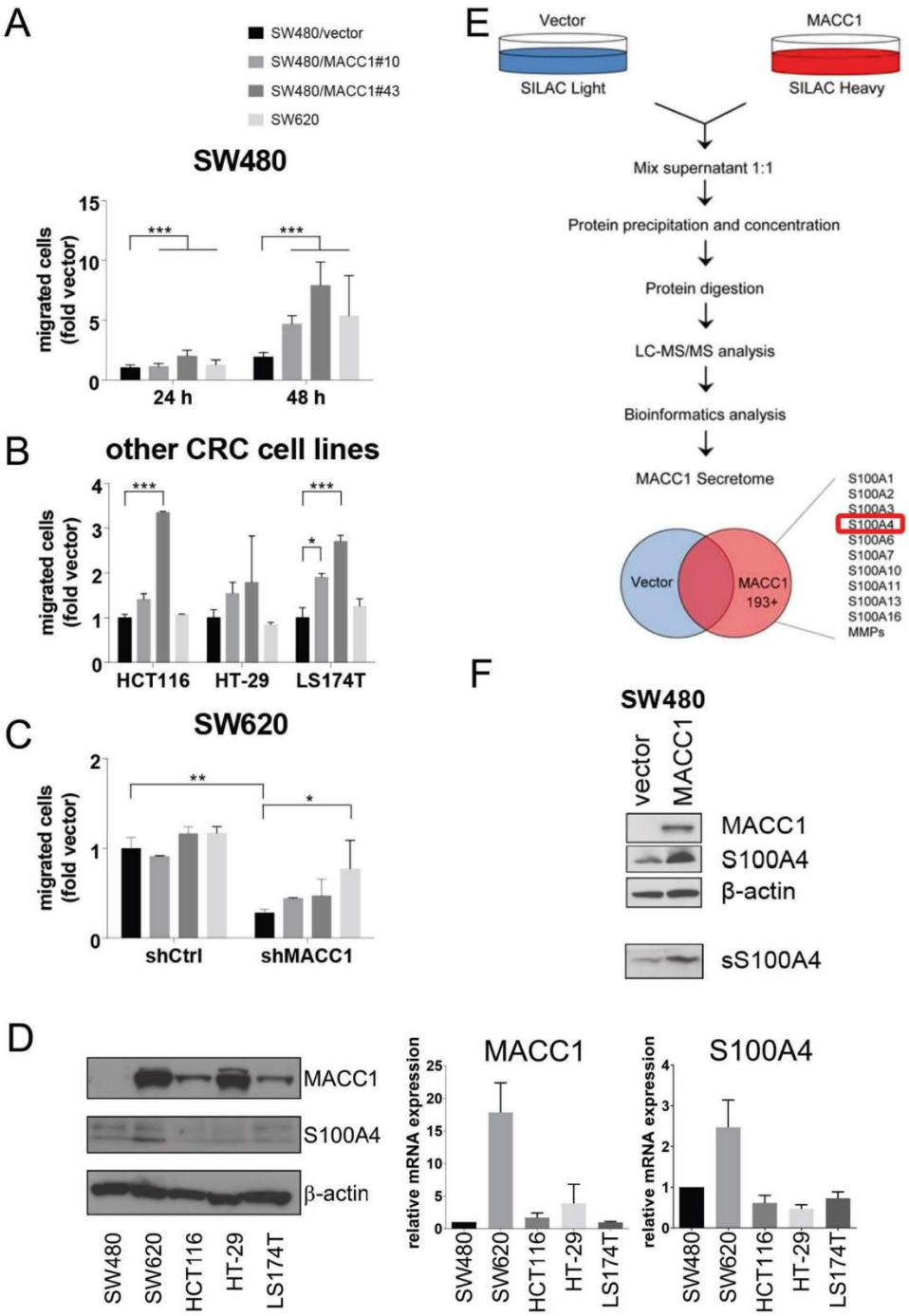

Fig. 1 The MACC1 secretome induces CRC cell migration via S100A4. Culture medium of MACC1-overexpressing cells stimulated migration of SW480 cells (**A**), and in HCT116, HT-29 and LS174T (**B**). The same culture supernatants rescued migration of SW620/shMACC1 that was diminished after depletion of MACC1 (**C**). Baseline protein (left) and mRNA (right) expression of MACC1 and S100A4 in the human colon carcinoma cell lines SW480, SW620, HCT116, HT-29 and LS174T (**D**). In a SILAC analysis of cell culture medium of SW480/vector and SW480/MACC1 cells, S100 proteins were secreted de novo in MACC1-overexpressing cells (**E**). Western blot from cell culture supernatant (sample volume proportional to respective cell count at time of medium harvest) confirmed increased presence of soluble S100A4 (sS100A4) in the secretome of SW480/MACC1 cells (**F**). Numeric results shown means ± SEM of 3 independent experiments, test for significance with ANOVA and Tukey correction for multiple testing.

cells. No statistically significant change in the S100A4-KO cells' migratory ability was seen, which demonstrated overall reduced motility (Fig. 4A). We inhibited S100A4 with its transcriptional inhibitor niclosamide and found significant reduction of transwell migration in HCT116/MACC1 and SW480/MACC1 cells, but not in HCT116/vector or SW480/vector cells, respectively (Fig. 4B, C). Prochlorpromazine, an FDA-approved phenothiazine drug and potent inhibitor of S100A4 interaction with myosin, proved similarly effective in migration inhibition (Fig. S1A) [40, 41]. Using knockout as well as pharmacological inhibition of S100A4 we show that MACC1-induced cell motility is largely dependent on S100A4 expression and function. S100A4 is a β-catenin signaling

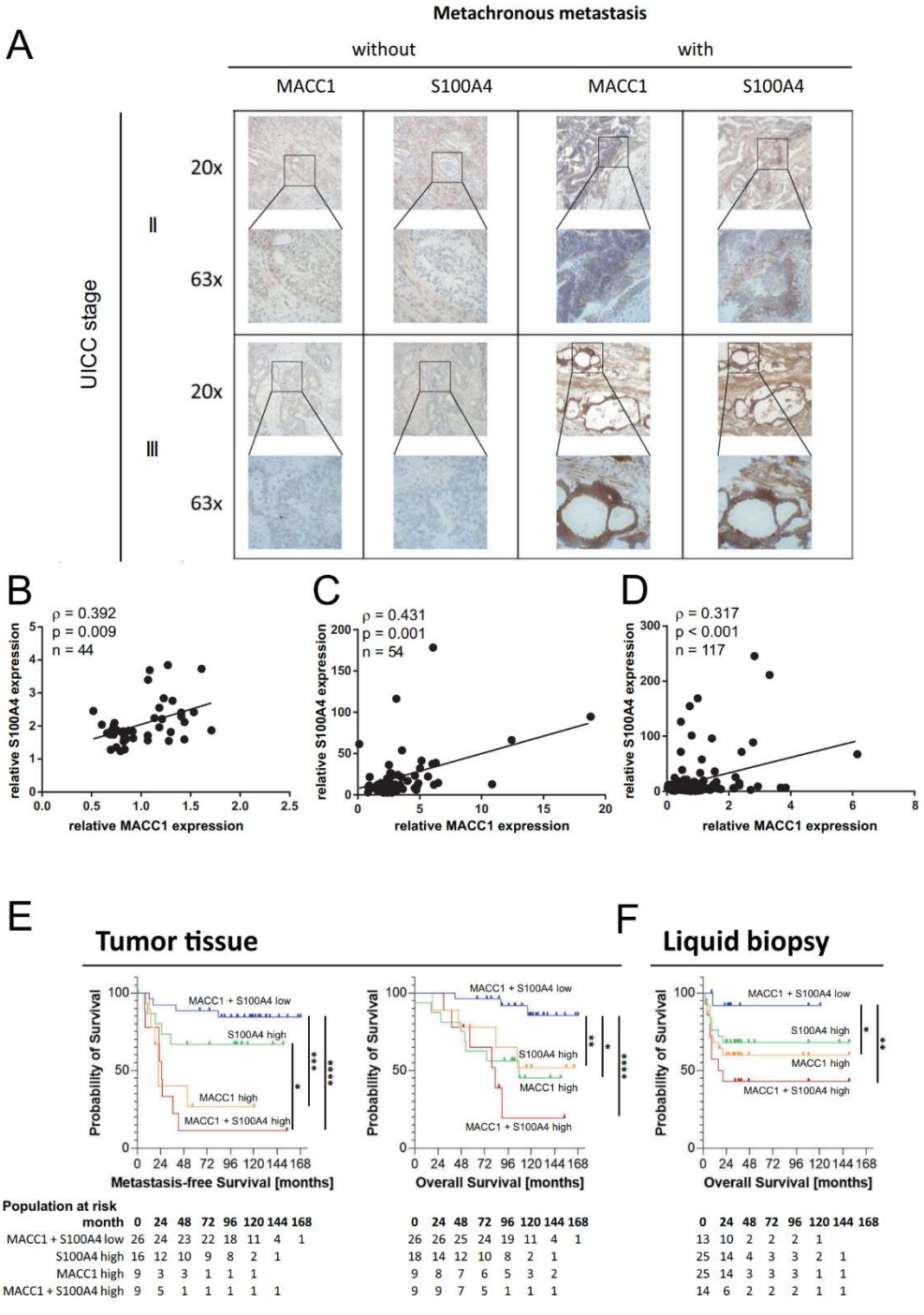

Fig. 2 MACC1 and S100A4 robustly identify high risk CRC patients. IHC of MACC1 and S100A4 in each 2 tumors of non-metastasized and metachronously metastasized primary tumors confirms overexpression of both biomarkers in CRC that yielded metachronous metastases well after surgical removal of the primary tumor (**A**). MACC1 and S100A4 expressions correlate in CRC tumors. Gene expression levels were analyzed in three additional cohorts of 44, 54 and 117 CRC tumors, respectively. Co-expression was examined with Spearman correlation, and we found a positive correlation of MACC1 and S100A4 expression levels in all datasets (**B**–**D**). Kaplan–Meier analysis for MFS and OS of patients based on the MACC1-S100A4 combination panel, test for significance with log rank (Mantel-Cox) test. Combined overexpression of MACC1 and S100A4 was associated with dismal MFS and OS in primary CRC tumors (**E**), and high levels of MACC1 and S100A4 mRNA transcripts detected in liquid biopsies (preoperative blood samples) predicted poor OS (**F**). Significant intergroup differences are indicated with asterisks, where applicable.

target gene itself [24]. Therefore, we tested whether β-catenin inhibitors would intercept the MACC1-dependent upregulation of S100A4. Indeed, niclosamide [25] and two other β-catenin inhibitors FH535 [42] and LF3 [43] hindered the upregulation of S100A4 in MACC1-overexpressing cells at mRNA and protein level in HCT116 cells (Fig. 4D). In SW480 cells, niclosamide dose-dependently downregulated the expression of S100A4 in both MACC1-overexpressing cells and in vector-transfected cells (Fig. S1B). These findings support that MACC1 regulates S100A4 expression through β-catenin/TCF4 signaling, creating the MACC1-β-catenin-S100A4 signaling axis.

MACC1 binds to β-catenin and stabilizes its interaction with TCF4

To comprehensively describe MACC1 interactions within β-catenin signaling we employed mass-spectrometry on co-immunoprecipitated MACC1 interaction partners and determined the MACC1-interactome. Intriguingly, we found β-catenin as an interaction partner of MACC1 (Fig. 5A). Co-Immunoprecipitation (Co-IP) experiments confirmed this protein-protein interaction (PPI) in whole cell lysates as well as in cytoplasmic and nuclear fractions (Fig. 5B). To probe whether this PPI is of direct nature or through other proteins, recombinant human MACC1 and β-catenin were co-incubated in an equimolar ratio in lysis buffer to carry out cell-free Co-IP experiments. Indeed, IP of MACC1 did precipitate β-catenin protein and vice versa, indicating that MACC1 and β-catenin maintain a direct PPI (Fig. 5C). We speculated that MACC1 interacts with β-catenin to mediate its posttranslational stabilization and transcriptional activity. While MACC1 overexpression increased the activity of the TOP-flash reporter for β-catenin/TCF4 signaling, mRNA levels of β-catenin where not affected. However, its target genes S100A4, cyclin-D1 and MMP7 were upregulated by MACC1 (Fig. 5D). Using DigiWest technology, we detected increased phosphorylation of β-catenin on Ser-552 (Fig. 5E), a post-translational modification (PTM) linked to stabilization and enhanced binding to TCF4, which was confirmed by western blot (Fig. 5F). In summary, MACC1 facilitates the phosphorylation of β-catenin at Ser-552 and improves β-catenin/TCF4 interaction to enhance the expression of β-catenin/TCF4 target genes including S100A4.

Combined transcriptional inhibition of MACC1 and S100A4 synergizes in restricting cancer cell motility and metastasis

We have shown the direct and causal functional link of MACC1 and S100A4 driving cell motility. To translate this finding into a novel therapeutic strategy we combined the transcriptional inhibition of both MACC1 and S100A4 by small molecules. For this, we investigated potential synergisms between inhibitors of MACC1 and S100A4 and applied atorvastatin or further members of the statin family fluvastatin and lovastatin (targeting MACC1 expression) and niclosamide (targeting S100A4 expression) as monotherapy or in combination. We analyzed the combination for reduced proliferation and motility in wound healing assays in HCT116 cells, which express both MACC1 and S100A4, at three different drug concentrations [17, 25].

Single treatments with atorvastatin (2.5 μM) and niclosamide (0.5 μM) significantly reduced wound closure. Combination of atorvastatin and niclosamide demonstrated a synergistic inhibitory effect, compared to the respective single treatments (Fig. 6A, Supplementary movie 1). This effect was shown to be dose-dependent (Fig. 6A, right panel).

Next, we tested two additional statins (fluvastatin and lovastatin) in combination with niclosamide. These statins also show a synergistic effect in combination with niclosamide (Fig. S4A, B, supplementary movies 2, 3). In summary, statins inhibit cellular motility synergistically with niclosamide even at lower concentrations (Figs. 5A and S3A, B). Synergy analyses indicated the synergism to be highest for 2.5 μM of a statin in combination with 0.5 μM niclosamide.

To test the combinatorial MACC1/S100A4 inhibition for metastasis intervention in vivo, SCID beige mice were intrasplenically xenotransplanted with stably luciferase overexpressing HCT116 cells. The tested statins and niclosamide were orally administered at human equivalent dosages [44]. Drug administration and monitoring of tumor growth and metastasis started 5 days after cell inoculation. The mice were treated with atorvastatin, fluvastatin or niclosamide alone, or with combinations thereof. A control group received solvent only. Solvent-treated mice developed extensive liver metastases over time as monitored by bioluminescence. Metastasis formation was quantified by human satellite DNA load in the livers. Single treatments with atorvastatin, fluvastatin or niclosamide significantly reduced liver metastasis by 41%, 40% and 50%, respectively (Fig. 6B–D). More importantly, the combinatorial treatment with atorvastatin and niclosamide restricted liver metastases, reflected by reduced bioluminescence. Human satellite DNA in mouse livers was reduced by 96% and 92%, respectively, in mice under atorvastatin/niclosamide and fluvastatin/niclosamide treatment (Fig. 6D). Synergistic effects are dosage dependent. Given at 100% human equivalent concentrations, all treatment regimens strongly reduced in vivo bioluminescence from mouse liver metastases, and combinatorial treatments were not superior to monotherapies (Fig. S4A). At 12.5% human equivalent dosage, neither treatment affected splenohepatic metastasis of CRC xenografts (Fig. S4B). Neither drug regimen exerted any discernible toxicity reflected in comparable relative body weight curves (Fig. S4C). We additionally stained human CRC cells within the murine liver via IHC of human CK19. In livers of mice receiving monotherapies diminished hCK19 immunoreactivity suggested a reduction of micrometastases compared to solvent-treated animals (1: solvent, 2: niclosamide, 3: fluvastatin, 4: atorvastatin). This effect was more pronounced in livers of combination treated animals (5: niclosamide + fluvastatin, 6: niclosamide + atorvastatin) (Fig. S4E). This is supportive for the efficacy of multiple hit intervention of the MACC1-β-catenin-S100A4 axis to reduce metastasis. The results were confirmed in a second CRC in vivo model. SW620 cells with high endogenous expression of MACC1 and S100A4 were intrasplenically xenografted in SCID beige mice. Treatment with the highest human equivalent dose of 328 mg/kg (human dose 2 g per day and patient) niclosamide or 13 mg/kg (human dose 80 mg per day and patient) of each statin alone failed to reduced liver metastasis.

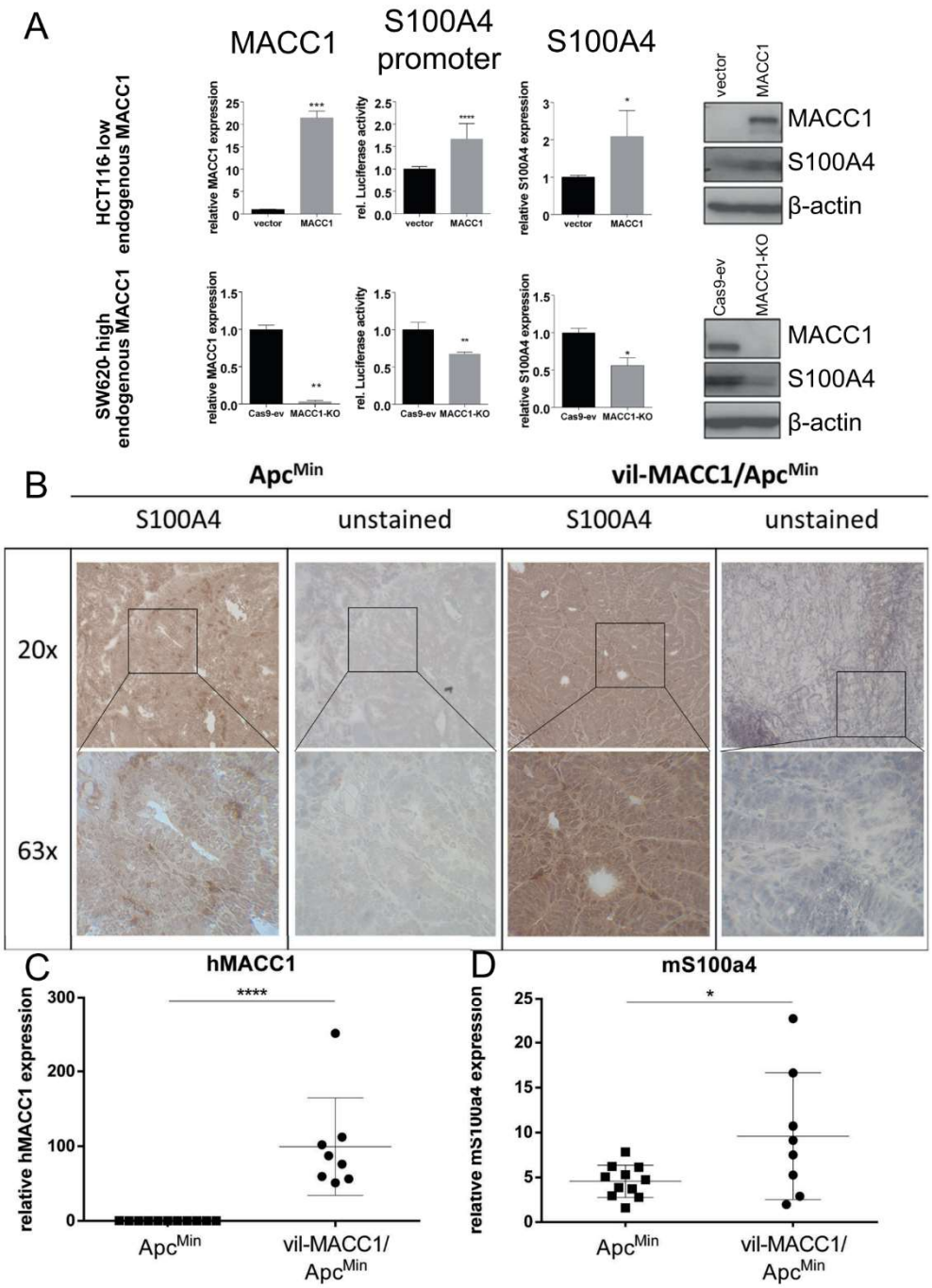

Fig. 3 MACC1 promotes S100A4 in vitro and in vivo. Ectopic MACC1 in HCT116 increased the activity of a S100A4 promoter-driven luciferase reporter. Concomitantly, S100A4 was increased in mRNA and protein levels (**A** top). Knockout of MACC1 in SW620 was followed by reduced S100A4-promoter-driven luciferase as well as decreased S100A4 mRNA and protein expression (**A** bottom). IHC of S100A4 in tumors of Apc^{Min} and vil-MACC1/Apc^{Min} mice confirms overexpression of S100A4 in MACC1-overexpressing littermates (**B**). In tumors of vil-MACC1/Apc^{Min} that overexpress human MACC1 (hMACC1, **C**), mouse-intrinsic S100a4 (mS100a4) was upregulated at RNA level (**D**).

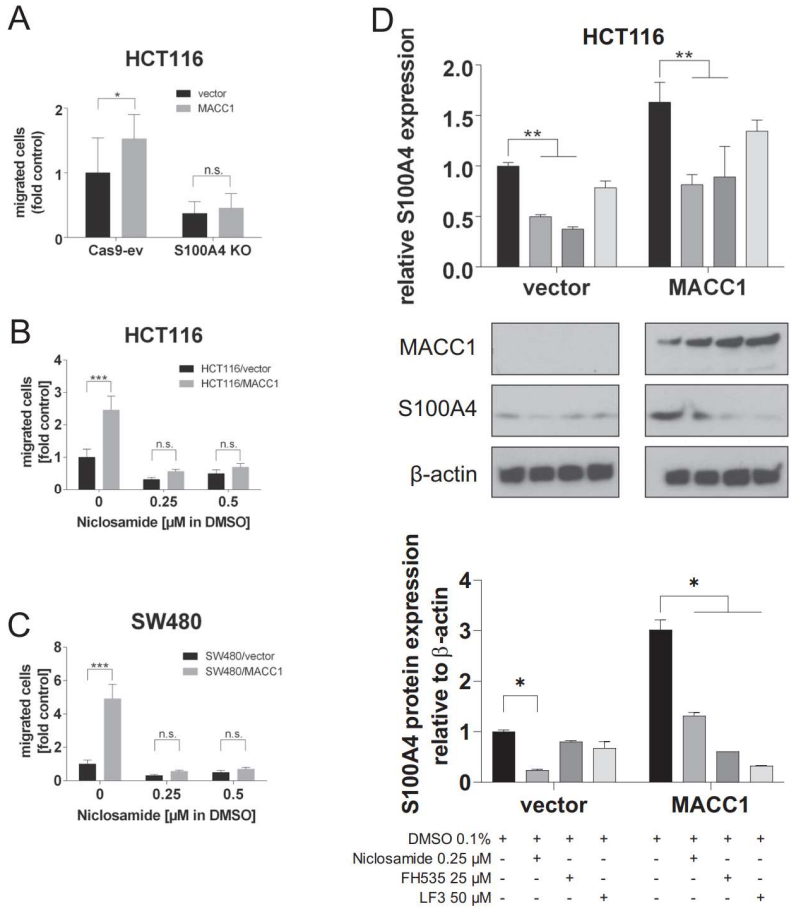

Fig. 4 MACC1 employs S100A4 through β-catenin signaling to drive cancer cell motility. MACC1-specific cell motility depends on S100A4. Overexpression of MACC1 in HCT116 cells induced transwell migration, but not in S100A4-KO counterparts (**A**). MACC1-induced cell migration in HCT116 and SW480 cells, and this effect was reverted by niclosamide, a transcriptional inhibitor of S100A4 (**B**, **C**). MACC1 increased S100A4 in presence of DMSO, and three independent β-catenin inhibitors (niclosamide, FH535 and LF3) largely reversed this upregulation on mRNA and protein level to expression levels of HCT116/vector cells (**D**). Numeric results shown as means ± SEM of 3 independent experiments, test for significance with Student's *t*-test, or ANOVA and Tukey correction for multiple testing.

However, combination of niclosamide and one of the two tested statins showed a strong reduction of liver metastasis for both approaches (Fig. S5A, B).

DISCUSSION

This is the first report to functionally link two metastasis-associated genes, MACC1 and S100A4, and to elucidate their cooperation as inducer (MACC1) and enforcer (S100A4) of CRC cell motility and metastasis in one functionally shared MACC1-β-catenin-S100A4 axis.

Mechanistically, MACC1 induces S100A4 overexpression on a transcriptional level, in that it interacts with β-catenin, induces its posttranslational stabilization and enhances its interaction with TCF4 [24].

Importantly, we found S100A4 to be instrumental in MACC1 mediated cell motility. MACC1 promoted transwell migration only in S100A4-proficient cells and failed to do so in S100A4-depleted cells and under pharmacological inhibition of S100A4 transcription or activity. MACC1 facilitated an activating PTM of β-catenin, which has been linked to enhanced transcriptional activity of its target genes [45–47]. MACC1 did not increase β-catenin expression, neither at mRNA nor protein level. However, the effect on Ser-552 phosphorylation might be crucial to permit MACC1 mediated hyperactivation of β-catenin signaling [48–50]. We speculate that MACC1, which lacks sequences suggestive of ATP-binding or kinase activity [6], rather acts as an adapter protein and recruits kinases to β-catenin. Further studies should probe for joined nuclear shuttling of MACC1 and β-catenin and examine the modulation of β-catenin-dependent transcription complexes. These findings have identified MACC1 as one decisive piece in the complex puzzle of intracellular signal transduction of cancer progression and metastasis.

The MACC1-β-catenin-S100A4 axis is functional in clinical cases of CRC, in which co-expression of MACC1 and S100A4 in tumors as well as patient blood hallmark high-risk CRC patients. We stratified CRC patients according to MACC1- and S100A4-transcript levels in primary tumors and in blood serum, respectively. The combined MACC1/S100A4 biomarker robustly identified CRC patients at high risk for poor MFS by tumor RNA analysis and predicted poor OS from liquid biopsy analyses. In sections of locally advanced, non-metastasized CRC (UICC stages II and III), MACC1 and S100A4

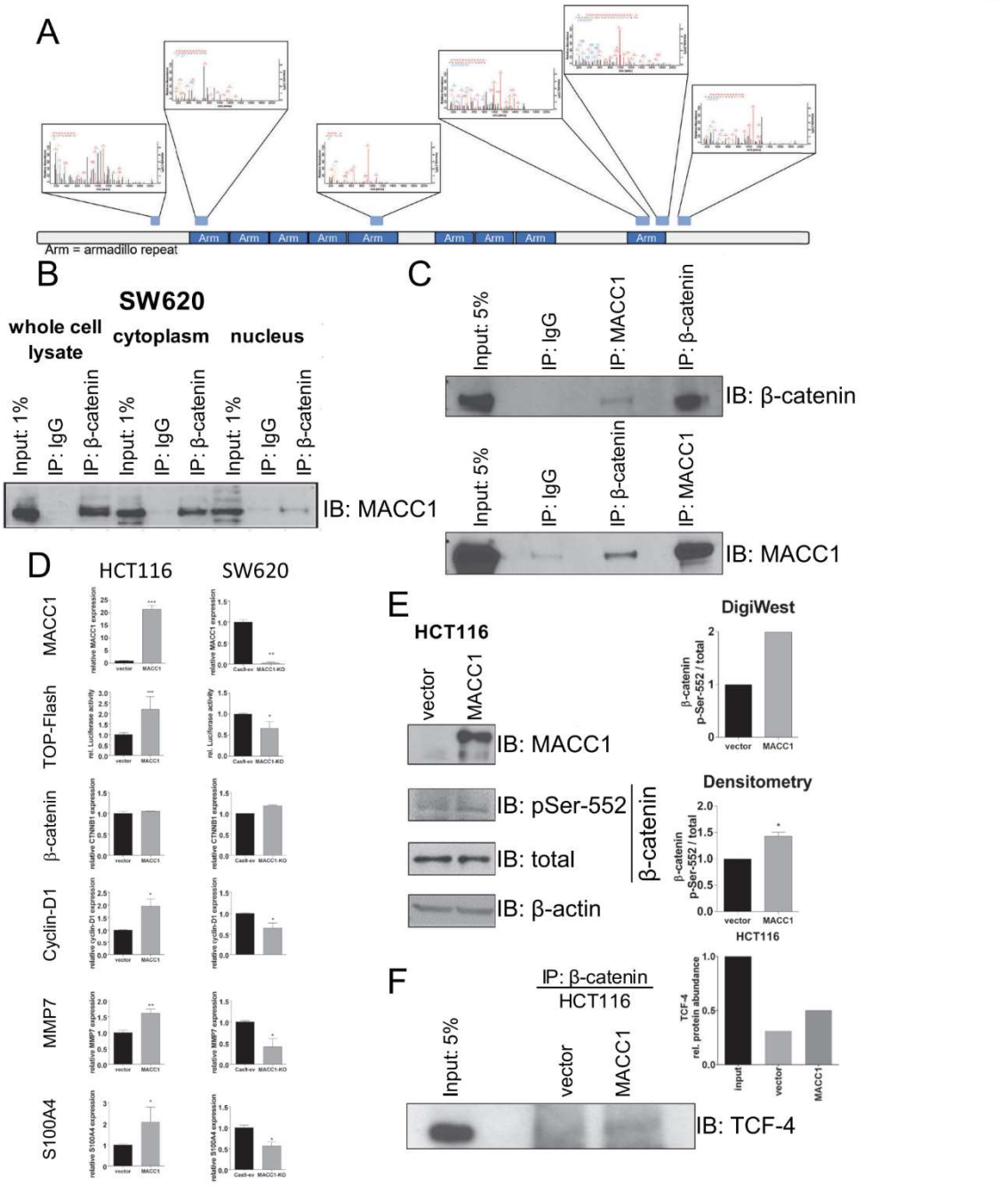

expression coincided, and discriminated metachronously metastasized cases from non-metastasized cases. Furthermore, both biomarkers correlated positively in three independent CRC cohorts.

The molecular background of a given tumor dictates its phenotype and aggressiveness and thus predicts patient survival. In light of this, several studies have identified molecular subtypes of CRC with distinct clinicopathological features impacting therapy response and survival [51, 52]. Personalized cancer medicine seeks to maximize therapeutic efficacy and minimize escape of tumor cells by resistance mechanisms by targeting the individual molecular makeup of a given tumor. We have previously described an association of MACC1 in KRAS-driven CRC, where

Fig. 5 MACC1 interacts with β-catenin and induces its transcriptional activity via post-translational modification. In a mass-spectrometry-based analysis of the MACC1 interactome in SW620 cells, several peptides interacting with MACC1 mapped to β-catenin, suggesting a direct PPI (**A**). Co-IP experiments on whole-cell lysates, cytoplasmic and nuclear protein of SW620 confirmed direct interaction between MACC1 and β-catenin (**B**). This finding was recapitulated by co-incubating recombinant MACC1 and β-catenin proteins in cell-free Co-IP assays (**C**). Impact of MACC1 overexpression or MACC1 knock-out is shown on TCF-reporter activity and mRNA expression of β-catenin and the β-catenin/TCF target genes Cyclin-D1, MMP7 and S100A4 in HCT116 and SW620 cells. In HCT116 cells MACC1 overexpression increases TCF reporter activity and TCF target gene expression, while β-catenin gene expression itself is unaffected. In SW620 cells MACC1 knockout decreases TCF reporter activity and TCF target gene expression, whereas β-catenin gene expression is also unaffected (**D**). In a DigiWest experiment, MACC1-overexpressing HCT116 cells demonstrated increased phosphorylation of p-Ser-552-β-catenin, confirmed in semiquantitative western blots, while total β-catenin protein was not altered (**E**). Comparative immunoprecipitation of β-catenin protein showed increased binding of TCF4 in HCT116/MACC1 cells, also shown by densitometry (**F**). Boxplots show means ± SEM of 3 independent experiments, test for significance with Student's *t*-test.

MACC1 overexpression combined with KRAS G13 mutation conferred poor MFS [53]. Conversely, absent MACC1 expression in mismatch-repair deficient CRC identifies low-risk patients who would not benefit from, and could be spared adjuvant chemotherapy [54]. Independently, our research as well as other studies confirm the prognostic value of S100A4 in CRC and other malignancies [33, 55, 56]. In this report we demonstrate that rationally combining two mechanistically linked biomarkers indeed improve prediction of CRC metastasis and cancer survival.

Our observation, that MACC1 and S100A4 form a signaling axis through β-catenin might add to characterization of molecular cancer subtypes with high metastatic potential and novel intervention points for improved anti-metastatic therapy. It seems likely that MACC1 and S100A4 also cooperate in other cancer entities, as the two biomarkers were described for improved prognosis of ovarian or gastric cancer, which underlines its considerable cross-entity potential [35, 36].

To test whether our hypothesis translates into clinical practice, we targeted the MACC1-β-catenin-S100A4 axis by combining transcriptional inhibitors of MACC1 (statins) and S100A4 (niclosamide) for cell motility and metastasis inhibition. We showed, that in combinatorial use, statins and niclosamide synergise in inhibiting CRC cell motility and invasion in vitro and metastatic dissemination in vivo. Metastasis remains the main challenge in the management of CRC patients and means of targeted metastasis intervention/inhibition or prevention is highly sought after. We demonstrate here that repositioning of statins and niclosamide, which are already in clinical use, could complement current therapy regimens for CRC [57, 58]. Long-term intake of statins, a mainstay of hypercholesterolemia management, has been associated with reduced cancer incidence in a variety of entities [59, 60]. The long term effects of niclosamide in cancer patients are currently tested in a clinical trial [61].

Here, we linked the metastasis inducer MACC1 to the metastasis enforcer S100A4 in a signaling axis through β-catenin, which promotes CRC progression and metastasis. Consequently, we simultaneously targeted inducer MACC1 and enforcer S100A4 within this axis of metastasis by combining clinically established drugs and generated efficient restriction of cancer cell motility and metastasis formation. These findings support the therapeutic value of our strategy with high translational potential, which warrants exploration in clinical trials for novel personalized, anti-metastatic therapies.

MATERIALS AND METHODS

Clinical samples

Tumor samples were obtained from 60 patients diagnosed with CRC of UICC stages I to III (no distant metastasis at time of diagnosis) undergoing R0 (no microscopic tumor residue) resections prior to tumor-specific adjuvant treatment. All patients had no history of hereditary colorectal cancer and did not have additional malignancies of any entity. Metachronous metastases developed in 23 patients (median follow-up: 167.2 months), 37 patients did not metastasize. The CRC cohort is identical with the cohort used in Stein et al. [5].

Blood samples were obtained from an independent cohort of 49 patients presenting at the Robert-Rössle-Clinic, Charité—Universitätsmedizin Berlin, with newly diagnosed CRC. Blood was taken on the day of diagnosis, prior to any surgical or adjuvant therapy, except of 16 patients diagnosed with locally advanced rectal cancer, who received neoadjuvant radio-chemotherapy of the primary tumor 3 to 6 days before blood was drawn. In these patients, no difference in circulating MACC1 transcript levels was detected in comparison to untreated rectal cancer patients. Presence of secondary malignancies in patient history or during follow-up was an exclusion criterion. The patient cohort is identical with the cohort studied by Stein, 2012 [34]. The follow-up period of survival was extended to a median of 806 days after primary diagnosis, followed by re-evaluation of prognosis with the Kaplan Meier estimator.

Cell culture, functional assays, and drug treatment

The CRC cell lines HCT116, SW480 and SW620 were maintained with RPMI or DMEM supplemented with 10% FBS in a humidified incubator at 37 °C and 5% CO_2. Overexpression of MACC1 was achieved by lentiviral transduction of HCT116 cells with a MACC1-GFP construct (vector = GFP) and transfection of SW480 with a pcDNA3.1-MACC1-V5-His vector (vector = pcDNA3.1-V5-His). To knockout MACC1 in SW620 cells with CRISPR-Cas9 technology, predesigned plasmids encoding Cas9, puromycin resistance and sgRNA (Applied StemCell Inc., Milpitas CA, USA) were co-transfected. Following selection with 4 µg/ml puromycin for 48 h, viable cells were single-cell sorted into 96-well plates. Expanding clones were tested for MACC1 expression by western blotting. The genomic locus of MACC1 was sequenced to verify indel mutations in MACC1-deficient clones (Fig. S2, Table S1).

The migratory capacity of CRC cells was assessed in transwell migration assays. Briefly, 1×10^6 cells were plated into 6-well plates. Complete medium was replaced by serum-free medium in the presence of inhibitors or DMSO, when indicated, and left overnight. 5×10^4 cells were seeded into the pre-soaked transwell inserts of 96-well transwell migration plates (Corning Inc., Corning NY, USA). After 18 h at 37 °C, migrated cells were collected with Trypsin-EDTA and quantified with CellTiter Glo (Promega, Madison WI, USA). Data are accumulated from at least three independent biological replicates and technical quadruplicates.

Wound healing was measured in an IncuCyte ZOOM instrument (EssenBiosciences, Ann Arbor MI, USA). 1×10^5 cells in 100 µl RPMI supplemented with 10% FCS were seeded into ImageLock 96-well plates (EssenBiosciences). After 6 h incubation to allow formation of monolayers, wounds were created with a WoundMaker tool (EssenBiosciences) and the wells were washed with PBS to remove floating cells. The plates were filled with complete medium, DMSO or inhibitors, when indicated, and wound closure was monitored continuously every 2 h. Analyses were performed by using the IncuCyte ZOOM 2016B software after generating confluence and wound masks with teaching image sets [62].

LF3, FH535, atorvastatin, fluvastatin, lovastatin, PCP (Selleckchem LLC, Houston TX, USA), and niclosamide (SigmaAldrich, St. Louis MO, USA) stocks were dissolved freshly for each experiment in DMSO (SigmaAldrich). The drugs were applied at concentrations indicated, while DMSO concentration was maintained at 0.1% in all treatments.

Secretome analysis

Cells were grown in DMEM SILAC media supplemented with heavy lysine and arginine ($^{15}N_2$ $^{13}C_6$ Lys, $^{15}N_4$ $^{13}C_6$ Arg). Secreted proteins were collected in the cell culture supernatant. The proteins were concentrated using a 30 kDa molecular filter cartridge (Millipore).

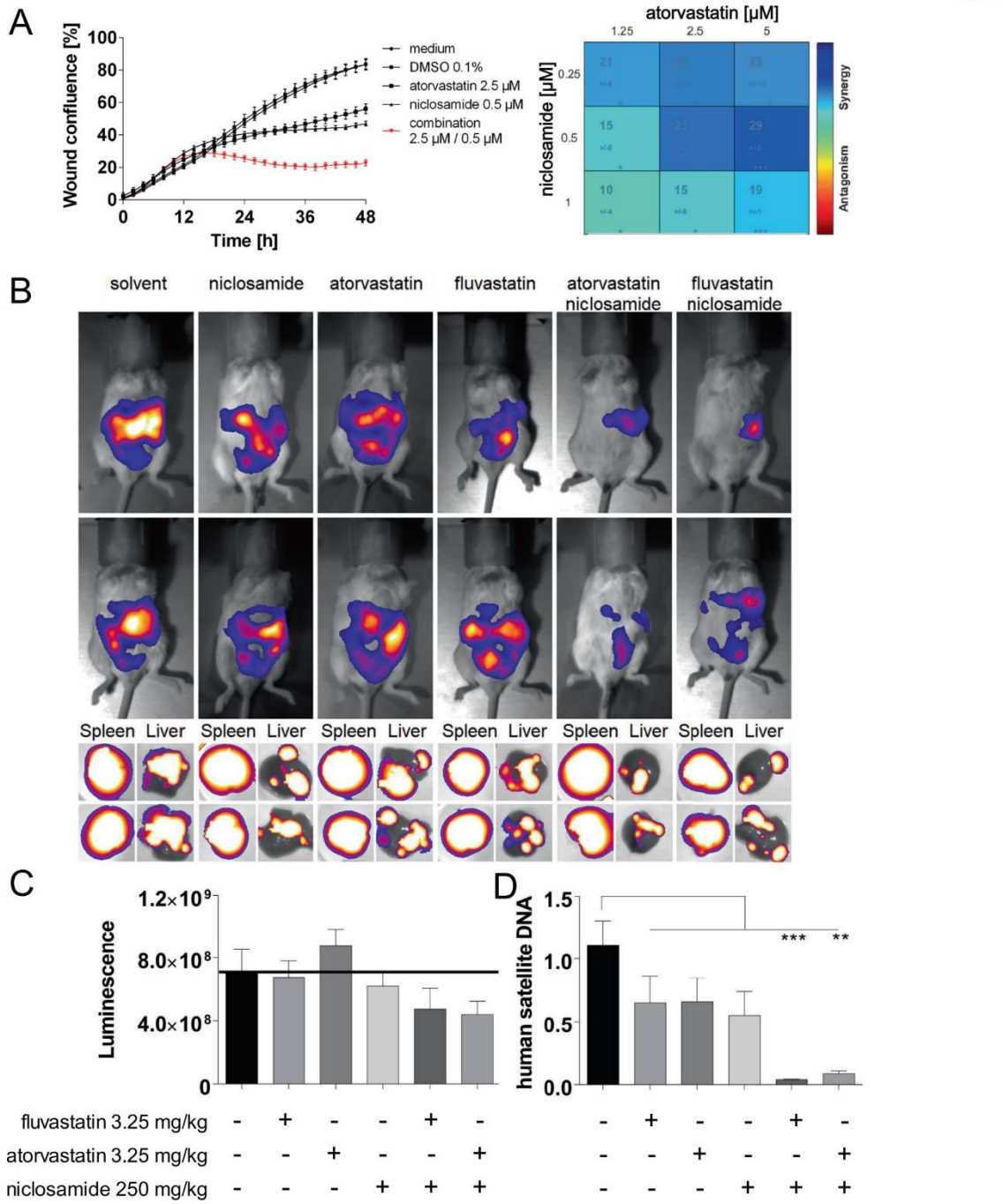

Xenografting and in vivo treatment

3×10^5 (HCT116/Luc) or 1×10^6 (SW620) cells in 30 µl PBS were injected into the parenchyma of the spleen of 6-week-old female SCID bg/bg mice ($n = 60$). After cell inoculation the mice were randomly assigned to 6 groups. Mice were treated 3 days after transplantation p.o. daily with 10 ml/kg solvent solution (10% Kolliphor EL (SigmaAldrich; 0.9% NaCl), 1.5–13 mg/kg atorvastatin or fluvastatin, or 164–328 mg/kg niclosamide in solvent). These amounts correspond to the human doses of 10 -80 mg per patient per day for the statins or 1–2 g per patient per day for niclosamide. Tumor growth and metastasis formation to the liver of HCT116 cell was monitored over time

Fig. 6 Statins and niclosamide synergize in suppression of CRC cell wound healing and metastasis. HCT116 human colorectal cancer cells with endogenous MACC1 and S100A4 expression were treated with three concentrations (1.25, 2.5 and 5 µM) of atorvastatin and niclosamide (0.25, 0.5 and 1 µM) alone and in combinations thereof (**A**). After drug application in vitro wound healing was monitored for 48 h using the IncuCyte live cell imaging system. Atorvastatin and niclosamide were able to reduce wound closure compared to control cells. Combining a statin with niclosamide increased this effect synergistically. Results are shown as means ± SEM of at least 3 experiments. Treating xenografted SCID beige mice ($n = 60$, 10 animals per group) with human equivalent doses of either atorvastatin (3.25 mg/kg, 20 mg per patient per day), fluvastatin (3.25 mg/kg, 20 mg per patient per day) or niclosamide (250 mg/day, 1.5 g per patient per day) alone reduced metastasis formation in the liver. Confirming the in vitro results, the combination of the tested drugs, each statin with niclosamide, was superior to single drug treatment (**B**, **D**). While visualization of xenografted cells by luminescence did not show significant reductions just before mouse killing (**C**), human cell load in the murine liver was quantifiably reduced in human satellite DNA specific qPCR (**D**). Numeric results are shown as mean ± SEM, and level of significance indicated as per ANOVA and Dunnett's correction for multiple testing.

using the ectopically overexpressed luciferase protein as described earlier) [17]. At the ethical end point, the animals were sacrificed, and the livers (site of distant metastasis) were snap-frozen in liquid nitrogen. To isolate tissue DNA from the livers including metastasis from human cells the liver tissue was randomly sliced using a cryomicrotome (Thermo Scientific, Waltham MA, USA). The amount of human satellite DNA in the liver tissue was detected by qPCR and immunohistochemistry (IHC) for human CK19, as previously described [25, 63].

Statistical analysis

Data were analyzed using GraphPad Prism 8 (GraphPad Software Inc., San Diego CA, USA) and SPSS Statistics 21 (IBM, Armonk NY, USA). To compare datasets, Student's *t*-tests (2 groups) and one-way ANOVA followed by correction for multiple comparison (Dunnett or Tukey, when comparing more than 2 groups) were employed. Statistical significance was assumed at a p-value < 0.05. Receiver operating characteristics (ROC) analysis was performed on mRNA expression levels to assess sensitivity and specificity for the primary endpoints "metachronous metastasis" and "death". Youden's J statistics were carried out to determine the optimal cut-off value to separate low and high MACC1 and S100A4 expression levels for subsequent survival analyses using Kaplan–Meier curves and logrank tests. Synergism of drug combinations on wound healing was analyzed at the 48 h time point using Combenefit v2.02 [64]. Bar graphs show mean and standard error of mean SEM.

DATA AVAILABILITY

The external CRC datasets [37, 38] are available via the Gene Expression Omnibus (https://www.ncbi.nlm.nih.gov/gds, accession number GSE28702 and GSE21510, respectively). Any other data used to support the findings of this study are available from the corresponding author on request.

REFERENCES

1. Schubert-Fritschle G, Combs SE, Kirchner T, Nüssler V, Engel J. Use of Multicenter Data in a Large Cancer Registry for Evaluation of Outcome and Implementation of Novel Concepts. Front Oncol. 2017;7. https://doi.org/10.3389/fonc.2017.00234.
2. Siegel RL, Miller KD, Goding Sauer A, Fedewa SA, Butterly LF, Anderson JC, et al. Colorectal cancer statistics, 2020. CA Cancer J Clin. 2020;70:145–64.
3. Siegel RL, Miller KD, Jemal A. Cancer statistics, 2020. CA Cancer J Clin. 2020;70:7–30.
4. Pita-Fernández S, Alhayek-Aí M, González-Martín C, López-Calviño B, Seoane-Pillado T, Pértega-Díaz S. Intensive follow-up strategies improve outcomes in nonmetastatic colorectal cancer patients after curative surgery: a systematic review and meta-analysis. Ann Oncol J Eur Soc Med Oncol. 2015;26:644–56.
5. Stein U, Walther W, Arlt F, Schwabe H, Smith J, Fichtner I, et al. MACC1, a newly identified key regulator of HGF-MET signaling, predicts colon cancer metastasis. Nat Med. 2009;15:59–67.
6. Radhakrishnan H, Walther W, Zincke F, Kobelt D, Imbastari F, Erdem M, et al. MACC1-the first decade of a key metastasis molecule from gene discovery to clinical translation. Cancer Metastasis Rev. 2019;37:805–20.
7. Arlt F, Stein U. Colon cancer metastasis: MACC1 and Met as metastatic pacemakers. Int J Biochem Cell Biol. 2009;41:2356–9.
8. Kobelt D, Perez-Hernandez D, Fleuter C, Dahlmann M, Zincke F, Smith J, et al. The newly identified MEK1 tyrosine phosphorylation target MACC1 is druggable by approved MEK1 inhibitors to restrict colorectal cancer metastasis. Oncogene 2021;40:5286–301.
9. Imbastari F, Dahlmann M, Sporbert A, Mattioli CC, Mari T, Scholz F, et al. MACC1 regulates clathrin-mediated endocytosis and receptor recycling of transferrin receptor and EGFR in colorectal cancer. Cell Mol Life Sci. 2021. https://doi.org/10.1007/s00018-020-03734-1.
10. Trochet D, Bitoun M. A review of Dynamin 2 involvement in cancers highlights a promising therapeutic target. J Exp Clin Cancer Res. 2021;40:238.
11. Stein U, Smith J, Walther W, Arlt F. MACC1 controls Met: What a difference an Sp1 site makes. Cell Cycle. 2009;8:2467–9.
12. Lemos C, Hardt MS, Juneja M, Voss C, Forster S, Jerchow B, et al. MACC1 Induces Tumor Progression in Transgenic Mice and Colorectal Cancer Patients via Increased Pluripotency Markers Nanog and Oct4. Clin Cancer Res. 2016. https://doi.org/10.1158/1078-0432.CCR-15-1425.
13. Stein U, Dahlmann M, Walther W. MACC1 - more than metastasis? Facts and predictions about a novel gene. J Mol Med. 2010;88:11–8.
14. Budczies J, Kluck K, Walther W, Stein U. Decoding and targeting the molecular basis of MACC1-driven metastatic spread: Lessons from big data mining and clinical-experimental approaches. Semin Cancer Biol. 2020;60:365–79.
15. Kopczyńska EK. The potential therapeutic applications and prognostic significance of metastasis-associated in colon cancer-1 (MACC1) in cancers. Contemp Oncol. 2016;20:273–80.
16. Kobelt D, Zhang C, Clayton-Lucey IA, Glauben R, Voss C, Siegmund B, et al. Pro-inflammatory TNF-α and IFN-γ Promote Tumor Growth and Metastasis via Induction of MACC1. Front Immunol. 2020;11:980.
17. Juneja M, Kobelt D, Walther W, Voss C, Smith J, Specker E, et al. Statin and rottlerin small-molecule inhibitors restrict colon cancer progression and metastasis via MACC1. PLoS Biol. 2017;15:e2000784.
18. Gohlke B-O, Zincke F, Eckert A, Kobelt D, Preissner S, Liebeskind JM, et al. Real-world evidence for preventive effects of statins on cancer incidence: A trans-Atlantic analysis. Clin Transl Med. 2022;12:e726.
19. Klaus A, Birchmeier W. Wnt signalling and its impact on development and cancer. Nat Rev Cancer. 2008;8:387–98.
20. Zhan T, Rindtorff N, Boutros M. Wnt signaling in cancer. Oncogene 2017;36:1461–73.
21. Fang D, Hawke D, Zheng Y, Xia Y, Meisenhelder J, Nika H, et al. Phosphorylation of ß-catenin by AKT promotes ß-catenin transcriptional activity. J Biol Chem. 2007;282:11221–9.
22. Gao C, Xiao G, Hu J. Regulation of Wnt/β-catenin signaling by posttranslational modifications. Cell Biosci. 2014;4:13.
23. Dammann K, Khare V, Harpain F, Lang M, Kurtovic A, Mesteri I, et al. PAK1 promotes intestinal tumor initiation. Cancer Prev Res. 2015;8:1093–101.
24. Stein U, Arlt F, Walther W, Smith J, Waldman T, Harris ED, et al. The Metastasis-Associated Gene S100A4 Is a Novel Target of ß-catenin/T-cell Factor Signaling in Colon Cancer. Gastroenterology. 2006;131:1486–500.
25. Sack U, Walther W, Scudiero D, Selby M, Kobelt D, Lemm M, et al. Novel effect of antihelminthic niclosamide on s100a4-mediated metastatic progression in colon cancer. J Natl Cancer Inst. 2011;103:1018–36.
26. Dahlmann M, Kobelt D, Walther W, Mudduluru G, Stein U. S100A4 in Cancer Metastasis: Wnt Signaling-Driven Interventions for Metastasis Restriction. Cancers 2016;8:59.
27. Li ZH, Bresnick AR. The S100A4 metastasis factor regulates cellular motility via a direct interaction with myosin-IIA. Cancer Res. 2006;66:5173–80.
28. Belot N, Pochet R, Heizmann CW, Kiss R, Decaestecker C. Extracellular S100A4 stimulates the migration rate of astrocytic tumor cells by modifying the organization of their actin cytoskeleton. Biochim Biophys Acta. 2002;1600:74–83.
29. Dahlmann M, Okhrimenko A, Marcinkowski P, Osterland M, Herrmann P, Smith J, et al. RAGE mediates S100A4-induced cell motility via MAPK/ERK and hypoxia signaling and is a prognostic biomarker for human colorectal cancer metastasis. Oncotarget 2014;5:3220–33.
30. Dahlmann M, Stein U. RNA Interference for Antimetastatic Therapy. Methods Mol Biol. 2015;1317:153–65.
31. Grum-Schwensen B, Klingelhöfer J, Beck M, Bonefeld CM, Hamerlik P, Guldberg P, et al. S100A4-neutralizing antibody suppresses spontaneous tumor progression,

pre-metastatic niche formation and alters T-cell polarization balance. BMC Cancer. 2015;15:44.
32. Hoshino A, Costa-Silva B, Shen T-L, Rodrigues G, Hashimoto A, Tesic Mark M, et al. Tumour exosome integrins determine organotropic metastasis. Nature 2015;527:329–35.
33. Fei F, Qu J, Zhang M, Li Y, Zhang S. S100A4 in cancer progression and metastasis: A systematic review. Oncotarget 2017;8:73219–39.
34. Stein U, Burock S, Herrmann P, Wendler I, Niederstrasser M, Wernecke K-DD, et al. Circulating MACC1 transcripts in colorectal cancer patient plasma predict metastasis and prognosis. PLoS One. 2012;7:e49249.
35. Burock S, Herrmann P, Wendler I, Niederstrasser M, Wernecke K-D, Stein U. Circulating Metastasis Associated in Colon Cancer 1 transcripts in gastric cancer patient plasma as diagnostic and prognostic biomarker. World J Gastroenterol. 2015;21:333–41.
36. Link T, Kuhlmann JD, Kobelt D, Herrmann P, Vassileva YD, Kramer M, et al. Clinical relevance of circulating MACC1 and S100A4 transcripts for ovarian cancer. Mol Oncol. 2019;13:1268–79.
37. Tsuji S, Midorikawa Y, Takahashi T, Yagi K, Takayama T, Yoshida K, et al. Potential responders to FOLFOX therapy for colorectal cancer by Random Forests analysis. Br J Cancer. 2012;106:126–32.
38. Tsukamoto S, Ishikawa T, Iida S, Ishiguro M, Mogushi K, Mizushima H, et al. Clinical significance of osteoprotegerin expression in human colorectal cancer. Clin Cancer Res. 2011;17:2444–50.
39. Schütte M, Risch T, Abdavi-Azar N, Boehnke K, Schumacher D, Keil M, et al. Molecular dissection of colorectal cancer in pre-clinical models identifies biomarkers predicting sensitivity to EGFR inhibitors. Nat Commun. 2017;8:14262.
40. Malashkevich VN, Dulyaninova NG, Ramagopal UA, Liriano MA, Varney KM, Knight D, et al. Phenothiazines inhibit S100A4 function by inducing protein oligomerization. Proc Natl Acad Sci. 2010;107:8605–10.
41. Garrett SC, Hodgson L, Rybin A, Toutchkine A, Hahn KM, Lawrence DS, et al. A biosensor of S100A4 metastasis factor activation: inhibitor screening and cellular activation dynamics. Biochemistry 2008;47:986–96.
42. Handeli S, Simon JA. A small-molecule inhibitor of Tcf/beta-catenin signaling down-regulates PPARgamma and PPARdelta activities. Mol Cancer Ther. 2008;7:521–9.
43. Fang L, Zhu Q, Neuenschwander M, Specker E, Wulf-Goldenberg A, Weis WI, et al. A small-molecule antagonist of the β-catenin/TCF4 interaction blocks the self-renewal of cancer stem cells and suppresses tumorigenesis. Cancer Res. 2016;76:891–901.
44. Nair AB, Jacob S. A simple practice guide for dose conversion between animals and human. J Basic Clin Pharm. 2016;7:27–31.
45. Ormanns S, Neumann J, Horst D, Kirchner T, Jung A. WNT signaling and distant metastasis in colon cancer through transcriptional activity of nuclear β-Catenin depend on active PI3K signaling. Oncotarget 2014;5:2999–3011.
46. Chowdhury MKH, Wu LE, Coleman JLJ, Smith NJ, Morris MJ, Shepherd PR, et al. Niclosamide blocks glucagon phosphorylation of serine 552 on β-catenin in primary rat hepatocytes via PKA signalling. Biochem J. 2016;473:1247–55. https://doi.org/10.1042/BCJ20160121.
47. Park MH, Kim DJ, You ST, Lee CS, Kim HK, Park SM, et al. Phosphorylation of β-catenin at serine 663 regulates its transcriptional activity. Biochem Biophys Res Commun. 2012;419:543–9.
48. He XC, Yin T, Grindley JC, Tian Q, Sato T, Tao WA, et al. PTEN-deficient intestinal stem cells initiate intestinal polyposis. Nat Genet. 2007;39:189–98.
49. Lee G, Goretsky T, Managlia E, Dirisina R, Singh AP, Brown JB, et al. Phosphoinositide 3-kinase signaling mediates beta-catenin activation in intestinal epithelial stem and progenitor cells in colitis. Gastroenterology 2010;139:869–81. 881.e1–9
50. Fang D, Hawke D, Zheng Y, Xia Y, Meisenhelder J, Nika H, et al. Phosphorylation of beta-catenin by AKT promotes beta-catenin transcriptional activity. J Biol Chem. 2007;282:11221–9.
51. Koulis C, Yap R, Engel R, Jardé T, Wilkins S, Solon G, et al. Personalized Medicine—Current and Emerging Predictive and Prognostic Biomarkers in Colorectal Cancer. Cancers 2020;12:812.
52. Guinney J, Dienstmann R, Wang X, de Reyniès A, Schlicker A, Soneson C, et al. The consensus molecular subtypes of colorectal cancer. Nat Med. 2015;21:1350–6.
53. Ilm K, Kemmner W, Osterland M, Burock S, Koch G, Herrmann P, et al. High MACC1 expression in combination with mutated KRAS G13 indicates poor survival of colorectal cancer patients. Mol Cancer. 2015;14:38.
54. Rohr U-P, Herrmann P, Ilm K, Zhang H, Lohmann S, Reiser A, et al. Prognostic value of MACC1 and proficient mismatch repair status for recurrence risk prediction in stage II colon cancer patients: the BIOGRID studies. Ann Oncol J Eur Soc Med Oncol. 2017;28:1869–75.
55. Stein U, Burock S, Herrmann P, Wendler I, Niederstrasser M, Wernecke K-D, et al. Diagnostic and prognostic value of metastasis inducer S100A4 transcripts in plasma of colon, rectal, and gastric cancer patients. J Mol Diagn. 2011;13:189–98.
56. Weidle UH, Birzele F, Krüger A. Molecular targets and pathways involved in liver metastasis of colorectal cancer. Clin Exp Metastasis. 2015;32:623–35.
57. Novac N. Challenges and opportunities of drug repositioning. Trends Pharm Sci. 2013;34:267–72.
58. Jiang W, Hu J-W, He X-R, Jin W-L, He X-Y. Statins: a repurposed drug to fight cancer. J Exp Clin Cancer Res. 2021;40:241.
59. Nielsen SF, Nordestgaard BG, Bojesen SE. Statin use and reduced cancer-related mortality. N. Engl J Med. 2012;367:1792–802.
60. Borgquist S, Broberg P, Tojjar J, Olsson H. Statin use and breast cancer survival - a Swedish nationwide study. BMC Cancer. 2019;19:54.
61. Burock S, Daum S, Keilholz U, Neumann K, Walther W, Stein U. Phase II trial to investigate the safety and efficacy of orally applied niclosamide in patients with metachronous or sychronous metastases of a colorectal cancer progressing after therapy: the NIKOLO trial. BMC Cancer. 2018;18:297.
62. Kobelt D, Walther W, Stein US. Real-Time Cell Migration Monitoring to Analyze Drug Synergism in the Scratch Assay Using the IncuCyte System. Methods Mol Biol. 2021;2294:133–42.
63. Becker M, Nitsche A, Neumann C, Aumann J, Junghahn I, Fichtner I. Sensitive PCR method for the detection and real-time quantification of human cells in xeno-transplantation systems. Br J Cancer. 2002;87:1328–35.
64. Di Veroli GY, Fornari C, Wang D, Mollard S, Bramhall JL, Richards FM, et al. Combenefit: an interactive platform for the analysis and visualization of drug combinations. Bioinformatics 2016;32:2866–8.

ACKNOWLEDGEMENTS

We are very grateful to Pia Herrmann, Janice Smith, Margarita Mokritzkij, Markus Hensel and Zeynep Hacer İpek (ECRC, Charité and MDC, Berlin, Germany) for their technical assistance and handling of patient-derived material. We thank Ole Daberkow and Britta Büttner (EPO GmbH, Berlin, Germany) for their assistance in performing the animal experiments, and Anja Arndt for her part in the DigiWest. We are thankful for the human S100A4 promoter to Dr. David Allard, University of Exeter (UK). We also thank the MDC FACS core facility and Dr. H.P. Rahn as well as the FMP for their invaluable technical services. This research was funded by grants from the BIH Innovations & SPARK-BIH Validation Fund, the Berlin School of Integrative Oncology (BSIO) and by the Germany Cancer Consortium (DKTK).

AUTHOR CONTRIBUTIONS

US initiated the entire study and conceived the MACC1 interactome and secretome studies. GD carried out all Mass-Spectrometry-based analyses of the MACC1 interactome and secretome. BK and HR analyzed gene co-expression, and BK performed all in vitro validation experiments and established KO cell lines. DK established lentiviral constructs for transgene overexpression, performed in vitro experiments on drug synergy, provided cells for and analysed data from all in vivo experiments. FZ and CS performed detection of differential protein activation using DigiWest. MD performed bioinformatics analyses. SB extended the follow-up of patient survival and carried out the survival analyses. UK provided expression data from the OncoTrack Consortium. BK and DK wrote the manuscript. US and WW critically revised the manuscript.by All co-authors vouch for the accuracy of their respective contribution and all data reported.

FUNDING

Open Access funding enabled and organized by Projekt DEAL.

COMPETING INTERESTS

All experiments were carried out in accordance with the guidelines approved by the institutional review board, number AA3/03/45, of the Charité—Universitätsmedizin Berlin, Germany. All patients gave written informed consent and the authors complied with all relevant ethical regulations for research involving human participants. For all studies, the welfare of the animals was maintained in accordance with the general principles governing the use of animals in experiments of the European Communities and German legislation. The study was performed in accordance to the United Kingdom Coordinating Committee on Cancer Research (UKCCCR) regulations for the Welfare of Animals and of the German Animal Protection Law and approved by the local responsible authorities, Berlin, Germany (State Office of Health and Social Affairs, Berlin, Germany), REG0010/19, G0333/18.CS works for NMI TT Pharmaservices, who offer DigiWest as a service. BK, HR, FB, SB, UK, MD, WW, GD, DK, and US declare no competing interests.

ETHICS APPROVAL AND CONSENT TO PARTICIPATE

All experiments were carried out in accordance with the guidelines approved by the institutional review board, number AA3/03/45, of the Charité—Universitätsmedizin Berlin, Germany. All patients gave written informed consent and the authors complied with all relevant ethical regulations for research involving human participants. For all studies, the welfare of the animals was maintained in accordance with the general principles governing the use of animals in experiments of the European Communities and German legislation. The study was performed in accordance to the United Kingdom Coordinating Committee on Cancer Research (UKCCCR) regulations for the Welfare of Animals and of the German Animal Protection Law and approved by the local responsible authorities, Berlin, Germany (State Office of Health and Social Affairs, Berlin, Germany), REG0010/19, G0333/18.

ADDITIONAL INFORMATION

Supplementary information The online version contains supplementary material available at https://doi.org/10.1038/s41388-022-02407-6.

Correspondence and requests for materials should be addressed to Ulrike Stein.

Curriculum vitae

Mein Lebenslauf wird aus datenschutzrechtlichen Gründen in der elektronischen Version meiner Arbeit nicht veröffentlicht.

My CV is not published in the electronic version of my work for data protection reasons.

Complete list of publications

Kortüm B, Radhakrishnan H, Zincke F, Sachse C, Burock S, Keilholz U, Dahlmann M, Walther W, Dittmar G, Kobelt D, Stein U. Combinatorial treatment with statins and niclosamide prevents CRC dissemination by unhinging the MACC1-β-catenin-S100A4 axis of metastasis. Oncogene. 2022 Aug 25; **IF 8.756**

Gohlke BO, Zincke F, Eckert A, Kobelt D, Preissner S, Liebeskind JM, Gunkel N, Putzker K, Lewis J, Preissner S, **Kortüm B**, Walther W, Mura C, Bourne PE, Stein U, Preissner R. Real-world evidence for preventive effects of statins on cancer incidence: A trans-Atlantic analysis. Clin Transl Med. 2022;12(2):e726. **IF 8.554**

Wust P, **Kortüm B**, Strauss U, Nadobny J, Zschaeck S, Beck M, Stein U, Ghadjar P. Non-thermal effects of radiofrequency electromagnetic fields. Sci Rep. 2020;10(1):13488. **IF 4.130**

4. Kobelt D, Dahlmann M, Dumbani M, Güllü N, **Kortüm B**, Vílchez MEA, Stein U, Walther W. Small Ones to Fight a Big Problem-Intervention of Cancer Metastasis by Small Molecules. Cancers (Basel). 2020 Jun 3;12(6). **IF 6.639**

5. Dahlmann M, Werner R, **Kortüm B**, Kobelt D, Walther W, Stein U. Restoring Treatment Response in Colorectal Cancer Cells by Targeting MACC1-Dependent ABCB1 Expression in Combination Therapy. Front Oncol. 2020;10:599. **IF 6.244**

6. Radhakrishnan H, Walther W, Zincke F, Kobelt D, Imbastari F, Erdem M, **Kortüm B**, Dahlmann M, Stein U. MACC1-the first decade of a key metastasis molecule from gene discovery to clinical translation. Cancer Metastasis Rev. 2019 Jan 3;37(4):805–20. **IF 6.400**

Kortüm B, Campregher C, Lang M, Khare V, Pinter M, Evstatiev R, Schmid G, Mittlböck M, Scharl T, Kucherlapati MH, Edelmann W, Gasche C. Mesalazine and thymoquinone attenuate intestinal tumour development in Msh2(loxP/loxP) Villin-Cre mice. Gut. 2015 Dec;64(12):1905–12. **IF 14.921**

Campregher C, Schmid G, Ferk F, Knasmüller S, Khare V, **Kortüm B**, Dammann K, Lang M, Scharl T, Spittler A, Roig AIAI, Shay JWJW, Gerner C, Gasche C. MSH3-deficiency initiates EMAST without oncogenic transformation of human colon epithelial cells. PLoS One. 2012 Jan [cited 2014 Feb 6];7(11):e50541. **IF: 3.730**

Ankersmit HJ, Nickl S, Hoeltl E, Toepker M, Lambers C, Mitterbauer A, **Kortuem B**, Zimmermann M, Moser B, Bekos C, Steinlechner B, Hofbauer H, Klepetko W, Schenk P, Dome B. Increased serum levels of HSP27 as a marker for incipient chronic obstructive pulmonary disease in young smokers. Respiration. 2012;83(5):391–9. **IF: 2.615**

Acknowledgements

This dissertation is dedicated to my mother, Christa-Maria, who taught me to count, and my father, Manfred Heinz, who taught me to read, and my siblings Friederike, Theresa, Konstanze, Barbara-Elisabeth, Dorothea, Viktoria, Clemens-August and Gregor-Cornelius.

I thank Prof. Ulrike Stein for adopting me in her laboratory and for supervising me all the way, by challenging me academically and professionally. She shared with me her vision of a calling to instrumentally apply one's potential in this world. Without Prof. Wolfgang Walther's careful, but neuralgic impacts on my scientific reasoning, I would not have managed to compile this dissertation. My gratitude also goes out to Prof. Pirus Ghadjar for offering me a stipend and for introducing me into the discipline of experimental and translational radio-oncology. I further acknowledge Prof. Claudia Baldus and Dr. Ralf Kühn for their indispensable expertise in revising and challenging the interim progress reports of my dissertation project. I also want to thank Prof. Gunnar Dittmar and Dr. Oliver Popp for advancing this project as well as my insight into the realm of proteomics, and the group of Prof. Walter Birchmeier for providing me with the small molecular means to probe the cellular systems with my humble hypotheses.

I thank Pia Herrmann, Janice Smith, Rita Mokritzkij, and Zeynep Hacer İpek for assisting me in at times arduous experiments. Without Dr. Dennis Kobelt, this study would not have taken shape at all. He always saw through what was necessary to show, and grounded me, who mostly looked for what would be interesting to see. Dr. Harikrishnan Radhakrishnan was a brotherly scout to me when I seemed to lose my way during my laboratory work. In Dres. Fabian Zincke, Mathias Dahlmann, Katharina Ilm, Jessica Pahlke, Francesca Imbastari, Christoph Treese and Inna Zaimenko, I found valuable sages who I could turn to for dispute, discussion and diversion. I regard Müge Erdem, Nazlı Güllü, Malti Dumbani, Miguel Vílchez and Paul Curtis Schoepe as my brothers and sisters whom I found along the way.

Prof. Constantin Alex and the Humbold University Orchestra gave me the invaluable experience of belonging, purpose, and duty within a greater musical organism.

Furthermore, I want to express my deep gratitude to the Berlin School of Integrative Oncology (BSIO) and the Charité – Universtitätsmedizin Berlin for offering me this most challenging and educative period of my career thus far! Prof. Clemens Schmitt and Prof. So-Young Lee have encouraged me in my non-canonical endeavor, and Dr. Eleanor Eife-Horn has helped me tremendously to formally settle in the doctorate program.

Finally, this dissertation is dedicated to my friend, my love and wife, Ana Airatovna Nasyrova. You have always stood by my side, challenging, teasing, encouraging me to complete and present whatever I have attempted. For this, and your unexplainable and inexhaustible zest for discovery and bafflement, I cannot thank you enough!